EFFECTS OF WHITE LIGHT EMITTING DIODES AND HALOGEN LAMP ON SPECTROSCOPIC MEASUREMENT OF SALA MANGO INTRINSIC QUALITIES

CHIONG WAN LONG

UNIVERSITI SAINS MALAYSIA

2017

EFFECTS OF WHITE LIGHT EMITTING DIODES AND HALOGEN LAMP ON SPECTROSCOPIC MEASUREMENT OF SALA MANGO INTRINSIC QUALITIES

by

CHIONG WAN LONG

Thesis submitted in fulfilment of the requirements

for the Degree of

Master of Science

May 2017

ACKNOWLEDGMENT

May all the glory and praise go to God the Almighty One for His grace and blessing upon completion of this thesis. He is the source of knowledge and wisdom and from Him, I received the strength to endure the whole research journey.

This thesis is possible with help and support from many individuals. I would like to extend my sincerity to each and every one of them.

First and foremost, I would like to thank my supervisor, Dr. Ahmad Fairuz Omar for his advice, support and encouragement throughout the research. Being more than a supervisor, he is a mentor and great role-model especially his great passion in research and education areas. Besides, special thanks to my co-supervisor, Professor Dr. Mohd. Zubir Mat Jafri for his advice and at the same time, being caring and sensitive to student's needs.

I would like to acknowledge the support of Federal Agriculture Marketing Authority (FAMA) (Perlis Branch) for their assistance in getting Sala Mango samples and Department of Agriculture particularly Mr. Haji Ahmad Puat bin Mat Kassim for sharing of his expertise regarding Sala Mango selection.

I am extremely thankful to Ministry of Higher Education and Universiti Sains Malaysia for financial support under MyBrain 15 scholarship and USM Fellowship scheme respectively.

I am also deeply indebted to lab assistants and technicians especially Mr. Mohtar Sabdin, Mr. Muhammad Anis Ibnu Hajar and Mr. Mohd. Noor Fakarruddin Abdullah for their full assistance while using the instruments and designing the lighting systems.

To my friends Ms. Ting Hie Kwang, Ms. Joice Tham Sin Yi and Ms. Then Li Yee, I am also thankful for your lending hand during experimental works especially when I have only limited time to finish the experiment.

Last but not least, to my beloved family and friends, I am blessed to have all of you in my life and thank you so much for the encouragement words and advices when I faced difficulties in my journey.

TABLE OF CONTENTS

ACKNOWLEDGEMENT ii

TABLE OF CONTENTS iv

LIST OF TABLES viii

LIST OF FIGURES x

LIST OF SYMBOLS AND ABBREVIATIONS xiii

ABSTRAK xiv

ABSTRACT xv

CHAPTER 1 – INTRODUCTION

1.1 Fruit Quality 1

1.2 Non-destructive Quality Measurement 3

1.3 Problem Statement 5

1.4 Research Objectives 6

1.5 Scope of the Research 6

1.6 Outline of the Thesis 7

CHAPTER 2 –THEORY AND LITERATURE REVIEW

2.1 Principle of Spectroscopy 8

2.2 Spectroscopic System 10

2.3 Lighting Fundamentals 11

2.3.1 Lighting Evolution 11

2.3.2 Light Emitting Diode 13

2.3.3 Application of White LED in Solid State Lighting 15

2.4 Chemometrics 16

2.4.1 Calibration and Prediction 17

2.4.2 Calibration Transfer 18

2.5 Fruit 19

2.5.1 Fruit Development and Physiology 20

2.5.2 Fruit Internal Quality 22

2.5.3 Optical Properties of Fruit 23

2.5.4 Colour and Appearance 24

2.5.5 Mango Overview 25

2.6 Application of Spectroscopy in Fruit Quality Analysis 26

CHAPTER 3 – METHODOLOGY

3.1 Overview of Research Methodology 29

3.2 Jaz Spectrometer 30

3.3 LED Lighting Panel Designation 32

3.4 Preliminary Study Using Colour Papers 33

3.4.1 Experimental Setup 33

3.4.2 Spectral Analysis 35

3.5 Real Case Study of Sala Mango 35

3.5.1 Fruit Material 36

3.5.2 Reflectance Measurement 37

3.5.3 Intrinsic Qualities Measurement 38

3.5.4 Data Processing 39

CHAPTER 4 – RESULTS AND DISCUSSION

4.1 White Diffuse Reflectance 42

4.2 Influence of LED CCT in Visible Spectroscopic Observation of RGB Sample 44

4.3 VIS Spectroscopic Measurement of Sala Mango Intrinsic Properties under Different Lightings 49

4.3.1 VIS Spectroscopic Analysis of Sala Mango 50

4.3.2 Calibration Models for pH and SSC 53

4.3.2(a) Acidity 54

4.3.2(b) Soluble Solids Content 61

4.3.2(c) Summary 69

4.4 Direct Calibration Transfer of Sala Mango Visible Spectra between Different Light Source 72

4.4.1 D35 as Master lighting 73

4.4.2 D45 as Master lighting 75

4.4.3 D57 as Master lighting 78

4.4.4 Halogen lamp as Master lighting 80

4.4.5 Summary 81

CHAPTER 5 – CONCLUSION AND FUTURE RECOMMENDATIONS

5.1 Conclusion 84

5.2 Future Recommendations 87

REFERENCES 88

LIST OF TABLES

		Page
Table 1.1	Components of qualities	2
Table 1.2	Non-destructive methodologies in Quality Measurement	3
Table 3.1	LED specifications	32
Table 3.2	Different Groups of Sala Mango Sample	36
Table 3.3	Properties of Sala Mango for 52 Samples	37
Table 4.1	Summary of Preliminary Study of Colour Papers	48
Table 4.2	Calibration and prediction results of Sala Mango acidity through reflectance measurement under D35 lighting	55
Table 4.3	Calibration and prediction results of Sala Mango acidity through reflectance measurement under D45 lighting	56
Table 4.4	Calibration and prediction results of Sala Mango acidity through reflectance measurement under D57 lighting	58
Table 4.5	Calibration and prediction results of Sala Mango acidity through reflectance measurement under halogen lamp lighting	60
Table 4.6	Calibration and prediction results of Sala Mango SSC through reflectance measurement under D35 lighting	62

Table 4.7	Calibration and prediction results of Sala Mango SSC through reflectance measurement under D45 lighting	64
Table 4.8	Calibration and prediction results of Sala Mango SSC through reflectance measurement under D57 lighting	65
Table 4.9	Calibration and prediction results of Sala Mango SSC through reflectance measurement under halogen lamp lighting	67
Table 4.10	Summary of best predictive model for acidity prediction of Sala Mango	69
Table 4.11	Summary of best predictive model for SSC prediction of Sala Mango	72
Table 4.12	Calibration and prediction results after Calibration Transfer using D35 as Master Lighting	74
Table 4.13	Calibration and prediction results after Calibration Transfer using D45 as Master Lighting	76
Table 4.14	Calibration and prediction results after Calibration Transfer using D57 as Master Lighting	78
Table 4.15	Calibration and prediction results after Calibration Transfer using halogen lamp as Master Lighting	81
Table 4.16	Summary of best predictive model results after direct calibration procedure between master and slave lightings	83

LIST OF FIGURES

		Page
Figure 1.1	Light Source Relative Irradiance vs. Spectral Content	5
Figure 2.1	The electromagnetic spectrum	9
Figure 2.2	Schematic diagram on a spectroscopic system	10
Figure 2.3	Fiber optic cable which consists of core, cladding and a supportive jacket. Refractive index of cladding, $n_{cladding}$ is lower than refractive index of inner core, n_{core}	11
Figure 2.4	Timeline of lighting evolution	12
Figure 2.5	A light-emitting diode	13
Figure 2.6	Correlated colour temperature scale and illumination of white LEDs	14
Figure 2.7	Chemometric analyser consists of three linked and interacting components	17
Figure 2.8	Interaction between Light and Fruit	23
Figure 3.1	Methodology flow of experiment	29
Figure 3.2	Jaz Spectrometer	30
Figure 3.3	Sampling System Overview by Jaz Spectrometer	31
Figure 3.4	(a) LED panel board and (b) cement type resistor	32
Figure 3.5	Colour series used in this study	33
Figure 3.6	Experimental setup for reflectance measurement of colour papers using Jaz Spectrometer	34

Figure 3.7	Green colour series (Non-Glossy) reflectance spectra under D45 illumination(left) and scatter plot of reflectance versus green values (right) with spectral gradient bolded in the equation	35
Figure 3.8	Sala Mango samples	36
Figure 3.9	Instrumentations used in intrinsic quality measurement; (a) refractometer and (b) pH meter	39
Figure 3.10	Direct Calibration Transfer Procedure	40
Figure 4.1	Spectra information showing (a) intensity of halogen lamp and (b) reflectance of 3 LEDs with halogen lamp as reference light source	43
Figure 4.2	Spectral gradient of red colour series for (a) glossy and (b) non-glossy surfaces with peak wavelength in bracket	44
Figure 4.3	Spectral gradients of green colour series for (a) glossy and (b) non-glossy surfaces with peak wavelength in bracket	46
Figure 4.4	Spectral gradient of blue colour series for (a) glossy and (b) non-glossy surfaces with peak wavelength in bracket	47
Figure 4.5	Reflectance spectra for Sala Mango Group 2 with sample coding from 10 to 19 under different light sources	51
Figure 4.6	Reflectance spectra for Sala Mango Group 4 with sample coding from 30 to 38 under different light sources	51
Figure 4.7	Reflectance spectra for Sala Mango Group 5 with sample coding from 42 to 52 under different light sources	52

Figure 4.8	Scatter plots of mango acidity prediction using D35 as light source	56
Figure 4.9	Scatter plots of mango acidity prediction using D45 as light source	57
Figure 4.10	Scatter plots of mango acidity prediction using D57 as light source	59
Figure 4.11	Scatter plots of mango acidity prediction using halogen lamp as light source	61
Figure 4.12	Scatter plots of mango SSC prediction using D35 as light source	63
Figure 4.13	Scatter plots of mango SSC prediction using D45 as light source	65
Figure 4.14	Scatter plots of mango SSC prediction using D57 as light source	67
Figure 4.15	Scatter plots of mango SSC prediction using halogen lamp as light source	68
Figure 4.16	Overview graph of 12 model performances for acidity prediction of Sala Mango	70
Figure 4.17	Overview graph of 12 model performance for SSC prediction of Sala Mango	71
Figure 4.18	Overview of model performance of different light sources	82
Figure 4.19	Illustration of forward and backward directions of direct calibration transfer	82

LIST OF SYMBOLS AND ABBREVIATIONS

CCT	Correlated colour temperature
CO_2	Carbon dioxide
CRI	Colour rendering index
GaN	Gallium nitride
Hg	Mercury
InGaN	Indium gallium nitride
K	Kelvin
LED	Light Emitting Diode
MLR	Multiple Linear Regression
NIR	Near infrared
R	Correlation coefficient
R^2	Coefficient of determination
RH	Relative humidity
RMSEC	Root mean square error of calibration
RMSEP	Root mean square error of prediction
SO_2	Sulphur dioxide
SSC	Soluble solids content
SSC/TA	Soluble solids to acid ratio
SD	Standard deviation
TA	Titratable acidity
U	Uranium
UV	Ultraviolet
VIS	Visible

KESAN DIOD PEMANCAR CAHAYA PUTIH DAN LAMPU HALOGEN TERHADAP PENGUKURAN SPEKTROSKOPI KUALITI INTRINSIK MANGGA SALA

ABSTRAK

Spektroskopi merupakan salah satu teknik yang paling berkesan dalam penilaian kualiti buah-buahan terutamanya mangga. Spektrum pantulan yang diperolehi daripada sistem spektrometer sangat dipengaruhi oleh cahaya yang digunakan dalam system ini. Dunia kian beralih kepada penggunaan diod pemancar cahaya putih (LED putih) kerana manfaat-manfaatnya berbanding dengan sumber cahaya konvensional. Oleh itu, kajian ini bertujuan untuk menggantikan sumber cahaya konvensional iaitu lampu halogen dengan LED putih sebagai sumber cahaya dalam pengukuran spektroskopi parameter intrinsik Sala Mango (keasidan dan kandungan pepejal larut). Pantulan spektrum mangga dalam julat cahaya nampak diperolehi menggunakan Jaz spektrometer di bawah pantulan lampu halogen dan LED putih dengan suhu warna 3500 K (D35), 4500 K (D45) dan 5700 K (D57). Data spektrum dianalisis menggunakan kaedah pelbagai regresi linear (MLR) untuk memilih model ramalan yang terbaik. Prosedur pemindahan kalibrasi langsung juga diaplikasikan antara algoritma yang terbentuk menggunakan lampu induk dan ramalan data yang diperoleh daripada lampu kerja. Prestasi yang baik telah tercapai dalam ramalan pengukuran keasidan untuk semua LED putih dengan hasil kajian yang setanding dengan lampu halogen. Hasil kajian juga menunjukkan prosedur pemindahan kalibrasi langsung telah berjaya dipraktikkan antara LED putih dalam ramalan keasidan Sala Mango.

EFFECTS OF WHITE LIGHT EMITTING DIODES AND HALOGEN LAMP ON SPECTROSCOPIC MEASUREMENT OF SALA MANGO INTRINSIC QUALITIES

ABSTRACT

Spectroscopy is among one of the most promising techniques for assessment of fruit quality particularly mango. Reflectance spectrum obtained from spectrometer system is greatly affected by lighting used in the system. The world is turning to white Light Emitting Diode (white LED) due to its benefits compared to conventional light sources. This study is therefore to replace conventional halogen lamp with white LED as light source in spectroscopic measurement of Sala Mango intrinsic parameters (acidity and soluble solids content). Reflectance spectra of mangoes were acquired using Jaz spectrometer over visible light range illuminated by halogen lamp and white LEDs with CCTs of 3500 K (D35), 4500 K (D45) and 5700 K (D57). Spectral data were analyzed using Multiple Linear Regression (MLR) method to choose the best predictive model. Direct calibration transfer technique also was applied between developed algorithm by master lighting and prediction data obtained from slave lightings. Good prediction performance was achieved for acidity measurement for all white LEDs with comparable results to halogen lamp. Results also showed direct calibration transfer procedure has successfully being implemented between white LEDs in acidity prediction of Sala Mango.

CHAPTER 1

INTRODUCTION

This chapter gives background of this research starting with fruit quality and secondly introducing the non-destructive fruit quality assessment developed by researchers including spectroscopy technique. Problem statement is included and further extended to objectives of this research work. Scope of research where work to be performed is described and lastly contents in every chapter are explained in outline of thesis.

1.1 Fruit Quality

Fruit is an important component in a balanced diet known widely as the food pyramid. Fruits are sources of mineral and certain vitamins especially vitamins A and C to humans. Besides, fruit also supply both digestible carbohydrate in form of sugar and starch and indigestible ones which are essential in prevention of constipation. Literatures also showed the preventive role of fruits and vegetables against health problems such as cancer, heart disease, stroke and Alzheimer disease (Liu, 2003; Van Duyn & Pivonka, 2000). Therefore, there is high demand of fresh fruit in market for regular supply of good quality, safe and nutritious fruit. Fresh fruit get rotten in a short period of time after harvest regardless of how well the fruit is stored or processed.

Quality control is vital in food industry to provide safe, acceptable and nutritional products to consumers. The main concern to consumers in buying fruit are the internal qualities such as sweetness, flavour and nutrition of the fruit although purchases mainly are produced on the basis of appearance and textural quality. Quality is defined to be the degree of preference or excellence. The term ‘quality’ is

subjective and complex as it is a combination of characteristics, attributes and properties which gives the overall value of the fruit (Siddiqui, 2015). Fruit quality can differ from consumer to consumer depending on the consumer's own preference and expectation. Repeated purchases are somehow dependent on the good eating quality (Knee, 2002). Since the term 'quality' is subjective, researchers have tried to quantify the term and the parameters are divided into external and internal attributes as shown in Table 1.1.

Table 1.1 Components of qualities (Titova *et al.*, 2015)

External Qualities	**Size**	Weight, Volume, Dimension
	Shape	Diameter/Depth ratio
	Color	Uniformity, Intensity
	Defect	Bruise, Stab, Spot
Internal Qualities	Flavour	Sweetness, Sourness, Astringency, Aroma
	Texture	Firmness, Crispness, Juiciness
	Nutrition	Carbohydrates, Proteins, Vitamins, Functional Property
	Defect	Internal Cavity, Water Core, Frost damage, Rotten

There are wide variations in quality of fruit as quality can be affected by external factors such as climate conditions, soil properties, cultivation techniques, etc. Even fruits taken from the same tree may have different qualities. Besides, as the number of fruit harvested each time is in large quantity, postharvest and grading of fruit have been a great challenge to the agricultural sector. Most of the sorting is still done in traditional way which is through manual sorting by farm workers. This method usually takes up a longer time and requires a lot of labours. Manual sorting is also unreliable because this method is subjective and inconsistent as the decision made is always dependent on the eye of the observer. Another method is by taking few fruits randomly from a tree as samples to make an overall assessment of the qualities of the fruits. Not only this method is destructive, yet it is still unreliable as each fruit would have different intrinsic qualities although obtained from the same tree. For fruit quality measurement, the conventional methods include firmness

measurement using a penetrometer, soluble solids content measurement using refractometer and acidity test using pH meter (Zerbini, 2006). These tests are all destructive and consequently, cost losses to farmers.

Hence, various efforts have been made to introduce non-destructive techniques for fruit quality assurance. Introduction of these non-destructive means of measurement eliminates the need to destroy fruits before measurement is done, time-saving and more reliable. Moreover, non-destructive quality evaluation can help to reduce the reliance on experienced workers in picking and sorting products with higher efficiency and better quality uniformity (Nip, 1993).

1.2 Non-destructive Quality Measurement

With advancement of science and technology, researchers have developed non-destructive methods to measure quality attributes of fruit. Table 1.2 lists down the methodology and techniques used in the measurement.

Table 1.2 Non-destructive methodologies in Quality Measurement (Nicolaï *et al.*, 2014; Omar & MatJafri, 2013)

Methodology	Technique	Components
Optics	(i) Image Analysis (ii) Reflectance, transmittance and absorbance Spectroscopy (iii) Laser Spectroscopy	Size, shape, colour, external defects Internal components, colour, defects Firmness, visco-elasticity, defects, shape
X-ray	X-ray image and CT	Internal cavity and structure, ripeness
Mechanics	(i) Vibrated Excitation (ii) Sonic (iii) Ultrasonic	Firmness, visco-elasticity, ripeness Firmness, visco-elasticity, internal cavity, density, sugar content Internal cavity and structure, firmness, tenderness
Electromagnetic	(i) Impedance (ii) Magnetic Resonance Imaging	Moisture content, density, sugar content, internal cavity Sugar content, oil, moisture content, internal defect and structure
Mass Spectrometry	(i) Gas Chromatography (ii) Advanced mass spectrometry	Aroma
Gas Sensors and Electronic noses		Aroma

Among the techniques, spectroscopy is the most popular non-destructive technique as it is the closest to practical use (Omar & MatJafri, 2013; Siddiqui, 2015). Reviews on this technique have been investigated by authors in publications such as Blanco and Villarroya (2002), Nicolai *et al.* (2007), Lin and Ying (2009) and (Ruiz-Altisent *et al.*, 2010). Researchers have applied mostly Visible (VIS) / Near Infrared (NIR) spectroscopy technique on different fruits such as apple (Bobelyn *et al.*, 2010; Luo *et al.*, 2011), apricot (Camps & Christen, 2009; Chen *et al.*, 2006), pear (Li *et al.*, 2013; Paz *et al.*, 2009), orange (Cen *et al.*, 2007; Jamshidi *et al.*, 2012), strawberry (Guo *et al.*, 2013; Shao & He, 2008), mango (Delwiche *et al.*, 2008; Jha *et al.*, 2012), banana (Davey *et al.*, 2009; Liew & Lau, 2012), blueberry (Sinelli *et al.*, 2008; Wang *et al.*, 2012), etc. This technique is proven to be successful in measuring the intrinsic qualities of fruits. However, the standard light sources used in all of these experiments were halogen lamps. Halogen lamp is recognised as standard light source for its continuous spectrum coverage from ultraviolet to infrared region in the electromagnetic spectrum (Figure 1.1) which is comparable to the real sunlight. This light source is also a good compromise between good performance and relatively low cost (Guidetti *et al.*, 2012).

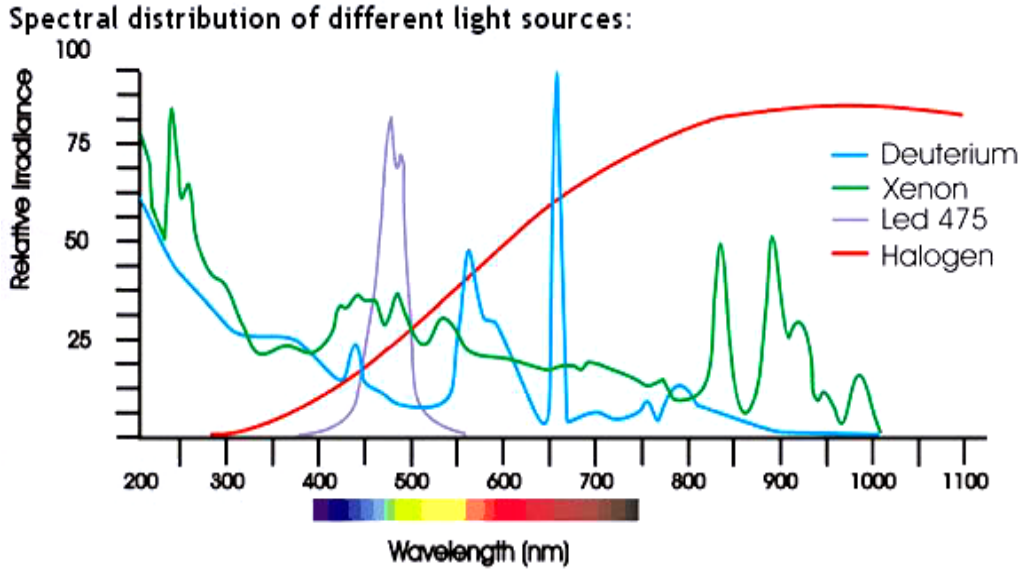

Figure 1.1 Light Source Relative Irradiance versus Spectral Content (Francis, 1995)

1.3 Problem Statement

Recently, white Light Emitting Diode (LED) has been invented and gradually gained popularity in lighting system due to its stability, cost-saving and long shelf-life (Narendran and Gu, 2005). It is also called as the 'smart' lighting application with higher efficiency and better light quality as compared to standard light sources of halogen lamp which give out a significant amount of heat during operation (Schubert and Kim, 2005; Shur and Zukauskas, 2005). One of the important components in spectroscopy system is the light source which is needed to provide light to illuminate samples in the system. As mentioned by Behar-Cohen *et al.* (2011), there is a probability for LED to be the main light source in the future. Thus, researches are focused to explore more on applications of LED including in spectroscopy technique.

1.4 Research Objectives

The main objective of this study is to replace the conventional halogen lamp with white LED as light source in spectroscopy measurement. Sub-objectives are aligned in order to achieve main objective of this research. The sub-objectives are:

1. To analyze the influence of different white LED correlated colour temperatures (lightings) in relation to halogen lamp on VIS spectroscopic measurement of acidity and soluble solids content of Sala Mango.
2. To determine the possibility of direct calibration transfer procedure in acidity prediction of Sala Mango using different lightings.

1.5 Scope of the Research

This research work focuses on the investigation of influence of Correlated Colour Temperature (CCT) of white LED on spectroscopic measurement. The choice of sample is Sala Mango taken from Perlis, Malaysia with wide colour variation (from green to yellow to orange) and wide pH and Soluble Solids Content (SSC) ranges (low pH and SSC when it is green to higher values when it is riper). The reflectance measurement using spectrometer is taken for all 52 samples and imported to computer for statistical analysis. Multiple Linear Regression (MLR) is then used to select few wavelengths that can generate the best combination giving highest coefficient of determination, R^2 and lowest Root Mean Square Error (RMSE) values with intrinsic parameters of Sala Mango for white LEDs and halogen lamp respectively. The focus of this study is assessment of acidity measurement of mango samples using VIS spectroscopy under different light sources and particularly investigation on the effect of LED CCT on spectroscopic measurement. Besides, this work also explores on direct calibration transfer procedure between similar light

sources (LEDs with different CCTs) and different types of light source (halogen lamp and LEDs).

1.6 Outline of the Thesis

This thesis is comprised of five chapters. Chapter 1 introduces the fundamental of fruit quality and the non-destructive measurement of fruit and subsequently associates to the objectives of the whole research. Chapter 2 discusses basic concepts and principles of spectroscopy, fruit and lighting, focusing mainly on several aspects that are relevant for this thesis. It starts with principle of spectroscopy, spectroscopic system and its relation with multivariate analysis. Then, it gives brief background on fruit and its properties, followed by reviews on spectroscopic assessment of fruit quality. The lighting part is explained last with Light Emitting Diode (LED) as the main light subject and its parameters. Chapter 3 explains detailed descriptions of steps and instruments used in this research in order to achieve the objectives of research. The first part is preliminary study using colour paper which is an initial work in discovering influence of LED spectra on colour measurement. The second part is dealing with the experiment on Sala Mango, a real case study for investigating influence of Correlated Colour Temperature of LED in prediction of intrinsic qualities of the fruit. Chapter 4 presents the analysis of data and discussion throughout the entire research. Similarly, this chapter is also divided into two parts; first on preliminary study and latter part on Sala Mango. Last but not least, Chapter 5 draws conclusion from this work and provides some suggestions for future work developments.

CHAPTER 2

THEORY AND LITERATURE REVIEW

This chapter gives the theory and principles of spectroscopy and its system, the lighting fundamentals and Light Emitting Diode (LED), chemometrics including calibration and prediction method and calibration transfer, fruit and its properties and colour and appearance. Literature review where past researches done by researchers on application of LED in solid state lighting and spectroscopy in fruit quality assessment are also discussed and elaborated in this chapter.

2.1 Principle of Spectroscopy

Spectroscopy technique works using optical methods at which matter will respond on ultraviolet ray (UV) (180-380) nm, visible (VIS) light (380-780) nm or near infrared ray (NIR) (780-2500) nm light to produce a range of wavelengths as the output (Noh & Choi, 2006). The spectra are then processed using multiple statistical analyses to obtain final results. The spectra are also correlated to predefined quality attributes using wavelength which fits in the best, commonly in terms of intensity (Omar & MatJafri, 2013). Spectroscopy is now widely used in many fields such as agricultural, medicinal, chemistry and others. Despite its advantages and contributions to science and technology, few know much about the origin of spectroscopy. In “The Early History of Spectroscopy” by Thomas (1991), the author discussed on the development of spectroscopy where science of spectroscopy begins when Sir Isaac Newton observed how sunlight was scattered into a series of colours after passed through a glass prism. He then reversed the experiment by passing individual colours through prism and white light was once again restored. From this simple experiment, Newton made a conclusion that white

light is actually composed of different colours which is known as the visible light spectrum (VIS).

Light or electromagnetic radiation is categorized according to wavelength into radiowaves, microwaves, infrared, visible light, ultraviolet ray, X-rays and gamma rays with each group in increasing frequency. Visible light covers from approximately 380 to 780 nm and is the only region which is observable to human eye known as the colour. Figure 2.1 shows the illustration of electromagnetic spectrum from gamma to radio waves.

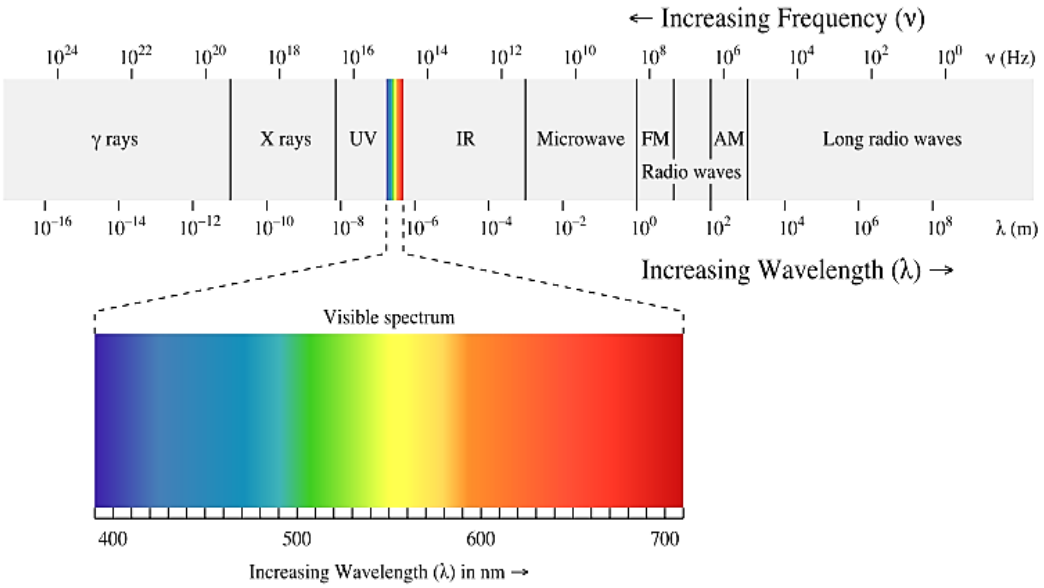

Figure 2.1 The electromagnetic spectrum (Leader Tech, 2016)

Colour can be assessed either through vision analysis or instrumental help. Eye is more flexible compared to instrument as eye is sensitive to geometric factors such as direction, pattern and shape of the object. However, the drawbacks are that evaluations are a subjective matter as different observers observe differently and might even change according to viewing conditions. Instrument holds advantage on these drawbacks as repeatable measurements are able to be made regardless time and place although only a specific attribute can be taken at a time (Hunter, 1987).

2.2 Spectroscopic System

A spectroscopic system includes a light source, a spectrometer, and a fiber optic cable. Light interacts with sample and sends back portion of the light via fiber optic cable to be analyzed by spectrometer. Spectrometer is considered as the heart of whole instrumentation system. Fiber optic sensor collects portion of the electromagnetic radiation after interaction with internal structure of sample and then transfers it to the spectrometer. The device will break down sample light beams into their spectral components, digitize the signal as a function of wavelength and finally data is shown in spectrum form on the screen of a computer. A simple diagram to illustrate spectroscopy instrumentation is shown in Figure 2.2.

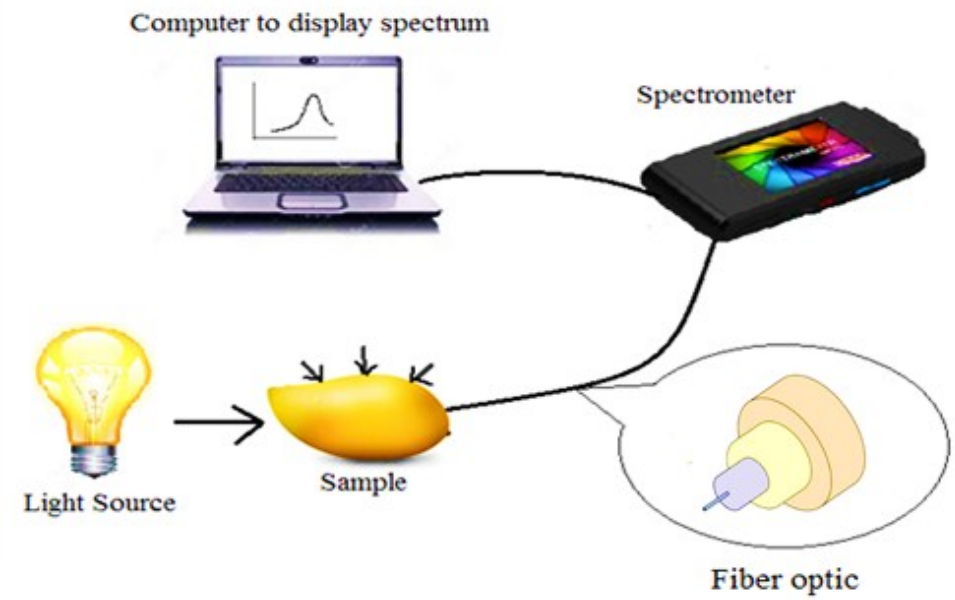

Figure 2.2 Schematic diagram on a spectroscopic system

Fiber optic cable consists of a core and a cladding with lower refractive index and supportive jacket at the outer layer. Figure 2.3 shows the inner core and cladding of an optical fiber. The core is usually made of pure silica but can also be plastics or special glasses while inner cladding is made of material with lower refractive index.

Supportive jacket acts as protector to prevent fiber from mechanical, thermal and chemical stress (Guidetti *et al.*, 2012). Light is transported using principle of total internal reflection where the refractive index of core is higher than refractive index of cladding in order for the phenomenon to occur (Utzinger & Richards-Kortum, 2003). Total internal reflection is highly efficient, 99.999% at each reflection compared to normal reflections from metallic or dielectric surface which may only up to 99% efficient (Jha, 2010).

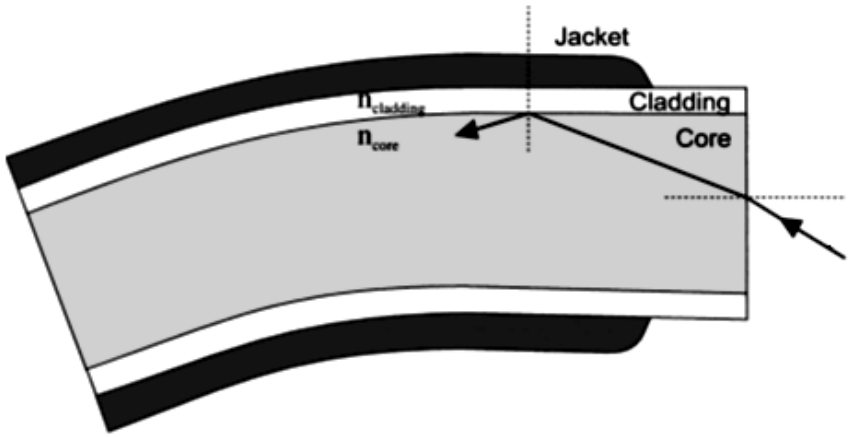

Figure 2.3 Fiber optic cable which consists of core, cladding and a supportive jacket. Refractive index of cladding, $n_{cladding}$ is lower than refractive index of inner core, n_{core} (Utzinger & Richards-Kortum, 2003)

2.3 Lighting Fundamentals

A basic understanding of lighting fundamentals is essential before we look into application of LED in solid state lighting. This section provides a brief overview of evolution of lighting since early ages, introduction to fundamentals of LED and lastly linkage of LED in application of solid state lighting particularly in food appearance.

2.3.1 Lighting Evolution

The sun is the main natural source of light in the world. Apart from keeping human beings warm and enabling biological processes to be carried out, sun is the

light source for human to view things during the daylight. However, when the sun sets and surroundings get dark, artificial light source is needed instead. From the ancient, fire is the oldest artificial light source followed by oil lamps, candles and gas lamps. The first invention of light bulb by Thomas Edison in 1879 marked a big progress in the human lighting history and after several attempts, he managed to replace electric bulb with a tungsten filament which is known as the incandescent lamp. Optics field had progressed so advanced that various engineering fields including lighting for illumination applications were improving from time to time as shown in Figure 2.4.

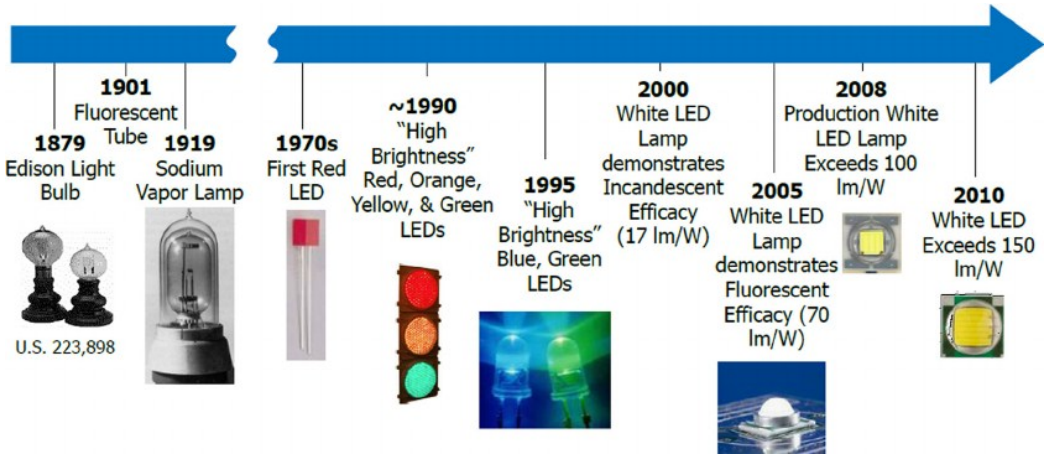

Figure 2.4 Timeline of lighting evolution (De Almeida *et al.*, 2014)

With light, human beings are provided with vision to see and perform out daily tasks. Understanding of light at fundamental levels had been explored by scientists at the past centuries. Sir Isaac Newton had claimed that light was made up of little particles or simply called "corpuscles" in the late 1660s. Christian Huygens found out in contraction that light behaves like wave instead which was validated by Thomas Young and Augustin-Jean Fresnel later using interference experiment. Riddle was solved when Max Planck and Albert Einstein used quantum mechanics approach to prove that actually light has wave-particle dual nature. Subsequently,

major developments in physics had increased, particularly the optics field leading to inventions such as light-emitting diodes (LEDs), lasers, fiber optics and etc.

2.3.2 Light Emitting Diode

A light-emitting diode (LED) is a p-n junction diode which emits light when sufficient voltage is applied to perform recombination process between electrons and holes and consequently, energy is released in the form of photons (light). LED which operates like conventional diode, allows electrical current to pass through the device in only one direction while blocking the current flow in opposite direction. Figure 2.5 shows the circuit symbol and real image of a LED.

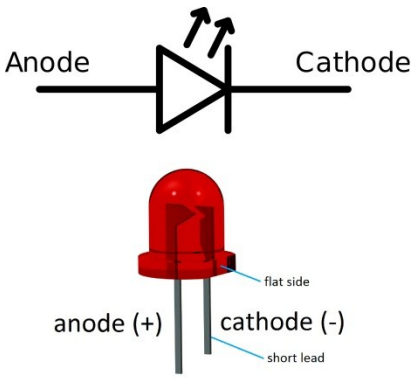

Figure 2.5 A light-emitting diode

Several methods are commonly used to generate white light such as mixing monochromatic LEDs of red, blue and green, addition of blue light and phosphor coating and placing of red, green and blue phosphor coatings over UV LED chip (Held, 2016; Prelovsek & Bizjak, 2006). White light illuminated from LED can be classified into warm, natural or cold based on the standard reference of white light emitted by ideal white light source, the Sun in particular expressed in Correlated Colour Temperature (CCT). CCT of a light source is the temperature of a blackbody radiator related to the appearance of the actual light source (Hunter, 1975).The

concept is derived from blackbody radiation at which colour of heated metal changes accordingly with its temperature. As metal gets heated, the colour of the metal changes from red, gradually to orange, yellow, white and then blue-white (Pode & Diouf, 2011). CCT is used to describe 'hot' or 'cold' of a white light and is expressed in Kelvin. Warm white light usually looks more reddish-yellow and often in CCT below 3500 K. Cold white light is more bluish-white colour and ranges from 5500K and above with 6500 K as standard daylight illuminant (Behar-Cohen *et al.*, 2011). Higher CCT LED tends to have more leading blue peaks indicating more blue radiation. This is one of the advantages of LED compared to incandescent and halogen lamps which are limited to CCT range about 2700 K to 3000 K only (Department of Energy, 2014). Figure 2.6 shows a correlated colour temperature diagram used to describe colour appearance of a white LED.

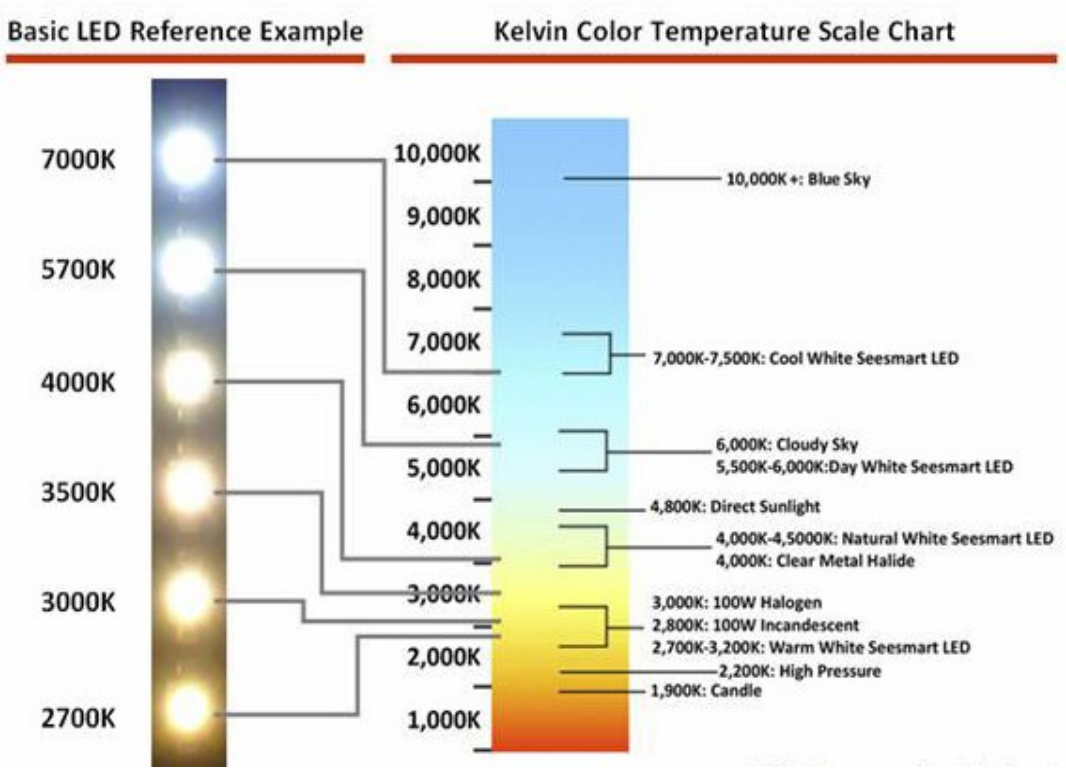

Figure 2.6 Correlated colour temperature scale and illumination of white LEDs (Wonderful Technology, 2016)

2.3.3 Application of White LED in Solid State Lighting

Solid State Lighting (SSL) based on LEDs is emerging fast with energy efficiency as the primary advantage compared to conventional lighting technologies. LEDs have already replaced traditional lamps in lighting systems such as traffic lights, sign boards, mobile phones, computer monitors and automotive lighting (De Almeida *et al.*, 2014). The functions of LED are expanding to not be limited only for display but also for lighting purpose as those traditional light sources such as incandescent and fluorescent lamps (Taguchi, 2008). As the world is changing towards the application of LEDs, researchers have made their efforts to discover more on LED lighting applications.

Comparison works have been conducted to investigate the difference of white LED and conventional light sources as lighting in colour perception of humans. It has been reported that different illumination sources give different perception on visual appearance of an object. As mentioned by Francis (1995) in "Quality as Influenced by Colour", the perception of colour will be affected by the type of lighting falling on an object. Researchers have conducted researches on consumer preferences and acceptability on food under different lightings. Barbut (2001) investigated the effect of three most commonly used light sources which are incandescent (INC), fluorescent (FL) and metal halide (MH) on appearance of fresh beef, pork and chicken meat. All the three meats looked most desirable under incandescent light. Jost-Boissard *et al.* (2009) also investigated the colour rendering of fruit and vegetables under LED and also standard sources (fluorescent and halogen) in terms of attractiveness, naturalness and suitability. It is found that LEDs seems to offer a plausible alternative to standard source although some LED mixings should be avoided. It is also mentioned that the colour temperature of the sources

does not seem to affect observers' preferences in term of attractiveness and naturalness. Cho *et al.* (2015) demonstrated that colour of lighting (in this case, white, yellow and blue lightings are used) in fact does alter meal size taken and blue lighting decreases significantly amount of food eaten in men but not women. Yang *et al.* (2015) also studied the effects of light colour on consumer's acceptability and willingness to eat apples and bell peppers.

However, all these researches are limited to qualitative means rather than quantitative ways with mostly using respondents for observation in food appearances. Researchers have been conducting the studies on effect of lighting on subjective parameters of food like attractiveness, naturalness and suitability, acceptability and willingness to consume food but the correlation between lighting and qualitative intrinsic qualities of food is still undetermined. Thus, further study has to be carried out to find the influence of lighting and its correlation to intrinsic qualities of food.

2.4 Chemometrics

Spectroscopic analysis is a technique to get information from spectra obtained as a consequence to interaction of matter with electromagnetic radiation. These spectra contain great deal of physical and chemical information about molecules of a material. Chemometrics is an important part of electromagnetic radiation spectroscopy analysis in food sector to correlate quality parameters with spectral data obtained. The method is such that first, to collect spectra of calibration set of samples for which the properties of interest are measured using conventional means. After that, a mathematical function of these spectra is created to represent the property using computer and regression software. Finally, prediction of property can be done by evaluating this mathematical function at the unknown sample's spectrum.

In sum, chemometric analyzer consists of three components (hardware, software and database) as shown schematically in Figure 2.7. Using chemometric modelling, estimation of sample properties becomes increasingly attractive since it is less time-consuming as spectra can often be collected in seconds.

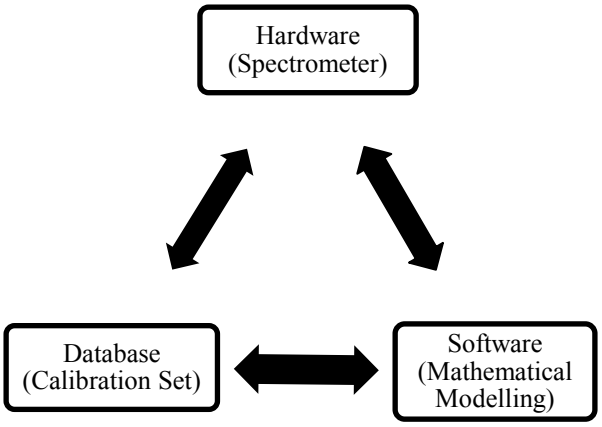

Figure 2.7 Chemometric analyser consists of three linked and interacting components

2.4.1 Calibration and Prediction

The main part of chemometrics in predicting quality parameters of food is building a calibration model and multivariate analysis has shown to be an effective tool in constructing the model. There are several multivariate tools used in analysis including multiple linear regression, principal component analysis, discriminant analysis, cluster analysis and partial least square (Abdi, 2003; Rencher, 2003). Multiple Linear Regression (MLR) is the most common multivariate technique among all the techniques. It gives the relationship between one or more dependent response variables (Y-variables) and two or more independent variables (X-variables) (Richarme, 2002). The developed model will then be tested using validation samples to verify the model accuracy. The statistic parameters involved

are such as coefficient of determination (R^2), root mean square error of calibration (RMSEC) and root mean square of prediction (RMSEP).

MLR has been widely used as analysis method in fruit quality assessment. For example, ElMasry *et al.* (2007) used MLR to obtain R^2 for moisture content, total soluble solids and acidity prediction of strawberry using hyperspectral imaging with results of 0.87, 0.80, and 0.92 respectively. Similarly, Rajkumar *et al.* (2012) utilized MLR models to predict quality attributes of banana using optimal wavelengths. R^2 found was to be 0.85, 0.87 and 0.91 for total soluble solids, moisture and firmness of banana respectively. A good calibration model is the crucial key in giving prediction of quality attributes and therefore, multivariate tool is important and have to be wisely applied for full advantage.

2.4.2 Calibration Transfer

Despite the advantages of spectroscopy being simple, fast and easy to handle, there is also limitation on multivariate calibration techniques when model generated is applied with new spectra measured under new environments or using different instruments. The solution to this limitation is recalibration process which is expensive and time-consuming as reported by Peng *et al.* (2011). Thus, researchers have tried to apply calibration transfer technique to avoid the need of generating calibration model again. The term 'calibration transfer' is mostly assumed to be transfer of model between different instruments although generally the term actually refers to transfer of model between different conditions.

Prior researches mostly are done for model transfer between different instruments. Calibration model developed from master instrument is transferred to predict quality parameter of second instrument (slave instrument). Fonollosa *et al.*

(2016) has successfully performed calibration transfer between chemical gas sensor arrays using direct standardization where signals of slave unit is transferable to space of a master unit. Salguero-Chaparro *et al.* (2013) also demonstrated calibration model transfer between diverse NIR spectrometers in quality evaluation of intact olives. Model transfer between two Fourier transform near infrared spectrophotometers has been successfully implemented in prediction of vitamin C Content of navel orange carried out by Hu and Xia (2011). Correlation coefficient (R) was found to be 0.887 while root mean square error of prediction (RMSEP) was 3.01mg/100g.

Calibration transfer technique is proven to be beneficial as acquiring new spectra for sample measurement and re-measuring is normally expensive and time-consuming. While most of the studies generally focused on calibration transfer between instruments, this method should be expanded to further explorations such as calibration transfer between different light sources in spectroscopy instrumentation system which are explored in this thesis.

2.5 Fruit

Understanding of fruit has been important in order to associate with its quality assessment. From its growth and ripening process to compositional studies, optical properties and comprehension of colour and appearance are all essential characteristics to be taken into account for evaluation purpose. All these fundamental properties are discussed throughout this whole section and lastly past literatures of fruit quality analysis using spectroscopy is also included.

2.5.1 Fruit Development and Physiology

'Mature' term in fruit harvest is derived from Latin word 'Maturus' by the meaning of ripen. It is the stage of fruit development where the fruit has attains its minimum edible quality at the ripening process on the tree. Ripe which is derived from Saxon word 'Ripi' and has the meaning of reap or gather. It is the condition where the fruit has attains its maximum edible quality after harvest. Ripening is a series of complex physiological processes involving increased rate of respiration, ethylene production, loss of chlorophyll, continued expansion of cells and conversion of complex metabolites into simple molecules (El-Ramady *et al.*, 2015). These processes take place within a week in fruit after maturity and result in physical changes in colour, texture and other sensory attributes (Omar & MatJafri, 2013). Ethylene is a plant hormone, particularly the fruit-ripening hormone responsible for regulating many aspects of plant growth including ripening process in climacteric fruits (Tharanathan *et al.*, 2006). Fruit ripening is an irreversible process leading to development of soft and edible fruit with desirable quality attributes (Seymour *et al.*, 2013).

One of the observations of fruit ripening is through the change in colour as a consequence of chlorophyll degeneration and appearance of other pigments. Therefore, fruit colour is often used as indicator to observe maturity for certain fruits such as banana, mango and tomato (Ruiz-Altisent *et al.*, 2010). Colour changes in mango fruit occur when chloroplasts are transformed to chromoplasts containing red or yellow pigments. Consequently, the reddish or yellowish colour of fruit eventually becomes perceptible due to carotenoids. Some cultivars also developed into reddish bluish colour, which has been attributed to anthocyanins (Singh *et al.*, 2013).

Another significant feature of fruit ripening is change in soluble carbohydrates mainly consist of sucrose, fructose and glucose. Ripening process breaks down starch into these simpler sugars and therefore the sugar levels within fruit tend to increase in this stage (Seymour *et al.*, 2012). Ripe mango contains 10 to 20% of total sugars on fresh weight basis depending on the cultivars and stage of ripeness of the fruit (Singh *et al.*, 2013). The total sugar content determines the sweetness of fruit and this attribute is one of the vital characteristics in determining fruit quality (Seymour *et al.*, 2013). It has been reported that the final eating quality is actually can be linked to total soluble solids at fully ripe stage (Subedi & Walsh, 2011).

The next feature to be discussed is acidity, which is due to the presence of organic acids, malic and citric acids found in most of the ripe fruits (Etienne *et al.*, 2013). The predominant organic acids in mature mango fruit are citric, succinic, malic and with citric acid as the major organic acid present in mango fruit and tartaric acid the lowest (Singh *et al.*, 2013). Acidity usually increases at early growth phase, reaches a peak and declines gradually until harvest. During ripening process, levels of acids will decrease presumably used as respiratory substances. The increase in sweetness and decrease in acidity simultaneously with accumulation of sugars and organic acids are responsible for the taste development of fruit (Tharanathan *et al.*, 2006).

Decrease of flesh firmness or textural softening is also another observation during fruit ripening, primarily due to the changes in cell-wall carbohydrate metabolism that result in decrease of cell wall components (Ignat, 2012). The softening process is part of the ripening in most of the fruits. Prior to ripening, fruit has rigid and well-defined cellular structures but after ripening process, the cell wall

becomes soft and diffused (Brownleader *et al.*, 1999). Mango also undergoes drastic and extensive textural softening from hard to soft ripe stage due to degradation of structural as well as storage polysaccharides (Tharanathan *et al.*, 2006).

2.5.2 Fruit Internal Quality

Although fruit purchase is greatly influenced by external attributes (appearance, colour, shape and size), the main concern to customers is actually the internal qualities that eventually give satisfaction to the buyers. Fruit internal qualities are often related to parameters such as soluble solids content (SSC), titratable acidity (TA), soluble solids to acid (SSC/TA) ratio and texture (Romano *et al.*, 2006). Sugar content and acidity have become significant parameters in determination of fruit internal quality as investigated by researchers (Gómez *et al.*, 2006; Li *et al.*, 2013; Omar, 2013; Wang *et al.*, 2012; Yuan *et al.*, 2015; Zhang *et al.*, 2008).

Jha *et al.* (2010) had done a review paper on quality parameters of mango and potential of non-destructive techniques for their measurement. According to the paper, major quality parameters such as size, shape, colour and aroma are used to define the overall quality of fruit. Major changes during ripening of mango are reduction in fruit weight, volume, length, thickness and firmness. Sucrose and fructose levels also increase relatively in all fruit with storage whereas polysaccharides content, particularly starch decreased dramatically. Most of the parameters mentioned are determined by wet chemistry method which destroy the samples and make them unfit for consumption (Jha *et al.*, 2010). Therefore, recent techniques for non-destructive techniques have been introduced to overcome this matter.

2.5.3 Optical Properties of Fruit

In order to evaluate the fruit quality, it is important to know the optical properties of the fruit itself. The basic of food quality analysis using optical properties is from the knowledge of interaction between light and fruit materials. Figure 2.8 shows a diagram on how light interacts with a fruit. Most of the fruit materials are not optically homogenous and therefore light is scattered in all directions when entered the numerous tiny internal interfaces. When beam of light strikes the fruit, roughly 4% of the incident light is reflected from the surface as regular reflectance and the rest is transmitted into the surface where it is either absorbed by the object, reflected back to the surface (body reflectance), or transmitted through the fruit. The amount of radiant energy in each of the processes depends on the properties of the fruit and the incident (Birth, 1976; Chen, 1978).

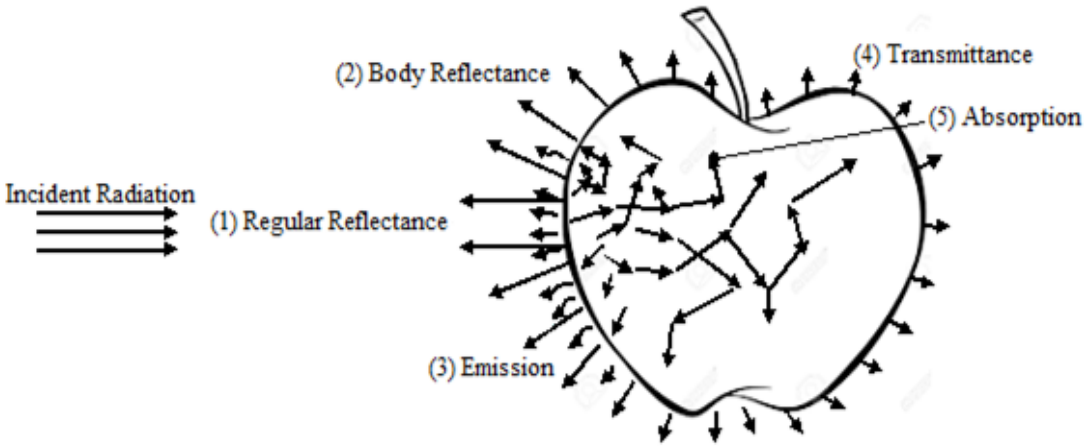

Figure 2.8 Interaction between Light and Fruit (Chen, 1978)

Measurement of body reflectance or generally known as reflectance is especially suitable for measuring quality factors such as external colours, surface damages, bruises and external differences between two objects. This technique measures the radiation reflected from sample, not on the surface but penetrates into the sample a few millimetres being absorbed partly and partly reflected back again (Guidetti *et al.*,

2012). This type of measurement can provide information of the region near surface of incidence point according to (Chen, 1978).

2.5.4 Colour and Appearance

According to 'Colour and Appearance' by Lawless and Heymann (2010), colour is defined to be "the perception in the brain that results from the detection of light after it has interacted with object." Few conditions to be satisfied in order for an object to be perceived by eyes are such that the source must be radiated in visible spectrum between 380 and 770 nm with observer possesses at least the normal colour vision and enclosure filled with clear optical medium and boundaries which are capable to reveal the object character. Besides, colour of an object perceived by an observer is also affected by type of lighting shines on the object, distance from observer to object and the surrounding environment. When light strikes on an object, it undergoes i) specular reflection due to gloss surface of the object skin, ii) scattering due to diffuse reflection and sometimes diffuse transmission, iii) absorption and iv) specular transmission which is directly through the object for transparent object. Tominaga and Wandell (1989) also reported that the colour appeared to our visual is actually both the light reflected from the object and nearby objects. The spectral reflectance of the reflected object is defined by the surface reflectance of the object and the light source shining on it.

Appearance is definitely one of the vital attributes of quality and colour is one of the subset in describing appearance of food or an object. Colour has to be within expected range else the other two major quality factors, flavour and texture are unlikely to be judged at all. This is especially true for fruits and vegetables

(Francis, 1995). For example, try to imagine banana flesh in purple or green in colour, the consumers would definitely reject to buy the fruit.

2.5.5 Mango Overview

Mango (*Mangifera indica*) is one of the popular tropical fruits produced in Malaysia with average annual production of 20022 tonnes from year 2009 to 2013 (Ministry of Agriculture and Agro-Based Industry, 2015). The mango fruit is a large, fleshy drupe which contains edible mesocarp with varying thickness (Litz, 2009). Mango is a climacteric fruit which continues to ripen even after detachment from parent plant at mature stage. The fruit normally reaches maturity in 4 to 5 months from flowering and harvested at green mature stage and kept under normal ripening. After that, it will take roughly 6 to 10 days to ripen depending on the environmental conditions and becomes overripe and spoiled within 15 days after harvest (Tharanathan *et al.*, 2006). Mango fruit is famous for its sweet taste, smooth texture, and juicy flesh with strong fragrant aroma. Mango is a natural source of Vitamin A and C which are important to human health in daily fiber intake. A huge variation exists among mango cultivars in fruit weight, shape and colour. There are roughly 216 clones of mango in Malaysia but the varieties well-known among consumers are such as Chokanan, Harumanis, Sala, Mas Muda, Siam Panjang and Maha 65. Mango fruit can be utilized into different products like juice, candy, pickles, jam and jelly although it is still preferably to be eaten fresh compared to other fruits (Ministry of Agriculture and Agro-Based Industry, 2016). The ripening process of a mango fruit can be assessed through correlation with skin colour commercially (Subedi & Walsh, 2011).

2.6 Application of Spectroscopy in Fruit Quality Analysis

As mentioned in Chapter 1, spectroscopy has been one of the most rising techniques in fruit quality analysis in the recent years. This non-destructive technique is often implemented with respect to attributes such as SSC, acidity, firmness, ripeness level and maturity. Examples of spectroscopy include Visible (VIS) Spectroscopy, Visible/Near-Infrared (VIS/NIR) Spectroscopy, Near-Infrared (NIR) Spectroscopy and Ultraviolet/Visible (UV/VIS) Spectroscopy. Each type of spectroscopy corresponds to different wavelength used in range but choice of spectroscopy usually dependent on properties of samples. The main focus would be on VIS spectroscopy as it is the one relevant in the whole research work.

Visible (VIS) spectroscopy which covers from 380 to 780 nm usually are used in assessment of fruit intrinsic quality through appearance especially skin colour as colour is located within the visible range. Spectra measured by spectroscopy show wavelengths in this range provide compositional information regarding chemical bonds where the main absorbers are such as chlorophylls, carotenoids, anthocyanins and other colour compounds. These pigments are those which give colour and appearance to the fruits and vegetables. Colour is often used as basis in sorting products into commercial grades, but it relates more directly to consumer in appearance while pigment concentration is more related to maturity (Abbott, 1999). Therefore, VIS spectroscopy is useful as it is able to evaluate fruit ripening stage and gives vital information when combined with multivariate analysis especially in prediction of fruits and vegetables quality.

Ziosi *et al.* (2008) introduced a new index based on absorbance difference (I_{AD}) between two wavelengths; 670 and 720 nm which are referred as chlorophyll-a absorption peak in characterizing peach ripening progression using VIS

spectroscopy. The I_{AD} obtained was proved to be able to identify physiological changes occurring in peach fruit and was a reliable marker of fruit ageing. Classification of durian maturity using visible spectroscopy of spine of durian was investigated by Timkhum and Terdwongworakul (2012). Spectrophotometer with wavelength region from 350 to 750 nm was used and best accuracy of classification was identified at 94.7%. The result was attributable to the absorbance of chlorophyll a, carotenoids and anthocyanins in the spine. Pholpho *et al.* (2011) applied visible reflectance spectroscopy and succeed to classify bruised and non-bruised longan accordingly. Reflectance of bruised fruits was lower than that of non-bruised fruits but both groups had highest reflectance at 700 nm and chlorophyll absorption at 670 nm.

VIS spectroscopy can be utilized more as a non-destructive evaluation of fruits and vegetables than just appearance attributes. Jha *et al.* (2005) used visible spectroscopy in prediction of sweetness, measured in ^{o}Brix of mango samples. Calibration models from different analyses were developed and MLR model of original spectra in range from 440 to 480 nm was found to be the best. The results obtained were good and convincing with standard error of calibration of 1.9^{o}Brix, validation (SEP) 1.98^{o}Brix and correlation coefficient (R) of 0.90. Subsequent year, same researchers applied the same technique to test on other attributes; namely firmness and yellowness but using different mathematical analyses (Partial Least Squares, Principal Component Regression and Multiple Linear Regression). All models were found to perform equally well in wavelength range from 530 to 550 nm but R for yellowness index was much better than that of firmness. The reasoning was that wavelength in visible range was better for surface attribute (yellowness index) than subsurface properties (firmness) (Jha *et al.*, 2006).

Yahaya *et al.* (2015) also utilized this technique to determine the acidity of Sala Mango using direct transfer calibration method between three different spectrometers. Multiple wavelengths were selected within visible range using Multiple Linear Regression (MLR) to develop calibration algorithm which subsequently transferred to another instrument to obtain prediction results. It was found that good results obtained for calibration transfer models despite different instruments were used to develop the prediction results.

While spectroscopy technique has been successfully utilized in fruit quality assessment in the past, no work has been published on white LED as substitute to halogen lamp as lighting in spectroscopic measurement of fruit. Thus, it is the main purpose of this research work in investigating the potential of substitution of halogen lamp in intrinsic qualities measurement of Sala Mango using spectroscopy technique and at the same time, checking on the influence of CCT of white LED in the measurement.

CHAPTER 3

METHODOLOGY

This chapter describes the detailed procedures of methodology used in this work in order to achieve objectives of the research. Among the steps include methodology for preliminary study and case study from research design to sample preparation, experimental work, data analysis and finally a conclusion is drawn.

3.1 Overview of Research Methodology

Figure 3.1 shows an overview of the research design of this experimental work. Further procedures are to be further elaborated in the next few sections.

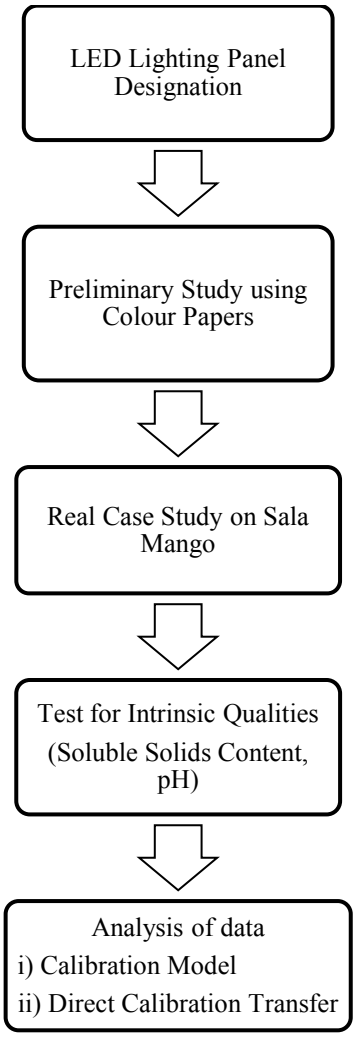

Figure 3.1 Methodology flow of experiment

3.2 Jaz Spectrometer

The main instrument used in this experiment is Jaz Spectrometer (Figure 3.2), a product from Ocean Optics Inc., USA. Jaz is light and portable, therefore enabling the spectrometer to be carried out for field work, lab or other process environment.

Figure 3.2 Jaz Spectrometer

In this research, however, Jaz was connected to computer via USB port since the experiment was conducted in lab and controlled by the Spectra Suite software. Being responsive from 200 to 1100 nm, Jaz has two different channels (Channel 0 and 1) with each of them having different wavelength coverage. Channel 0 covers from 200 to 850 nm while Channel 1 ranges from 650 to 1100 nm. Channel 0 was used in this work as it covers whole range of visible region. Basically, sampling system using spectrometer is explained as flowchart in Figure 3.3.

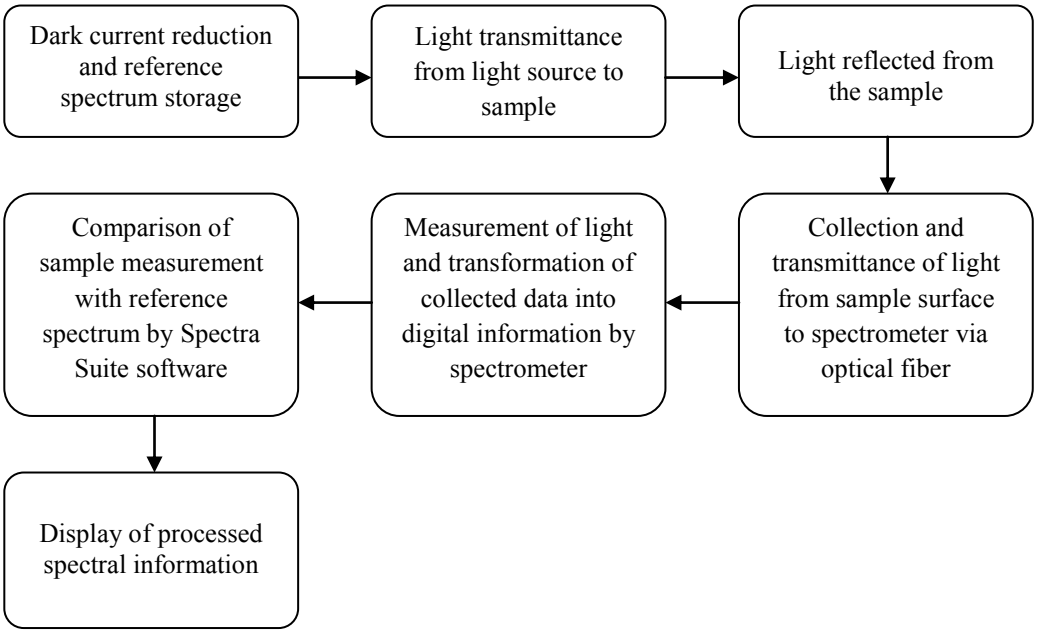

Figure 3.3 Sampling System Overview by Jaz Spectrometer (Ocean Optics, 2010)

Optical measurement can be carried out in different modes such as transmittance, absorbance and reflectance. In this research, reflectance mode which is reported to be the easiest mode is used instead due to the reasons as stated below (Chen, 1978; Hemming, 2013):

1. Its suitability to measure quality factor which is related to external colour (skin colour) especially this research is taking the skin colour of mango under influence of different lighting into account.

2. Its relative high intensity which make measurement easier to use for quality evaluation. The source needs not to be of high intensity or the detector to be very sensitive.

3. Reflectance measurement is not adversely to be affected by low-intensity background.

3.3 LED Lighting Panel Designation

The main components in this research are the white LEDs with different CCTs. The LEDs are products from Osram Opto Semiconductor with specifications of LEDs are shown as in Table 3.1. For the sake of simplicity, each white LED is labeled accordingly to CCT throughout whole thesis using shorthand where white LED with CCT of 3500 K as D35, 4500 K white LED as D45 and 5700 K LED as D57. The LED panels are designed to be 4 LEDs connected in series with 3 cement type resistors of 10 Watt 2.2 Ω ±5% connected in parallel. Figure 3.4 shows the LED panel designed and resistor used in this research.

Table 3.1 LED specifications (Osram Opto, 2011, 2015a, 2015b)

	D35	D45	D57
Correlated Colour Temperature (CCT)	3500 K	4500 K	5700 K
Product Type	LCW W5AM-KXKY-409Q	LCW W5AM-PC-KRKT-4J8K	LUW W5AM-KYLX-4E8G
Colour of Emission	Warm White	Natural White	Cool White
Viewing angle	170°	170°	170°
Forward Current (mA)	350	350	350
Forward Voltage (V)	3.2	3.2	3.2
Luminous Flux (lm)	71-97	82-104	82-130
Colour Rendering Index	80	70	70

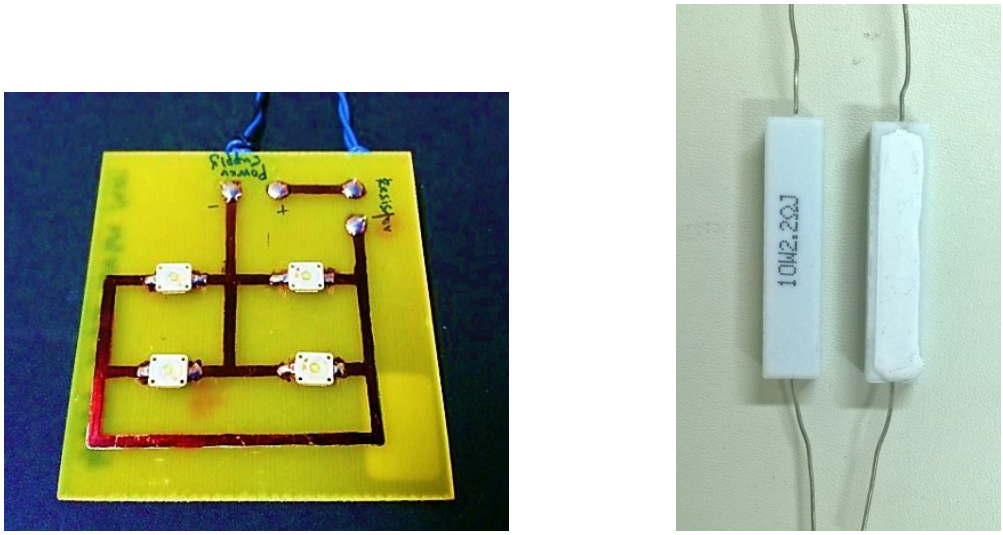

(a) (b)

Figure 3.4 (a) LED panel board and (b) cement type resistor

3.4 Preliminary Study Using Colour Papers

This study is an initial step in understanding the interactions between spectral characteristics of light sources and basic colours. Colour papers were used as representation of colour measurement with special RGB colour code. The colour papers used were of monochromatic colour of red, blue and green colours with two different surfaces; glossy and non-glossy. A monochromatic colour scheme is scheme with only single hue in varying shades (McMurry, 2006). Each colour series was in increasing values of 20, 40, 60, 80, 100, 120, 140, 160, 180, 200, 225 and 255 as viewed in laptop screen. Although printed version of these colour series were no longer in RGB colour system, these numerical numbers were just being a reference to increasing gradient in hue for colour measurement. Monochromatic colours were investigated as changes in series can be observed significantly without influence of the other two colour elements. Figure 3.5 shows the colours which were used in this experiment. Two type surfaces were used to explore possibility of different results obtained due to CCT of LED.

Figure 3.5 Colour series used in this study

3.4.1 Experimental Setup

Figure 3.6 shows the experimental setup for this experiment. The experiment was conducted in a dark room using Jaz Spectrometer with spectral response of 200-850 nm. Reference spectrum was obtained by shining halogen lamp (ASD Inc.) as

standard light source at 45^{o} onto WS-1-SL, a white diffuse reflectance standard with reflectivity above 95% for wavelength coverage from 250 to 2000 nm. The probe used in this experiment is R600-7-SR-125F with 600 μm core diameter. The height between colour paper and fiber tip and the distance between LED panel and fiber probe were kept constant throughout the experiment which were 1.0 cm and 23.5 cm respectively. The spectroscopy was then calibrated using the spectrum reference and used for reflectance measurement. The colour paper was put under the fiber optic probe perpendicularly with two LED panels supplied with 1.6 A illuminating from both sides at the angle of 45^{o}. The Spectra Suite software uses the following Equation (3.1) to evaluate each pixel on the detector and produce the reflectance spectra:

$$R_\lambda = \frac{S_\lambda - D_\lambda}{W_\lambda - D_\lambda} \times 100 \qquad (3.1)$$

where R_λ= the reflectance at the wavelength of λ

S_λ=the sample intensity at the wavelength of λ

D_λ=the dark intensity at the wavelength of λ

W_λ= the reference intensity at the wavelength of λ

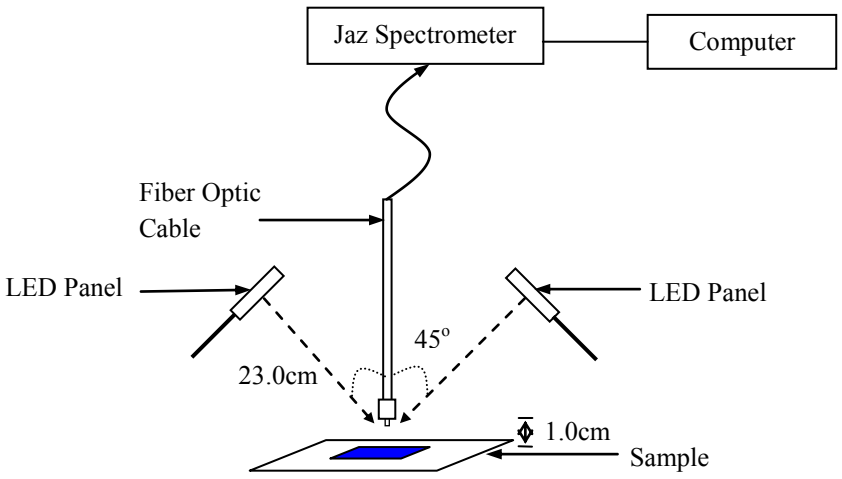

Figure 3.6 Experimental setup for reflectance measurement of colour papers using Jaz Spectrometer

3.4.2 Spectral Analysis

The spectral reflectance of colour papers were saved and further analysed using mathematical analysis. For analysis of the spectra from colour papers, gradient of the graph of reflectance against colour series for selected wavelengths was used. High gradient indicates a small increase in colour series is sufficient to detect change in reflectance of the colour paper (better responsivity). This analysis technique was applied instead of direct interpretation from reflectance spectra due to the raw spectra does contain peaks from white LED itself which is not useful in colour measurement. Figure 3.7 shows an example of raw reflectance spectra with two peaks at wavelength bands from (i) 420 to 460 nm for blue radiation from white LED and ii) 500 to 600 nm for real colour spectrum measured. In order to eliminate the former one, the gradient technique was utilized. Results are to be discussed in Chapter 4, Results and Discussion.

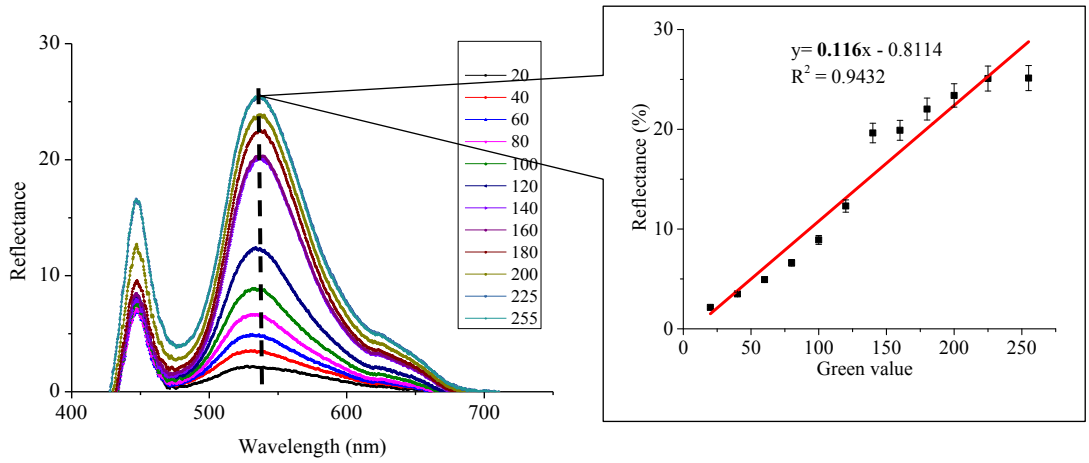

Figure 3.7 Green colour series (Non-Glossy) reflectance spectra under D45 illumination(left) and scatter plot of reflectance versus green values (right) with spectral gradient bolded in the equation

3.5 Real Case Study of Sala Mango

For investigation of white LED as light source in spectroscopy system for fruit quality assessment, the sample used in this research work is Sala Mango which has

wide variation in colour, Soluble Solids Content (SSC) and acidity. The wide variations are to ensure extensive coverage in obtained results for higher reliability results.

3.5.1 Fruit Material

52 Sala Mango (Figure 3.8) were harvested randomly and classified into different groups according to ripeness levels as described in Table 3.2. The fruit samples were collected and arranged by courtesy of Federal Agricultural Marketing Authority (Perlis Branch) with assistance of expert from Department of Agriculture at an orchard located in Perlis. The different categories are to investigate how reflectance spectra differ from one group to another with large variations in samples covered.

Figure 3.8 Sala Mango samples

Table 3.2 Different Groups of Sala Mango Sample

Group	Code	Description
1	1-9	Immature, Green
2	10-19	Mature but still green in colour
3	20-29	Mature and turn into yellowish-green colour
4	30-38	Fruits wrapped in black paper (Free from bruises)
5	42-52	Artificially ripened using calcium carbide for 3 days
6	39-41	Artificially ripened using calcium carbide for 4 days

Subsequent to the harvest, the samples were transported to Engineering Lab, School of Physics, Universiti Sains Malaysia where the experimental procedures were carried out. 14 out of 52 samples were artificially ripened using calcium carbide for 3 and 4 days respectively to get wider variation of sample groups. The other samples were stored in air-conditioned room at 17^{o}C and 65% relative humidity (RH). After the samples were ready, each sample was labeled accordingly in number from 1 to 52 and later was weighed using weighing balance. The diameter of mangoes also was measured using thread and meter ruler to obtain the average size of the mango samples. Table 3.3 gives the properties of Sala Mango samples.

Table 3.3 Properties of Sala Mango for 52 Samples

	Min	Max	Mean	Standard Deviation
Weight(kg)	0.232	1.009	0.539	0.156
Outer Diameter (cm)	19.3	30.2	25.3	2.2
SSC (^{o}Brix)	7.3	15.5	10.5	2.0
Acidity (pH)	2.75	5.24	3.80	0.81

The weight and outer diameter of the whole samples were in the range of 0.232-1.009 kg and 19.3-30.2 cm, respectively while the range of SSC and acidity were from 7.3 to 15.5 ^{o}Brix and pH 2.75 to 5.24, respectively. The samples were wide in range because different maturity levels of mango were used in this experiment.

3.5.2 Reflectance Measurement

For reflectance measurement of mango samples using Jaz Spectrometer, similar experimental setup was used as shown in Figure 3.5, difference was just that the colour papers were replaced with mango samples. The spectra of the 52 samples were obtained using wavelength ranges of 200 to 850 nm (Channel 0) with custom setup of integration time of 100 ms, spectra averaged of 5 and boxcar smoothing of 1. Channel 0 of the spectrometer covers visible light which is from the wavelength of

380 to 780 nm. The spectrometer was first calibrated using white diffuse reflectance standard having halogen lamp as light source shining at 45^{o} to the white diffuse. The optical fiber probe was placed 1.5 cm directly perpendicular above the white diffuse. After calibration was done, reflectance measurement on mango surface was taken for mango samples with halogen lamp as light source. Three measurements were taken randomly from one surface of each mango sample and later were averaged to obtain a single spectrum which represents the sample. The overall set of data was used to develop the calibration algorithm. Similar measurements were repeated from another surface of mango sample and the obtained spectra were used for prediction purpose. When the measurement was done, the light source was replaced with two LED panels shining from two directions on mango surface as shown in Figure 3.5 and reflectance measurement was repeated for D35, D45 and D57 lightings. The acquired data were properly stored for analysis purpose.

3.5.3 Intrinsic Qualities Measurement

After spectroscopy measurement was done for all the mango samples, destructive tests were carried out to obtain the intrinsic qualities of the samples. The fruits were peeled off skin and blended using a blender to collect the juice for measurement. The Soluble Solids Content (SSC) of mango juice was measured by using PAL-3 refractometer from Atago Co. (Tokyo, Japan) with range of measurement from 0 to 93 ^{o} Brix, resolution of 0.1 ^{o}Brix and accuracy of ±0.2 ^{o}Brix as shown in Figure 3.9 (a). A refractometer basically is an optical device which applies the refraction of light concept when light passes through a liquid. Denser liquid refracts more light indicating higher SSC in the liquid. 1^{o}Brix arbitrarily indicates 1 g of sucrose in 100 g of solution (Kenkel, 2010). Meanwhile, acidity of fruit was measured using Exstik

pH meter (Figure 3.9 (b)) from Extech Instruments (Watham, Massachusetts, USA) with range of measurement between 0-14 pH, resolution of 0.01 pH and accuracy of ±0.01 pH.

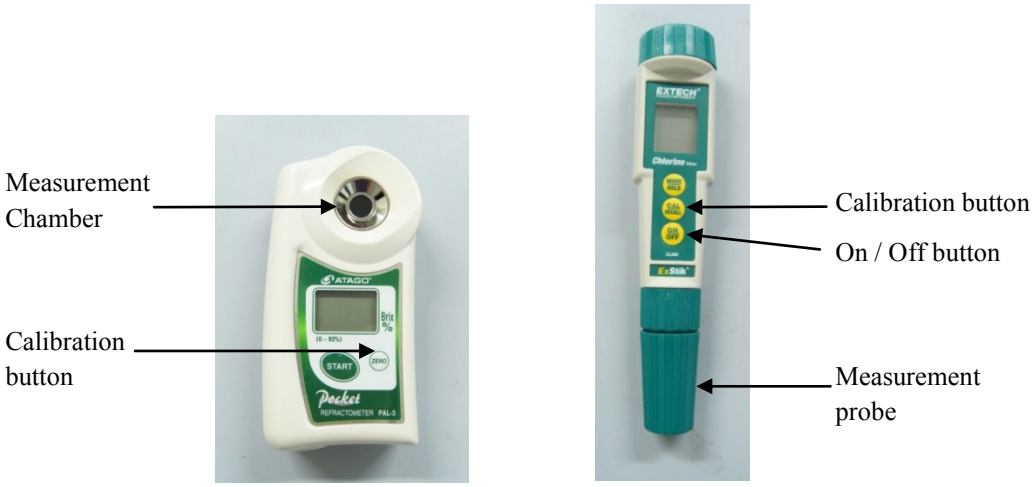

Figure 3.9 Instrumentations used in intrinsic quality measurement; (a) refractometer and (b) pH meter

3.5.4 Data Processing

Acquired spectral data were imported to OriginPro8.1 Service Release (Patch) 3(SR3) (OriginCorp., USA) and graphs were plotted as shown in Chapter 4. All the statistical analyses to find the calibration algoritm correlating reflectance and intrinsic qualities were run with Minitab 14 (Minitab Inc., USA), a statistical software powerful for data analysis. Multiple Linear Regression (MLR) was applied to selected wavelengths to get different models and performance of each model was evaluated using several parameters such as coefficients of determination (R^2) of calibration and prediction, root mean square errors of calibration (RMSEC) and prediction (RMSEP). High value of R^2 for both calibration and prediction is preferred to show stability of model developed. RMSEC and RMSEP are defined as Equation (3.2) (Esbensen *et al.*, 2002):

$$RMSEC/RMSEP = \sqrt{\frac{\sum_{i=1}^{n}(\hat{y}_i - y_i)^2}{n}} \quad (3.2)$$

where $\hat{y}_i$ = predicted value of ith observation

y_i = measured value of ith observation

n = number of observations in calibration (RMSEC)/ prediction set (RMSEP)

Both of these parameters are direct estimation of modeling error and a good model possesses a small difference between them.

For second part of the analysis on real study of Sala Mango, direct calibration transfer procedure was applied between halogen lamp and LEDs to observe possibility of direct transfer of calibration model from master lighting to slave lightings without recalibration process. Figure 3.10 shows an overview of direct calibration transfer procedure between different lightings.

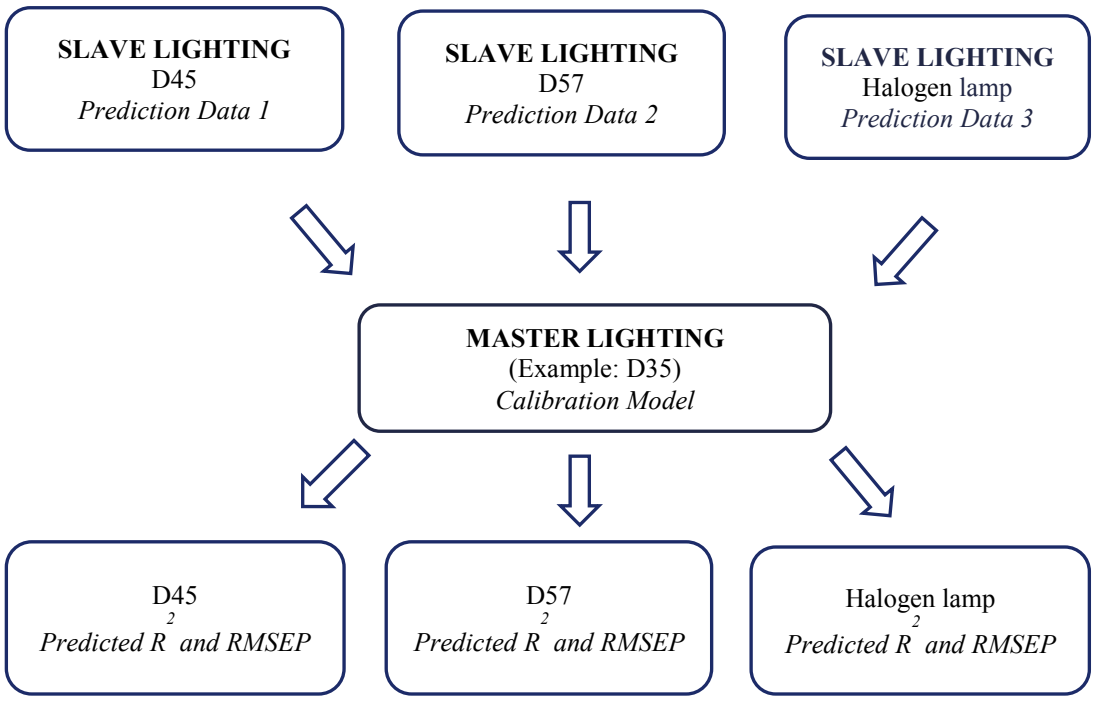

Figure 3.10 Direct Calibration Transfer Procedure

From Figure 3.10, calibration model developed from master lighting (in this case, D35) is transferred into prediction data measured by spectrometer under other lightings or slave lightings (D45, D57 and halogen lamp) to get predicted R^2 and RMSEP results for all the three slave lightings. The performance of the model was once again evaluated using the statistical parameters.

CHAPTER 4

RESULTS AND DISCUSSION

This chapter discusses both on preliminary study of colour papers and real case study of Sala Mango including data analysis, graphs, and regression results. For real case study on Sala Mango, the analysis is separated into two different parts which the part part is on calibration and prediction models and second part is on direct calibration transfer technique. After results are presented, discussions on the analyzed data are elaborated and supported proof from literature review on the results obtained are also given.

4.1 White Diffuse Reflectance

Since the main objective of this research work is to explore influence of LED CCT on spectroscopic measurement of Sala Mango, it is important to first understand the spectral data of LED itself before interaction with sample to obtain reflectance data. White LEDs used in the study are of combination of blue light and phosphor. However, there are differences in proportion which produce white LEDs with different CCT. Figure 4.1(a) shows the intensity spectrum of halogen lamp and Figure 4.1(b) is the spectra of white diffuse reflectance under illumination of three different LEDs with halogen lamp as reference light source. As shown in Figure 4.1(b), there is slight shift in peaks between the LEDs. The high peaks at blue region (400-480 nm) for D35 is at 445 nm, 446 nm for D45 and 440nm for D57 while slight curves at the range of 500-700 nm indicating the component for yellow phosphor of white LED. Increasing reflectance for D35 spectra to D57 explains very much influence of the luminous intensity and flux of the LEDs under the same current applied. It is notable that the differences in blue peaks are quite large between the

LEDs due to the CCT. The spectra from 500nm onwards for D35 and D45 are very near to each other with D45 spectrum appears slightly higher than D35. For D57 spectrum, it has a small peak at 530 nm before intersects with the other LEDs spectra at around 595 nm. The intersection signifies the three white LEDs having the similar reflectance and least difference in intensity.

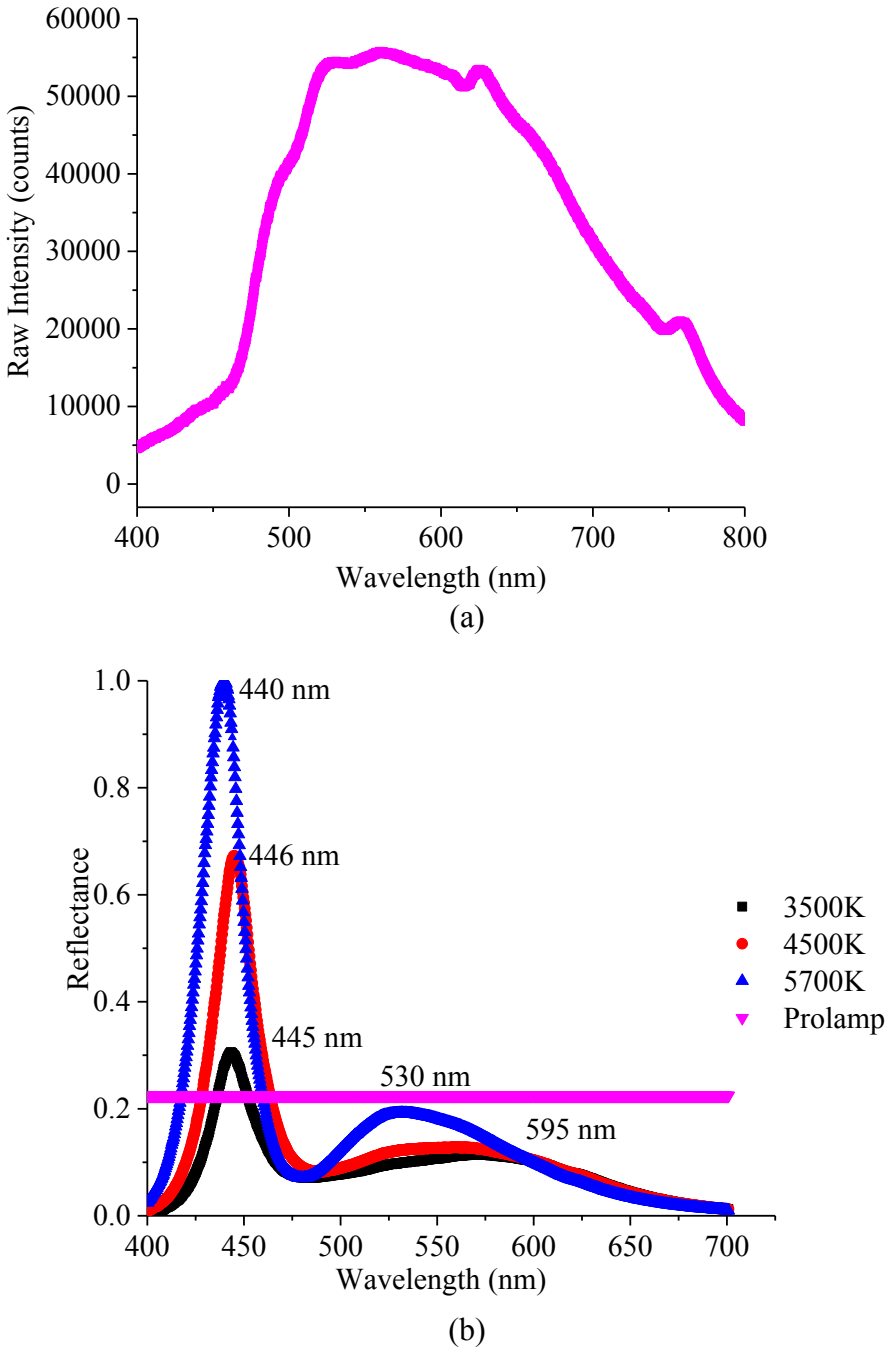

Figure 4.1 Spectra information showing (a) intensity of halogen lamp and (b) reflectance of 3 LEDs with halogen lamp as reference light source

4.2 Influence of LED CCT in Visible Spectroscopic Observation of RGB Sample

As mentioned in Chapter 3, for analysis of spectra from colour papers, gradient of the graph of reflectance against colour series for selected wavelengths was used. Figure 4.2, 4.3, and 4.4 show the relationships between spectral gradient and wavelengths for red, blue and green series of glossy and non-glossy surfaces. Both type of surfaces basically have the same trend but differ in gradient values. For red series, D35 has the highest spectral gradient followed by D45 and lastly D57.

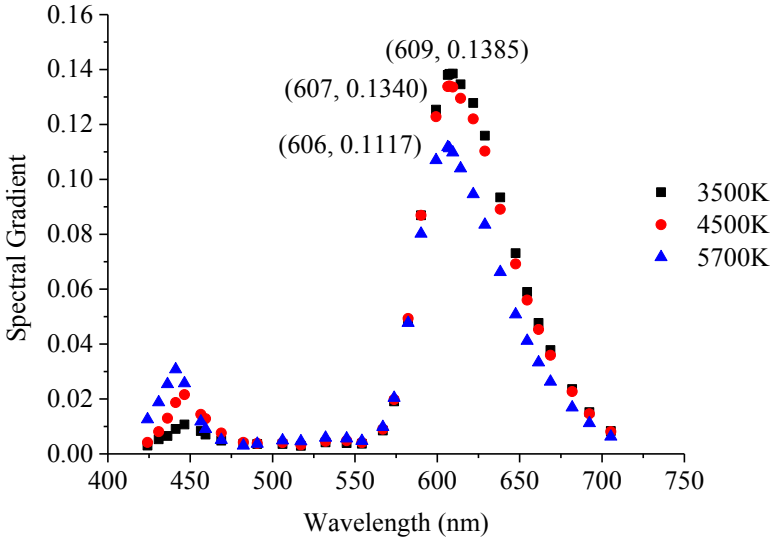

(a)

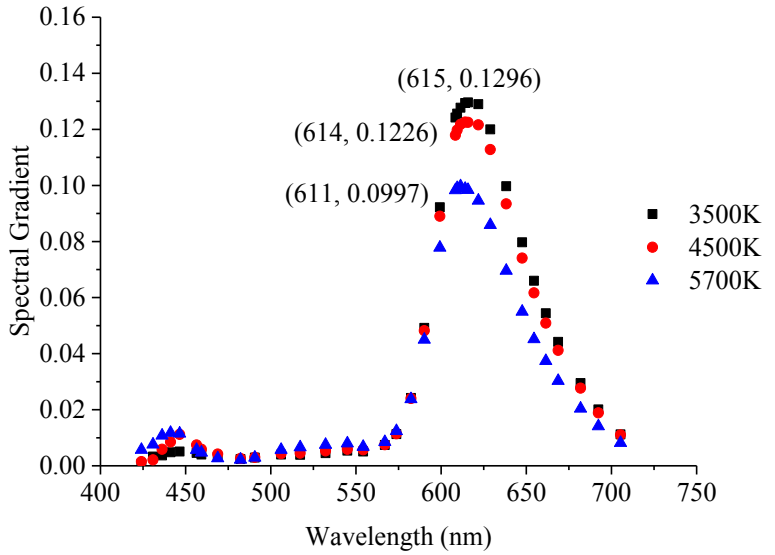

(b)

Figure 4.2 Spectral gradient of red colour series for (a) glossy and (b) non-glossy surfaces with peak wavelength in bracket

The result obtained does not match with spectra of white diffuse reflectance (Figure 4.1(b)). Therefore, it can be deduced that LED with lower CCT which looks warmer has improved the observation of red colour compared to cool white LED which in this case is D57. D35 has a little higher reflectance compared to D45 and D57 with the lowest reflectance at wavelengths after the intersection point. Different surfaces produce peaks at different wavelengths but in similar decreasing trend for increasing CCT. For glossy surfaces, the peak wavelengths for the increasing CCT of LEDs are of 609 nm, 607 nm and 606 nm while the peak wavelengths for non-glossy surfaces are 615 nm, 614 nm and 611 nm. Spectrometer is indeed a powerful tool which is able to detect small difference of the peak wavelengths. The difference of peak wavelength between one LED to another is small (±3 nm) and hence, different CCT of LED does not really affect the appearance of the colour. However, the differences in peak wavelengths of the surfaces indicate that type of object's surface does affect shifting of peak wavelength under spectroscopic view. As for the small peaks at the blue region, it is noteworthy that the peaks for non-glossy surface are less significant as compared to the glossy ones which matches with common observation that glossy surface should have higher reflectance compared to non-glossy surface.

For green colour series, Figure 4.3 shows the spectral gradient plotted for both glossy and non-glossy surfaces. The green spectra demonstrate maximal gradient at wavelengths of 537 nm (glossy) and 539 nm (non-glossy) for D35, 535 nm (glossy) and 537 nm (non-glossy) for D45 and 531 nm (glossy) and 533 nm (non-glossy) for D57. By referring to Figure 4.3, the spectra at around 530nm also have the same trends as in Figure 4.1 where D57 has leading reflectance and D45 has slightly higher reflectance as compared to D35. For region of 400-470 nm, the small

peaks for both surfaces have similar trend and the difference in spectral gradient is not as significant as in for the red colour series. This indicates the type of surfaces for green colour series does not affect the blue component of white LED.

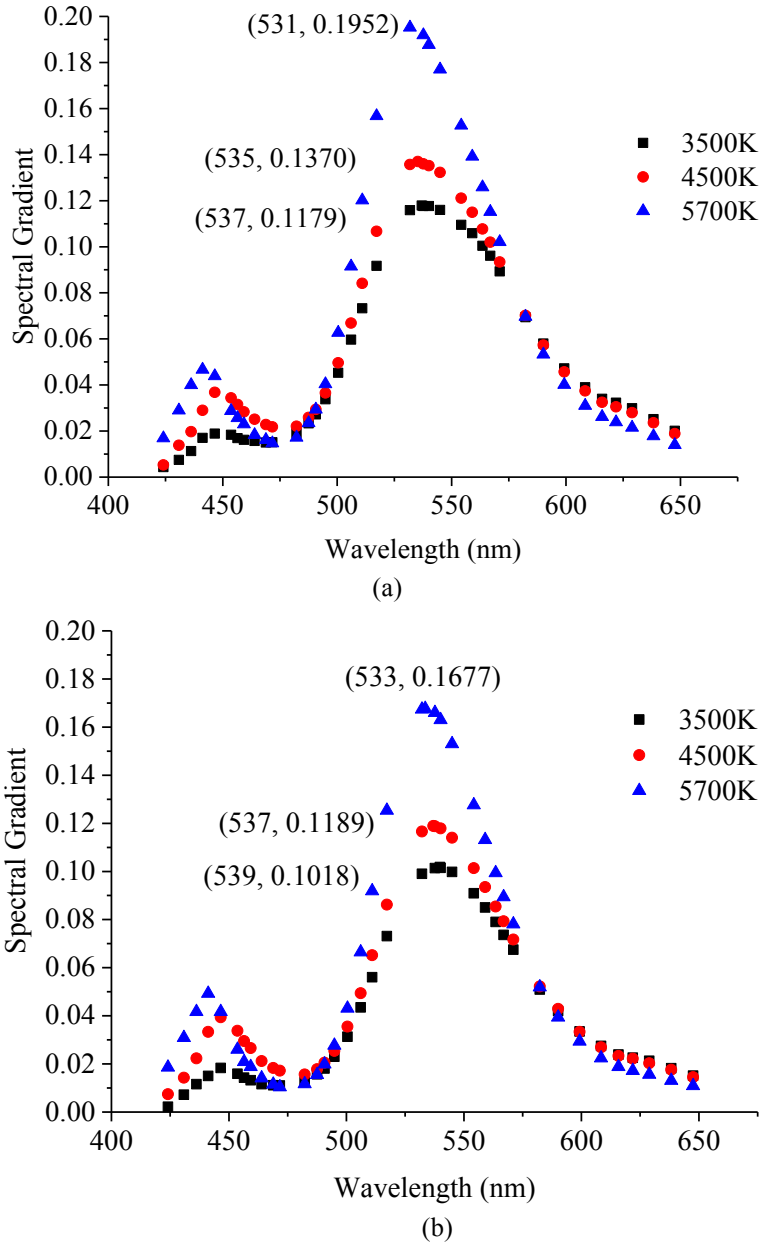

Figure 4.3 Spectral gradients of green colour series for (a) glossy and (b) non-glossy surfaces with peak wavelength in bracket

Next, observation for blue colour series is discussed instead. The peak wavelengths of white diffuse standard reflectance are 445 nm, 446 nm, and 440 nm

in increasing CCTs. D57 has peak at the smallest wavelength followed by D35 and D45 in decreasing order.

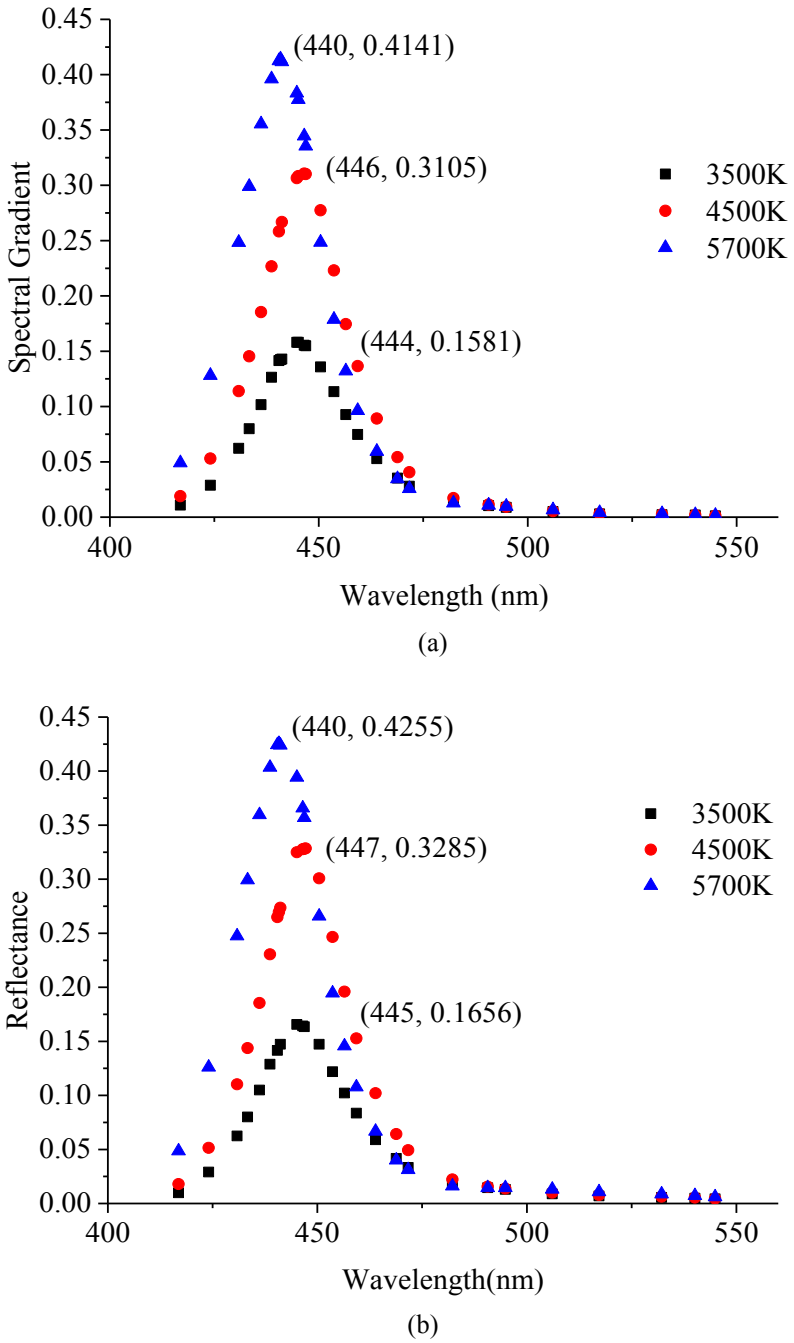

Figure 4.4 Spectral gradient of blue colour series for (a) glossy and (b) non-glossy surfaces with peak wavelength in bracket

For glossy surfaces, the peaks wavelengths are 444 nm, 446 nm and 440 nm in increasing CCTs while in non-glossy case, the peak wavelength for D35 is 445

nm, 447 nm for D45 and 440 nm for D57 respectively. The results are not in an observable trend as in for red and green series. The influence from blue light of the white LED itself has contributes to the inconsistency of the peak wavelengths of blue colour series.

Table 4.1 summarizes the results from preliminary study for colour papers. From the results, it can be shown that the peak wavelength for blue and green colour series only differ a little from halogen lamp and therefore it can be deduced that colour correlated temperature of LED does not affect much the position of peak wavelength for these two colour series. In contrast, red colour series has huge peak differences with halogen lamp at 631 nm (non-glossy) and 627 nm (glossy) while LEDs peak wavelengths range from 611 to 615 nm (non-glossy) and 606 to 609 nm (glossy). This observation suggests sample colour should be taken into consideration while doing measurement using spectroscopy.

Table 4.1 Summary of Preliminary Study of Colour Papers

Colour Series	Light source	Observation				
		Peak Wavelength (nm)		Spectral Gradient		
		Glossy	Non-Glossy	Glossy	Non-Glossy	*Difference
White Diffuse	D35	445		-		
	D45	446				
	D57	440				
Blue	D35	444	445	0.1581	0.1656	-0.0075
	D45	446	447	0.3105	0.3285	-0.0180
	D57	440	440	0.4141	0.4255	-0.0114
	Halogen lamp	444	448	0.1116	0.1113	
Green	D35	537	539	0.1179	0.1018	0.0161
	D45	535	537	0.1370	0.1189	0.0181
	D57	531	533	0.1952	0.1677	0.0275
	Halogen lamp	531	534	0.2714	0.2344	
Red	D35	609	615	0.1385	0.1296	0.0089
	D45	607	614	0.1340	0.1226	0.0114
	D57	606	611	0.1117	0.0997	0.0120
	Halogen lamp	627	631	0.3702	0.3823	

**Difference=Glossy-Non-Glossy Values*

On the other hand, spectral gradient gives more significant result compared to peak wavelength. The increasing or decreasing values of spectral gradient with increasing CCT gives result whether the colour observation has been improved or vice versa. Blue and green series have increasing spectral gradient with increasing CCT indicating better responsivity at higher LED CCT but red series is proved to have higher responsivity using lower CCT LED. Besides, the difference between spectral gradient values of glossy and non-glossy surfaces give an odd observation for blue series as negative result is obtained. Glossy surface is expected to give higher reflectance and indirectly contributes to higher spectral gradient and positive difference value. Blue series which its wavelength band is located between 400 and 470 nm is obviously affected by the blue radiation from white LED contributing to the odd result obtained. Therefore, it is recommended that blue colour object is not measured under this type of white LED lighting. However, further studies are required to confirm the fact.

4.3 VIS Spectroscopic Measurement of Sala Mango Intrinsic Properties under Different Lightings

The main focus of this research is to investigate the effect of white LED CCT on spectroscopy measurement and at the same time correlating it with the intrinsic qualities of sample which is Sala Mango. The result from Section 4.2 has proven successfully that different light sources would affect the spectroscopic view of RGB samples. LED CCT does shift the peak wavelength of object though in insignificant way and the spectral gradient would change order with increasing CCT depending on the colour of the object. Therefore, in the next section, correlation between LED CCT with intrinsic parameters of Sala Mango is investigated instead.

4.3.1 VIS Spectroscopic Analysis of Sala Mango

A detailed analysis on different groups of sample is done to discover possibility of different observations. Mango is a climacteric fruit such that it continues to ripen after harvesting with colour change (green to yellow) observable on the fruit skin (Zhang *et al.*, 2014). As the fruits starts to ripen, other external parameters such as size, firmness and texture change as well apart from skin colour transition. Internal changes involve change in absorbing pigments in mango such as chlorophylls, carotenoid and anthocyanin pigments. These pigments would usually be indicated by peaks and valleys in reflectance spectra.

Reflectance spectra for different groups of mango sample under D35, D45, D57 and halogen lamp illuminations are shown as in Figure 4.5, 4.6 and 4.7. For mango samples in Group 1 to 3, the spectra are similar to one another with only difference is increasing reflectance from Group 1 to 3. Generally, the reflectance spectra are observed to be in similar patterns with peaks in the (i) 420-470 nm, (ii) 540-580 nm range and a valley in the (iii) 650-690 nm range. The first peak range is due to the blue radiation emitted from white LEDs with highest intensity by D57 followed by D45 and lastly D35. The second peak is related to carotenoid pigment while the valleys indicate strong absorption which corresponds to the peak absorbance of chlorophyll-a (Zerbini *et al.*, 2015).

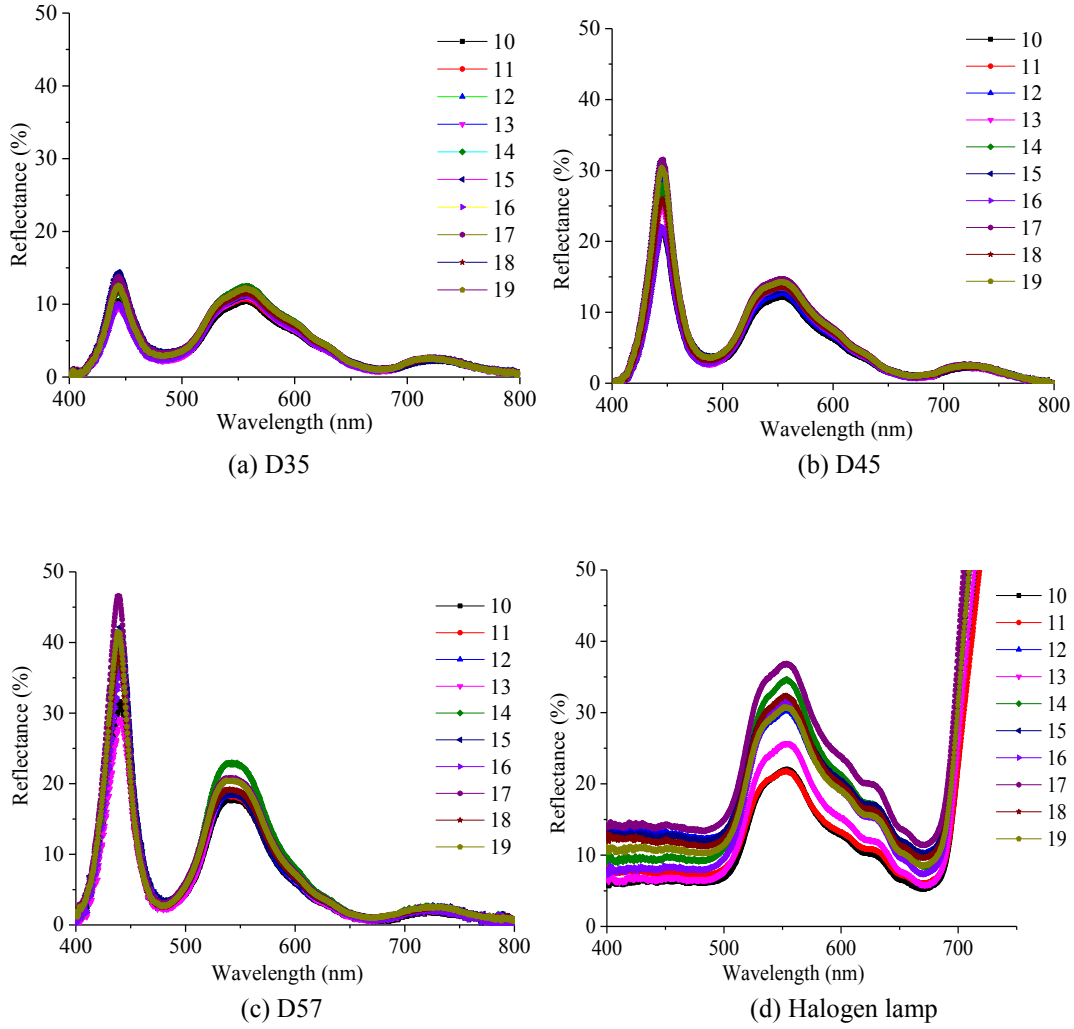

Figure 4.5 Reflectance spectra for Sala Mango Group 2 with sample coding from 10 to 19 under different light sources

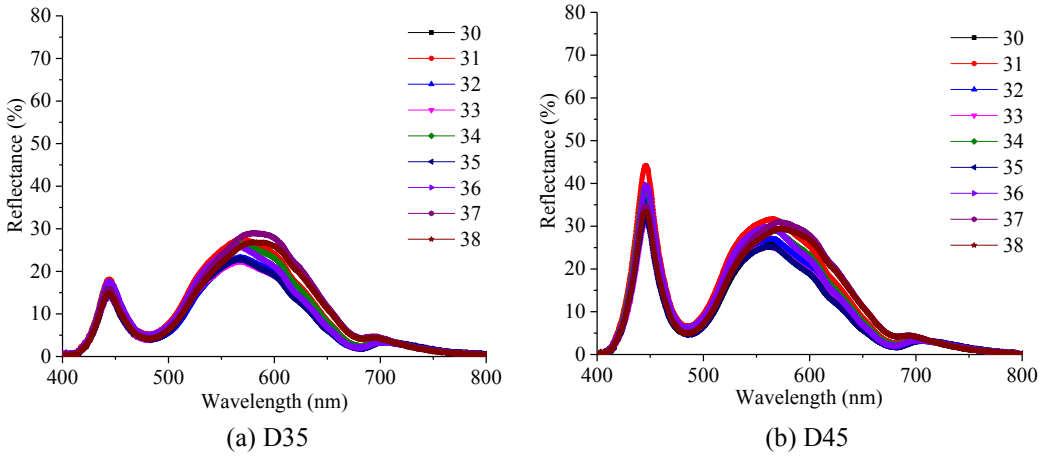

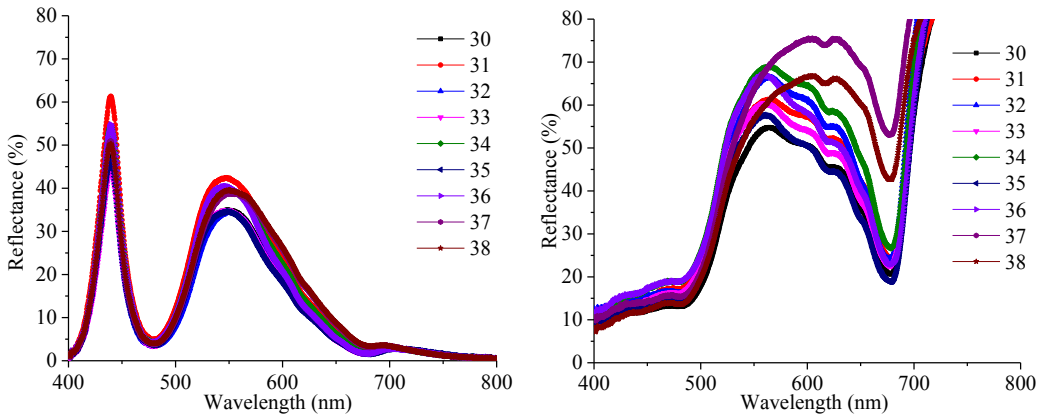

(c) D57 (d) Halogen lamp

Figure 4.6 Reflectance spectra for Sala Mango Group 4 with sample coding from 30 to 38 under different light sources

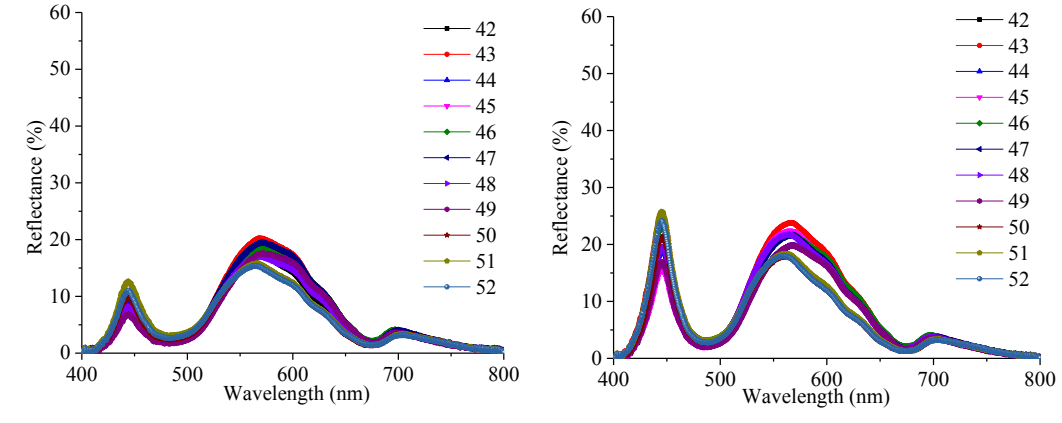

(a) D35 (b) D45

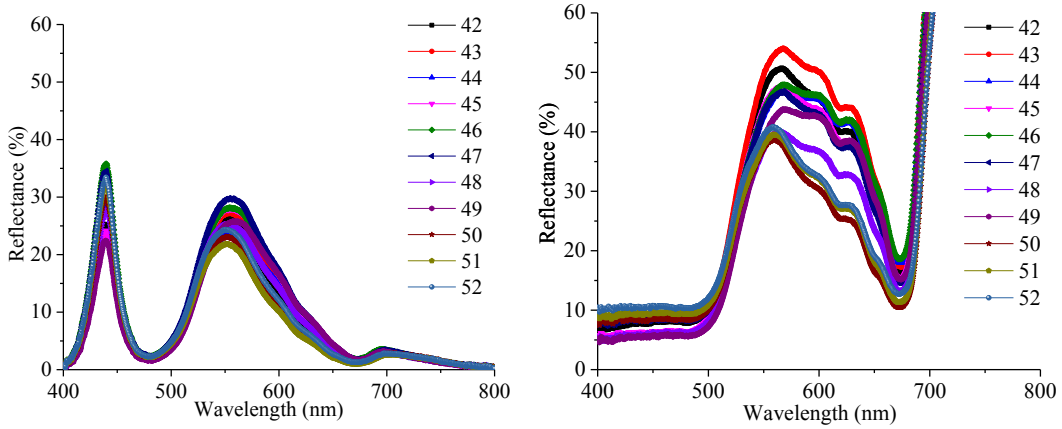

(c) D57 (d) Halogen lamp

Figure 4.7 Reflectance spectra for Sala Mango Group 5 with sample coding from 42 to 52 under different light sources

The spectral shapes clearly show that reflectance spectra can be used as indicators to estimate chlorophyll content in fruit ripening. The peaks and valleys in the spectra indicates dominancy of blueness in green colour and deficiency of red colour in mango respectively (Jha *et al.*, 2006). The raw reflectance spectra of mangoes studies by Jha *et al.* (2012) and Yahaya *et al.* (2015) also showed the similar pattern. According to Wanitchang *et al.* (2011), reflectance is found to increase as the fruit is more mature in the 600-700 nm range. However, from all the previous spectra, only halogen lamp spectra show the significant differences in reflectance compared to LEDs spectra. Compositions from white LED have influenced the reflectance spectra and this might be a drawback if maturity of mango fruits is to be assessed. Moreover, spectra from halogen lamp seem to have more specific curve than LEDs' which can be shown from small valleys around 600-640 nm. The valleys are the evidence of chlorophyll-b absorption in mango fruit (Spinelli *et al.*, 2013). Although not as weighty as carotenoid and chlorophyll-a pigments in mango, halogen lamp spectra are the only ones which are able to show the valleys in all different groups of samples. This may be an advantage for halogen lamp as lighting in spectroscopy measurement as the spectra obtained are clearer, more transparent and visible indicating more information can be extracted.

4.3.2 Calibration Models for pH and SSC

Multivariate analysis is performed to find quantitative relationship between reflectance spectra and internal qualities of mango. Different wavelengths in the visible range are selected to develop calibration models for predicting SSC and pH of mango using Multiple Linear Regression (MLR). Visible range is split to its three most dominant regions of red, green and blue. Models 1 to 3 are models developed

using wavelengths from only one region (blue (λ_B) , green (λ_G) or red(λ_R)) while Models 4 to 6, developed from combination of two regions (blue-green ((λ_{B+G}), red-green((λ_{R+G}), or red-blue (λ_{R+B})) and the rest are from the three regions (λ_{B+G+B}). The algorithms are compared in terms of coefficients of determination (R^2) of calibration and prediction, root mean square error of calibration (RMSEC) and prediction (RMSEP). The best model is chosen based on highest R^2 with lowest RMSEC and RMSEP as well as small difference between RMSEC and RMSEP.

4.3.2(a) Acidity

Table 4.2 shows results for different wavelength selections in obtaining acidity calibration models for the four light sources. The spectral range considered for this work is in visible range as colour is only perceived in this special region. The acidity values for samples ranged from 2.75 to 5.24 pH.

i. D35

Table 4.2 shows results for MLR analysis of acidity measurement of Sala Mango under D35 illumination. The best predictive model is shown in highlight. Wavelengths used in an algorithm indeed are important as variations of R^2 obtained are wide from 0.1657 to 0.9341.

For Models 1 to 3, only wavelengths from red, blue or green region are used respectively. 5 wavelengths used from solely green or red region still able to produce satisfactory results with R^2 of 0.8479 and 0.8416. In contrast, wavelengths used from only blue region produced very poor result with R^2 of 0.1657. These results show that blue wavelengths in an algorithm are not sufficient to predict the acidity of mango samples as blue region only contains information from blue radiation of LED.

Table 4.2 Calibration and prediction results of Sala Mango acidity through reflectance measurement under D35 lighting

Model	Grouping	Wavelength(nm)	Calibration		Prediction	
			R^2	RMSEC (pH)	R^2	RMSEP (pH)
1	λ_B	400,410,420,430,440	0.1657	0.7783	0.0560	0.7940
2	λ_G	510,520,530,540,550	0.8479	0.3323	0.8621	0.3035
3	λ_R	600,625,650,670,700	0.8416	0.3391	0.8764	0.2873
4	λ_{B+G}	420,450,480,520,550	0.8630	0.3154	0.8557	0.3105
5	λ_{G+R}	520,540,580, 620, 670	0.8661	0.3118	0.8435	0.3233
6	λ_{B+R}	420,450,480, 620,670	0.8502	0.3298	0.8489	0.3185
7	λ_{B+G+R}	420,470,550,615,675	0.7887	0.3917	0.7768	0.3861
8		450,520,580,615,650	0.8866	0.2869	0.8987	0.2601
9		455,520,550,675,700	0.8971	0.2733	0.9189	0.2328
10		470,520,570,675,700	0.9030	0.2654	0.9227	0.2271
11		430,520,540,690,700	0.9117	0.2532	0.9192	0.2323
12		430,520,640,690,700	0.9341	0.2187	0.8939	0.2662

When two regions of wavelengths are used in algorithms (Models 4 to 6), the results are almost similar but a slight lower for algorithm developed from blue and red regions. This observation due to deficiency in green region wavelengths is justifiable as the region contains information about skin colour of the mangoes. For the rest of the models, results show R^2 are all higher and therefore wavelengths from three regions (red, green and blue) should be covered in acidity prediction algorithm of Sala Mango. Despite having the highest R^2 and lowest RMSEC, prediction R^2 of Model 12 drops around 4% from 0.9341 to 0.8934 which might due to latent variables in the model. Therefore, the best algorithm for D35 as lighting is found to be Model 10 as highlighted in Table 4.2 which has smaller difference in R^2 of calibration and prediction with increment by 2%. Figure 4.8 presents the scatter plot for this predictive model.

Calibration:

$$pH = 2.332 + 0.370\ R_{470} - 0.4052\ R_{520} + 0.1327\ R_{570} - 0.4382\ R_{675} + 0.769\ R_{700} \quad (4.1)$$

$R^2 = 0.9030$; RMSEC=0.2654 pH

Prediction:

$R^2 = 0.9227$; RMSEP= 0.2271 pH

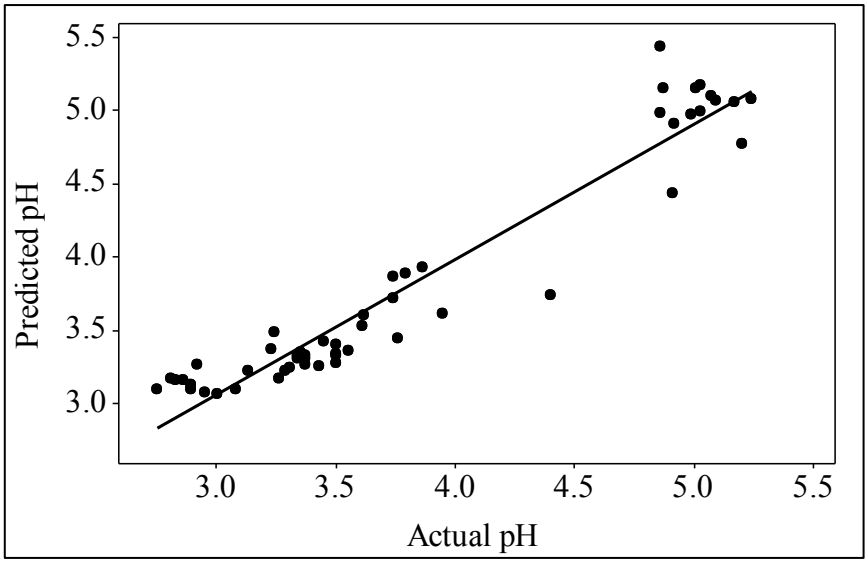

Figure 4.8 Scatter plots of mango acidity prediction using D35 as light source

ii. D45

Table 4.3 shows the model performance of generated algorithm under D45 lighting illumination on acidity measurement of Sala Mango. The best predictive model is shown in highlight.

Table 4.3 Calibration and prediction results of Sala Mango acidity through reflectance measurement under D45 lighting

Model	Grouping	Wavelength(nm)	Calibration		Prediction	
			R^2	RMSEC (pH)	R^2	RMSEP (pH)
1	λ_B	400,410,420,430,440	0.6293	0.5188	0.2933	0.6870
2	λ_G	510,520,530,540,550	0.8461	0.3343	0.8265	0.3404
3	λ_R	600,625,650,670,700	0.8674	0.3103	0.8384	0.3286
4	λ_{B+G}	420,450,480,520,550	0.8652	0.3128	0.8725	0.2919
5	λ_{G+R}	520,540,580, 620, 670	0.8634	0.3149	0.8615	0.3041
6	λ_{B+R}	420,450,480, 620,670	0.7752	0.4039	0.7885	0.3769
7	λ_{B+G+R}	420,470,550,615,675	0.7795	0.4001	0.7511	0.4078
8		450,520,580,615,650	0.8807	0.2943	0.9004	0.2579
9		455,520,550,675,700	0.8942	0.2772	0.9241	0.2251
10		470,520,570,675,700	0.9121	0.2526	0.9308	0.2150
11		430,520,540,690,700	0.8952	0.2758	0.9126	0.2417
12		410,560,570,690,700	0.9310	0.2238	0.9034	0.2540

For Models 1 to 3 (single region wavelengths), wavelengths from blue region give surprisingly good calibration R^2 (0.6293) compared to D35 result (0.1657). But still, the predicted R^2 gives a poor result of 0.2933 which rejects this model for

acidity prediction of mango samples. For Models 2 and 3, similar results obtained as compared to D35 with red wavelengths having slightly higher R^2 and lower RMSEC and RMSEP. For algorithms generated using two regions wavelengths (Models 4 to 6), Model 6 only possesses R^2 of 0.7752 while Models 4 and 5 with quite satisfactory results of 0.8652 and 0.8634 suggesting the significance of green region wavelengths in correlating reflectance spectra of mango and acidity measurement. Algorithms involving wavelengths from the three regions found to give better results as in D35 case. The best predictive model is given by Model 10 (as highlighted) which has lower R^2 and bigger RMSEC compared to Model 12 but has better R^2 of prediction and lower RMSEP. The algorithm and scatter plot for this model are shown in Equation (4.2) and Figure (4.9) respectively.

Calibration:

$$pH = 2.359 + 0.2650\, R_{470} - 0.3363\, R_{520} + 0.1223\, R_{570} - 0.4634\, R_{675} + 0.749\, R_{700} \quad (4.2)$$

$R^2 = 0.9121$; RMSEC=0.2526 pH

Prediction:

$R^2 = 0.9308$; RMSEP= 0.2150 pH

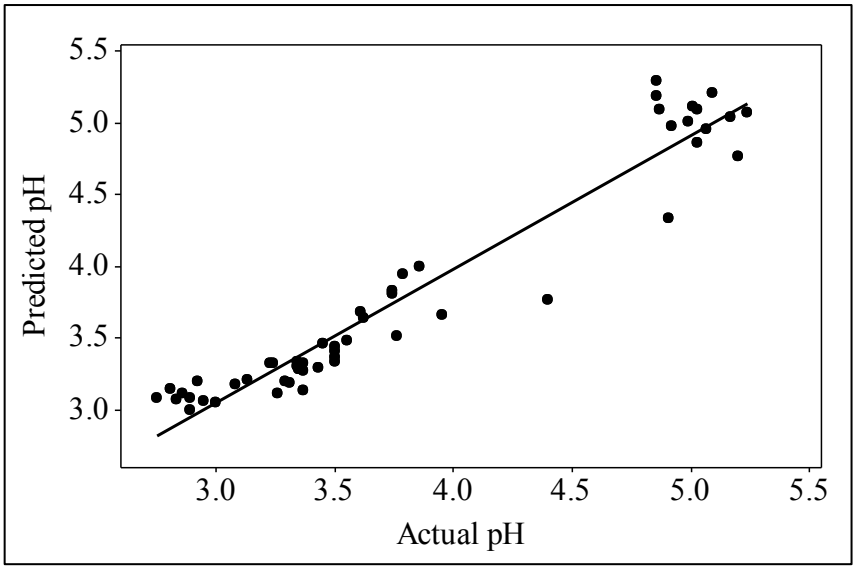

Figure 4.9 Scatter plots of mango acidity prediction using D45 as light source

iii. D57

Table 4.4 shows the model performance for prediction of acidity using D57 as lighting in reflectance measurement of Sala Mango. The best predictive model is shown in highlight.

Table 4.4 Calibration and prediction results of Sala Mango acidity through reflectance measurement under D57 lighting

Model	Grouping	Wavelength(nm)	Calibration		Prediction	
			R^2	RMSEC (pH)	R^2	RMSEP (pH)
1	λ_B	400,410,420,430,440	0.1826	0.7703	0.2212	0.7212
2	λ_G	510,520,530,540,550	0.8537	0.3259	0.8524	0.3140
3	λ_R	600,625,650,670,700	0.8203	0.3612	0.8467	0.3200
4	λ_{B+G}	420,450,480,520,550	0.8564	0.3229	0.8586	0.3073
5	λ_{G+R}	520,540,580, 620, 670	0.8798	0.2954	0.8636	0.3019
6	λ_{B+R}	420,450,480, 620,670	0.8241	0.3574	0.8795	0.2845
7	λ_{B+G+R}	420,470,550,615,675	0.7565	0.4204	0.7959	0.4120
8		450,520,580,615,650	0.8824	0.2922	0.9041	0.2531
9		455,520,550,675,700	0.8938	0.2777	0.9100	0.2452
10		470,520,570,675,700	0.8979	0.2722	0.9145	0.2390
11		430,520,540,690,700	0.8712	0.3058	0.8681	0.2968
12		455,540,550,690,700	0.9194	0.2418	0.8956	0.2641

D57 which has the highest blue radiation among the LEDs indeed has slight different observations compared to D35 and D45. For algorithms generated from single region wavelengths, the similar result is that lowest R^2 is still the one produced by using only blue wavelengths. However, in contrast to D35 and D45 where red region wavelengths produced better R^2 than green region wavelengths, D57 produces higher R^2 for green region wavelengths instead. It can be deduced that as the blue radiation of LED increases, red wavelengths are needed to balance up the extra blue spectra from LED in algorithm as blue and red components. For combination of three region wavelengths, the R^2 obtained are observed to be lower than D35 and D45. The highest R^2 of calibration is 0.9194 while D35 and D45 are able to generate R^2 of 0.9341 and 0.9310 respectively. R^2 of prediction of 0.9145 is also lower compared to 0.9227 for D35 and 0.9308 for D45. The differences might

deduce that acidity prediction of Sala Mango is the best using lower CCT of LED. Thus, the best model for prediction of pH for D57 lighting is Model 10 and the predictive model is plotted in scatter plot as shown in Figure 4.10.

Calibration:

$$pH = 2.532 + 0.388R_{470} - 0.233R_{520} + 0.144R_{570} - 0.712R_{675} + 0.712R_{700} \quad (4.3)$$

$R^2 = 0.8979$; RMSEC=0.2722 pH

Prediction:

$R^2 = 0.9145$; RMSEP= 0.2390 pH

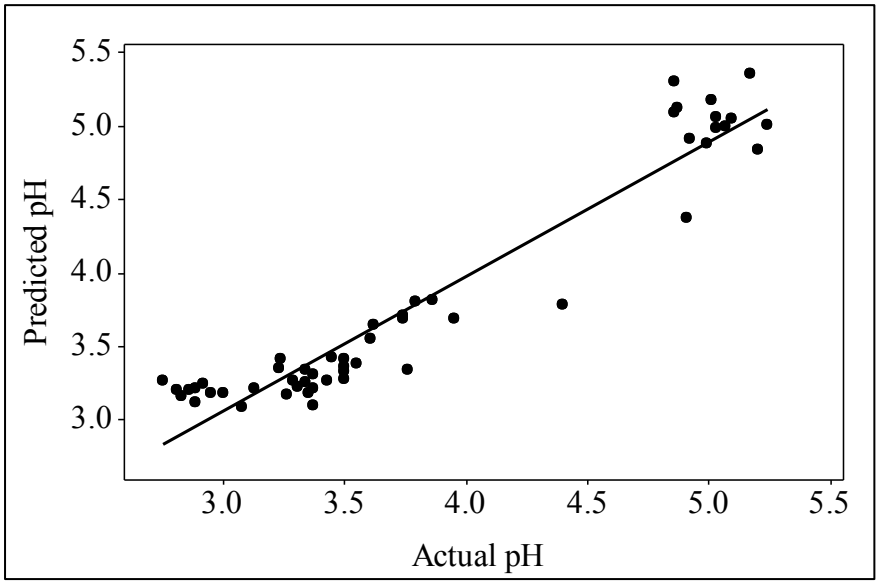

Figure 4.10 Scatter plots of mango acidity prediction using D57 as light source

iv. Halogen Lamp

Halogen lamp acts as the reference lighting and is the only light source without significant blue radiation affecting reflectance spectra of mango sample as the LEDs. Hence, the spectra obtained using halogen lamp lighting are truly from spectra of mango samples without influence of the lighting spectrum. Table 4.5 shows the results for acidity measurement of Sala Mango under halogen lamp. The best predictive model is shown in highlight.

Table 4.5 Calibration and prediction results of Sala Mango acidity through reflectance measurement under halogen lamp lighting

Model	Grouping	Wavelength(nm)	Calibration		Prediction	
			R^2	RMSEC (pH)	R^2	RMSEP (pH)
1	λ_B	400,410,420,430,440	0.0652	0.8238	0.0865	0.7811
2	λ_G	510,520,530,540,550	0.8527	0.3270	0.8577	0.3083
3	λ_R	600,625,650,670,700	0.8506	0.3294	0.8589	0.3070
4	λ_{B+G}	420,450,480,520,550	0.8468	0.3335	0.8539	0.3124
5	λ_{G+R}	520,540,580, 620, 670	0.8566	0.3227	0.8542	0.3120
6	λ_{B+R}	420,450,480, 620,670	0.8296	0.3517	0.8668	0.2991
7	λ_{B+G+R}	420,470,550,615,675	0.8276	0.3538	0.8715	0.2929
8		450,520,580,615,650	0.8751	0.3012	0.8952	0.2646
9		455,520,550,675,700	0.8833	0.2911	0.8943	0.2658
10		470,520,570,675,700	0.8995	0.2702	0.9114	0.2432
11		430,520,540,690,700	0.8828	0.2917	0.8794	0.2838
12		430,520,640,690,700	0.9310	0.2238	0.9034	0.2540

From Table 4.5, for models developed using single region wavelengths (Models 1 to 3), the algorithm generated solely using blue wavelengths seem to give poorest result (R^2 of 0.0652 and RMSEC of 0.8238 pH). Green and red region wavelengths are able to produce satisfactory correlations with acidity with R^2 of 0.8527 and 0.8506 respectively. For Models 4 to 6, the results are the same as D35 and D45 whereby combination of blue and red wavelengths gives the lowest R^2 but the differences are not as huge as D45. For the rest of the models, the results are also better when three regions wavelengths are used to produce predictive models in acidity measurement of mango. The best model chosen is plotted as shown in Figure 4.11.

Calibration:

$$pH = 2.501 + 0.124\, R_{470} - 0.128 R_{520} + 0.044\, R_{570} - 0.044 R_{675} + 0.045\, R_{700} \quad (4.4)$$

$R^2 = 0.8995$; RMSEC=0.2702 pH

Prediction:

$R^2 = 0.9114$; RMSEP= 0.2432 pH

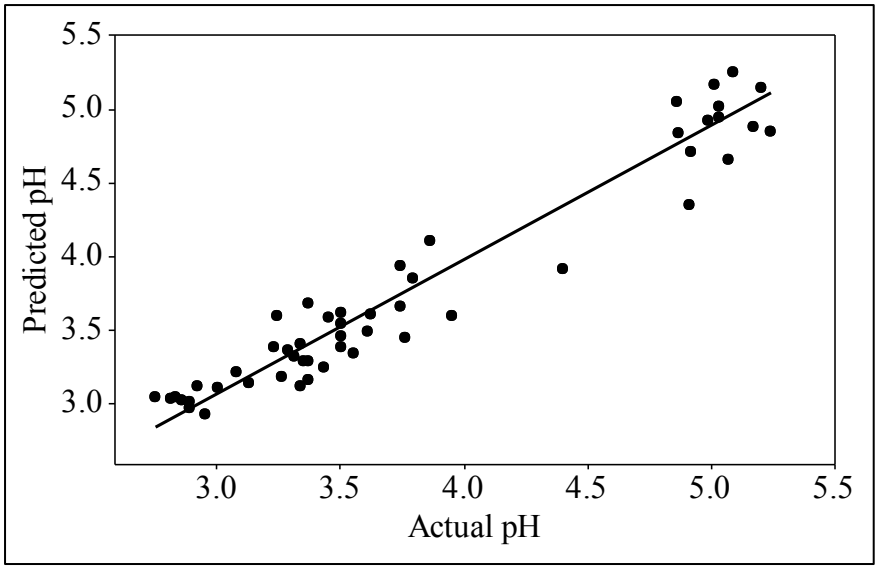

Figure 4.11 Scatter plots of mango acidity prediction using halogen lamp as light source

4.3.2(b) Soluble Solids Content

The following are the results of Soluble Solids Content (SSC) calibration and prediction of Sala Mango using reflectance spectroscopic measurement under D35, D45, D57 and halogen lamp illuminations. The SSC values in all samples ranged from 7.3 to 15.5^{o} Brix.

i. D35

Table 4.6 shows SSC spectroscopic measurement of Sala Mango under D35 lighting. The best predictive model is shown in highlight. From Table 4.6, it is shown that overall results of calibration between SSC and reflectance spectra (R^2<0.7) is poorer compared to acidity (R^2>0.8). This might due to the fact that SSC is better correlated in NIR region (1100-1250 nm) as reported by Cortés *et al.* (2016) or mango itself is better correlated to acidity instead of SSC. This might due to the fact that the range for SSC (7.3-15.5 ^{o}Brix) is wider compared to acidity (2.75

to 5.24 pH). Therefore, the latent variables are higher and affecting the results indirectly.

Table 4.6 Calibration and prediction results of Sala Mango SSC through reflectance measurement under D35 lighting

Model	Grouping	Wavelength(nm)	Calibration		Prediction	
			R^2	RMSEC (^{o}Brix)	R^2	RMSEP (^{o}Brix)
1	λ_B	400,410,420,430,440	0.1875	1.9011	0.0561	1.9655
2	λ_G	510,520,530,540,550	0.5795	1.3678	0.6593	1.1807
3	λ_R	600,625,650,670,700	0.5448	1.4231	0.5525	1.3533
4	λ_{B+G}	420,450,480,520,550	0.6199	1.3004	0.6935	1.1200
5	λ_{G+R}	520,540,580, 620, 670	0.5732	1.3779	0.5958	1.2862
6	λ_{B+R}	420,450,480, 620,670	0.5931	1.3454	0.7109	1.0877
7	λ_{B+G+R}	420,470,550,615,675	0.5901	1.3504	0.6220	1.2437
8		450,520,580,615,650	0.5876	1.3544	0.6500	1.1969
9		455,520,550,675,700	0.5909	1.3491	0.6627	1.1749
10		470,520,570,675,700	0.5899	1.3507	0.6670	1.1723
11		430,520,540,690,700	0.6361	1.2723	0.6903	1.1258
12		400,520,670,690,700	0.6830	1.1875	0.5932	1.2903

Munawar *et al.* (2013) also found acidity of mango to give better prediction results (R = 0.98) compared to SSC (R= 0.82) while Fu *et al.* (2009) which investigated on SSC and acidity of loquats showed SSC has better results than acidity. For Model 1 to 3, model developed from blue region wavelengths (Model 1) once again produces the lowest R^2 of 0.1875 and RMSEC of 1.9011^o Brix. Green wavelengths produce slightly better correlation than red wavelengths algorithm showing SSC is more related to the skin colour of mango. For two region wavelengths combination models (Model 4 to 6), the results varied significantly compared to acidity (Table 4.2). It was surprising to find that combination of green and red wavelengths (λ_{G+R}) give the lowest R^2 as compared to other two combinations. This observation suggests that blue wavelengths are important in correlating SSC properties of Sala Mango rather than the other two regions. For algorithms using combinations of three regions wavelengths, the results are observed to be slightly better than one and two regions algorithms. The best predictive model is given by scatter plot as shown in Figure 4.12.

Calibration:

SSC (^{o}Brix) =4.160+ 0.572R_{430}- 1.440R_{520}+ 0.846R_{540} - 1.786R_{690}+ 2.820R_{700} (4.5)

R^2= 0.6361; RMSEC=1.2723 ^{o}Brix

Prediction:

R^2= 0.6903; RMSEP= 1.1258 ^{o}Brix

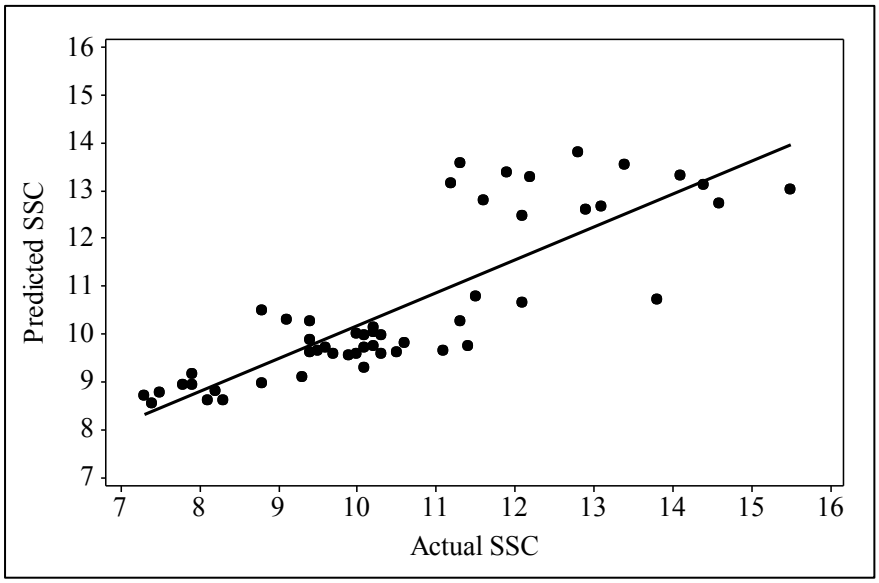

Figure 4.12 Scatter plots of mango SSC prediction using D35 as light source

ii. D45

Table 4.7 shows the results for D45 as lighting in SSC measurement of Sala mango using reflectance mode of Jaz spectrometer. The best predictive model is shown in highlight. From Table, for Model 1 to 3, it is found that green wavelengths (λ_G) give the best correlation as compared to blue (λ_B) and red (λ_R) wavelengths with R^2 of 0.5787 and RMSEC of 1.3690 ^{o}Brix while prediction R^2 of 0.6355 and RMSEP of 1.2214 ^{o}Brix. This result matches well with the result obtained from D35.

Table 4.7 Calibration and prediction results of Sala Mango SSC through reflectance measurement under D45 lighting

Model	Grouping	Wavelength(nm)	Calibration		Prediction	
			R^2	RMSEC (^{o}Brix)	R^2	RMSEP (^{o}Brix)
1	λ_B	400,410,420,430,440	0.4669	1.5400	0.2101	1.7979
2	λ_G	510,520,530,540,550	0.5787	1.3690	0.6355	1.2214
3	λ_R	600,625,650,670,700	0.5366	1.4358	0.5737	1.3209
4	λ_{B+G}	420,450,480,520,550	0.6418	1.2624	0.5910	1.2938
5	λ_{G+R}	520,540,580,620,670	0.5384	1.4330	0.5847	1.3038
6	λ_{B+R}	420,450,480,620,670	0.5178	1.4646	0.4771	1.4629
7	λ_{B+G+R}	420,470,550,615,675	0.4776	1.5244	0.6007	1.2783
8		450,520,580,615,650	0.5699	1.3832	0.6751	1.1530
9		455,520,550,675,700	0.5690	1.3847	0.6686	1.1646
10		470,520,570,675,700	0.5970	1.3390	0.6955	1.1210
11		430,520,540,690,700	0.5842	1.3600	0.6518	1.1938
12		480,520,650,690,700	0.6602	1.2295	0.6404	1.2132

For combination of two region wavelengths, Model 6 (λ_{B+R}) is observed to have the poorest result which is compatible with the previous result showing the importance of green wavelengths in correlation to SSC property of Sala Mango. Meanwhile, R^2 for Model 4 decreases from 0.6418 to 0.5910 with RMSEC of 1.2624 ^{o}Brix increases to RMSEP of 1.2938 ^{o}Brix showing the importance of red wavelengths in the SSC prediction algorithm of mango samples. For three-regions-combined-algorithms, all the predicted results seem to be higher showing the stability of the algorithms. The best predictive model is Model 10 which is chosen based on criteria explained earlier with high R^2 for calibration and prediction, low RMSEC and RMSEP with small difference between the two variables and is presented as scatter plot in Figure 4.13.

Calibration:

$$\text{SSC } (^o\text{Brix}) = 7.500 + 0.700R_{470} - 0.770R_{520} + 0.265R_{570} - 0.896R_{675} + 1.431R_{700} \quad (4.6)$$

$R^2 = 0.5970$; RMSEC=1.3390 ^{o}Brix

Prediction:

$R^2 = 0.6955$; RMSEP= 1.1210 ^{o}Brix

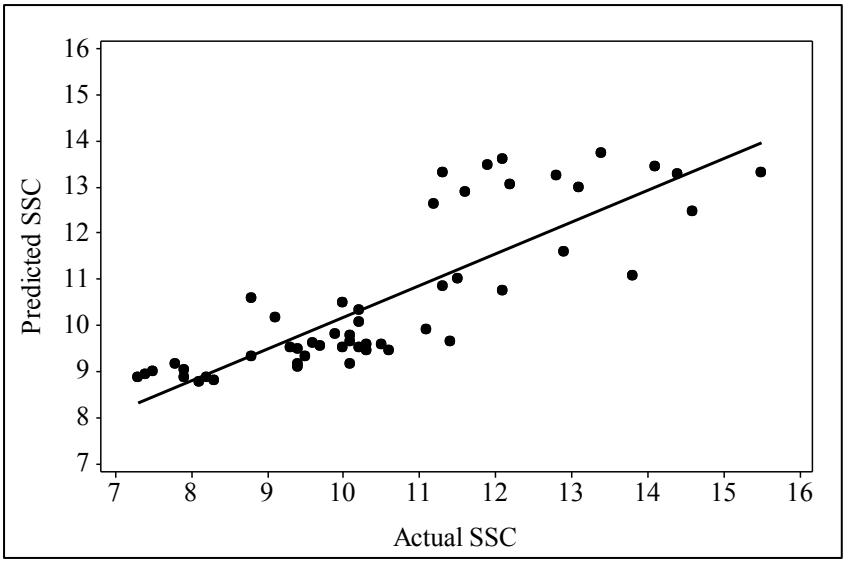

Figure 4.13 Scatter plots of mango SSC prediction using D45 as light source

iii. D57

Table 4.8 shows the results for different wavelength selections of algorithms produced using MLR technique using reflectance spectroscopic measurement under D57 lighting. The best predictive model is shown in highlight.

Table 4.8 Calibration and prediction results of Sala Mango SSC through reflectance measurement under D57 lighting

Model	Grouping	Wavelength(nm)	Calibration		Prediction	
			R^2	RMSEC (^{o}Brix)	R^2	RMSEP (^{o}Brix)
1	λ_B	400,410,420,430,440	0.1235	1.9746	0.1570	1.8574
2	λ_G	510,520,530,540,550	0.5598	1.3993	0.5949	1.2877
3	λ_R	600,625,650,670,700	0.5420	1.4274	0.5424	1.3685
4	λ_{B+G}	420,450,480,520,550	0.5587	1.4011	0.6346	1.2229
5	λ_{G+R}	520,540,580, 620, 670	0.5596	1.4000	0.5719	1.3236
6	λ_{B+R}	420,450,480, 620,670	0.5434	1.4252	0.6715	1.1595
7	λ_{B+G+R}	420,470,550,615,675	0.4871	1.5105	0.5136	1.4109
8		450,520,580,615,650	0.5860	1.3571	0.6424	1.2097
9		455,520,550,675,700	0.5957	1.3410	0.6322	1.2269
10		470,520,570,675,700	0.5951	1.3421	0.6159	1.2591
11		430,520,540,690,700	0.6127	1.3126	0.5845	1.3040
12		440,520,610,690,700	0.6849	1.1840	0.5348	1.3798

For models generated from single region wavelengths (Model 1 to 3), the highest R^2 still belongs to green wavelengths (Model 2) with R^2 calibration of 0.5598 increases to predicted R^2 of 0.5949 and RMSEC of 1.3993 ^{o}Brix decreases to RMSEP of

1.2877 ^{o}Brix. Red wavelengths produce satisfactory result while blue wavelengths solely produce inacceptable result just like as shown in D35 and D45 cases. For Models 4 to 6, the lowest R^2 is found to be combination of green and red wavelengths. This result shows the significance of blue wavelengths in algorithm correlated to mango SSC despite having poor result for single region wavelengths. On the other hand, absence of green wavelengths in contrast gives the best results with R^2 calibration of 0.5434 increases to R^2 prediction of 0.6715 while RMSEC of 1.4252 ^{o}Brix drops to RMSEP of 1.1595 ^{o}Brix. This observation can deduce that combination of wavelengths in visible region is indeed independent and cannot be accounted from just one view. Besides, for this lighting, three-region-combined-algorithms only produce slightly better results compared to D35 and D45. It is obvious that CCT of LED indeed does influence the correlation and prediction of mango intrinsic quality. The best predictive model is Model 8 and is presented as scatter plot in Figure 4.14.

Calibration:

$$\text{SSC } (^{o}\text{Brix}) = 7.89 + 0.1280R_{450} - 0.453R_{520} + 0.427R_{580} + 0.89R_{615} - 2.42R_{650} \quad (4.7)$$

R^2= 0.5860; RMSEC=1.3571 ^{o}Brix

Prediction:

R^2= 0.6424; RMSEP= 1.2097 ^{o}Brix

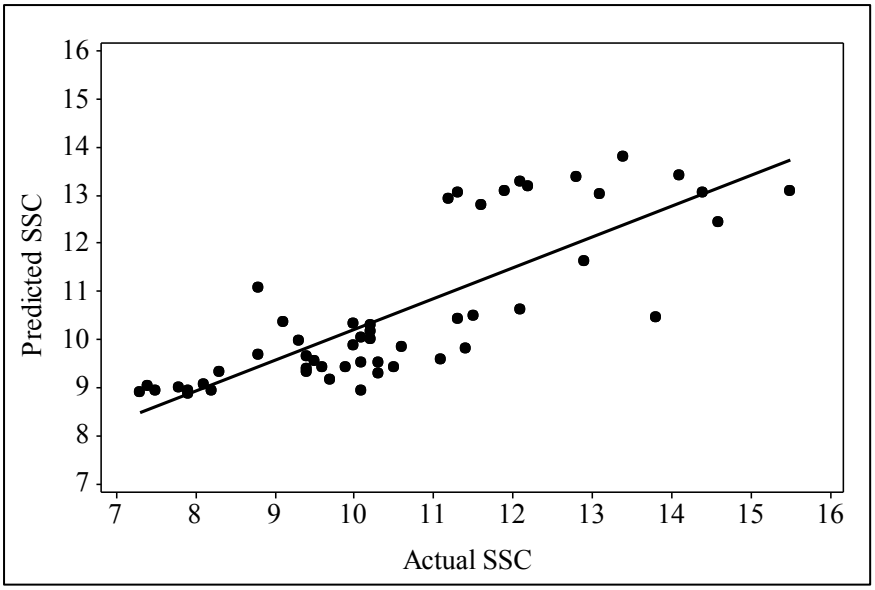

Figure 4.14 Scatter plots of mango SSC prediction using D57 as light source

iv. Halogen Lamp

Table 4.9 shows the results for different wavelength selections of algorithms produced using MLR technique using reflectance spectroscopic measurement under halogen lamp lighting. The best predictive model is shown in highlight. For halogen lamp, overall results are better with R^2 of some models reaching more 0.7 compared to LEDs results as shown in Table 4.6, Table 4.7 and Table 4.8.

Table 4.9 Calibration and prediction results of Sala Mango SSC through reflectance measurement under halogen lamp lighting

Model	Grouping	Wavelength(nm)	Calibration		Prediction	
			R^2	RMSEC (^{o}Brix)	R^2	RMSEP (^{o}Brix)
1	λ_B	400,410,420,430,440	0.1365	1.9600	0.0197	2.0030
2	λ_G	510,520,530,540,550	0.6134	1.3113	0.7129	1.0839
3	λ_R	600,625,650,670,700	0.5155	1.4681	0.6390	1.2156
4	λ_{B+G}	420,450,480,520,550	0.6064	1.3232	0.6789	1.1464
5	λ_{G+R}	520,540,580, 620, 670	0.5862	1.3568	0.5999	1.2797
6	λ_{B+R}	420,450,480, 620,670	0.5561	1.4052	0.6813	1.1421
7	λ_{B+G+R}	420,470,550,615,675	0.5397	1.4310	0.7181	1.0741
8		450,520,580,615,650	0.6051	1.3253	0.6963	1.1149
9		455,520,550,675,700	0.6087	1.3193	0.7085	1.0922
10		470,520,570,675,700	0.6059	1.3241	0.7276	1.0603
11		430,520,540,690,700	0.6204	1.2995	0.7018	1.1047
12		430,540,570,620,670	0.6280	1.2864	0.6188	1.2491

For single region algorithms (Models 1 to 3), the results also match with other LEDs such that green wavelengths used solely are best in predicting SSC of Sala Mango with R^2 of calibration of 0.6134 increases to 0.7129 and RMSEC of 1.3113 ^{o}Brix decreases to RMSEP of 1.0839 ^{o}Brix. On the other hand, for two-region-algorithms, the poorest result goes to combination of green and red wavelengths algorithm (Model 5) with matching results for LED cases except D45. Combinations for λ_{B+G} and λ_{B+R} give approximately similar prediction R^2 suggesting importance of blue wavelengths in an algorithm. For the rests of the model, better R^2 are also observed when three regions wavelengths are used to generate an algorithm. All the results are not much in differ but the best model is still chosen based on high R^2 of calibration and prediction and low RMSEC and RMSEP. The best predictive model is Model 10 and is presented as scatter plot in Figure 4.15.

Calibration:

$$SSC(^{o}Brix)=7.560+0.428R_{470}- 0.326R_{520} +0.104R_{570}- 0.087R_{675}+0.083R_{700} \quad (4.8)$$

R^2= 0.6059; RMSEC=1.3241 ^{o}Brix

Prediction:

R^2= 0.7276; RMSEP= 1.0603 ^{o}Brix

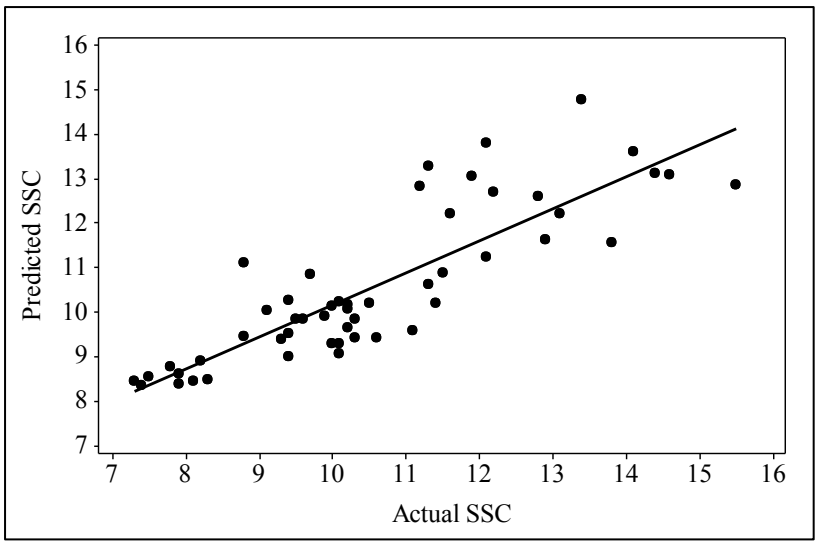

Figure 4.15 Scatter plots of mango SSC prediction using halogen lamp as light source

4.3.2(c) Summary

This study showed the capability of VIS spectroscopy to predict acidity and soluble solids content attributes of Sala Mango despite different light sources are used. Calibration and prediction models' performance of these attributes are accessed to observe influence of lighting on spectroscopic measurement using Jaz spectrometer. Table 4.10 shows the list of best predictive model for acidity measurement of Sala Mango.

Table 4.10 Summary of best predictive model for acidity prediction of Sala Mango

Light Source	Calibration Algorithm	Calibration		Prediction	
		R^2	RMSEC (^{0}Brix)	R^2	RMSEP (^{0}Brix)
D35	$pH = 2.332 + 0.370R_{470} - 0.405R_{520} + 0.133R_{570} - 0.438R_{675} + 0.769R_{700}$	0.9030	0.2654	0.9227	0.2271
D45	$pH = 2.359 + 0.265R_{470} - 0.336R_{520} + 0.122R_{570} - 0.463R_{675} + 0.749R_{700}$	0.9121	0.2526	0.9308	0.2150
D57	$pH = 2.532 + 0.388R_{470} - 0.233R_{520} + 0.144R_{570} - 0.712R_{675} + 0.712R_{700}$	0.8979	0.2722	0.9145	0.2390
Halogen lamp	$pH = 2.501 + 0.124R_{470} - 0.128R_{520} + 0.044R_{570} - 0.0440R_{675} + 0.045R_{700}$	0.8995	0.2702	0.9114	0.2432

From the Table, it was found that despite huge difference in reflectance spectra of Sala Mango between LEDs and halogen lamp, performance of calibration and prediction models for acidity measurement for LEDs are able to give comparable results with the halogen lamp's. Wavelength selection of the best predictive models for all light sources is the same (470,520,570,675,700 nm) proving LED spectra didn't alter spectroscopic acidity measurement of Sala Mango. Wavelengths chosen in this work also indicate prominent wavelengths that match with the colour attributes of mango fruit. Figure 4.16 gives an overview on the 12 model performances (Refer Table 4.2 - 4.5) of the four light sources plotted in bar graphs.

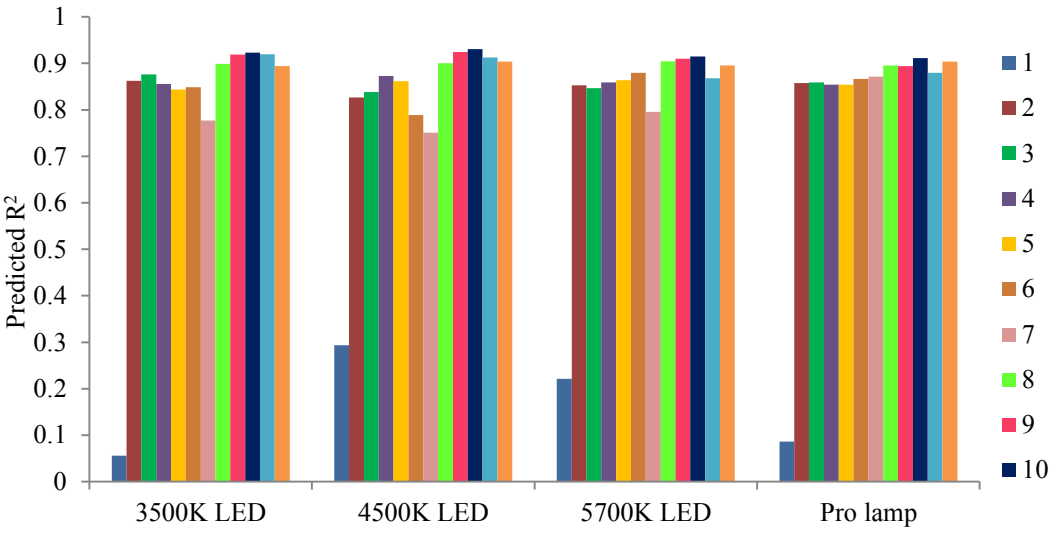

Figure 4.16 Overview graph of 12 model performances for acidity prediction of Sala Mango

It is observed that halogen lamp shows more stable performances compared to LEDs indicating wavelength selection used in calibration model under LED lighting is more limited. Regardless, the R^2 of calibration and prediction produced by LEDs are still high with proper wavelengths chosen and therefore, it can be deduced that LED can be an alternative to halogen lamp as light source in spectroscopic acidity measurement of Sala Mango.

On the other hand, the results obtained for SSC are not as good as pH with lower R^2 obtained for calibration and prediction. Figure 4.17 shows an overview of the 12 model performances (Refer Table 4.6 - 4.9) of SSC prediction of the four light sources. Halogen lamp shows better performance compared to LEDs showing stability of the light source as lighting in SSC spectroscopic measurement of Sala Mango.

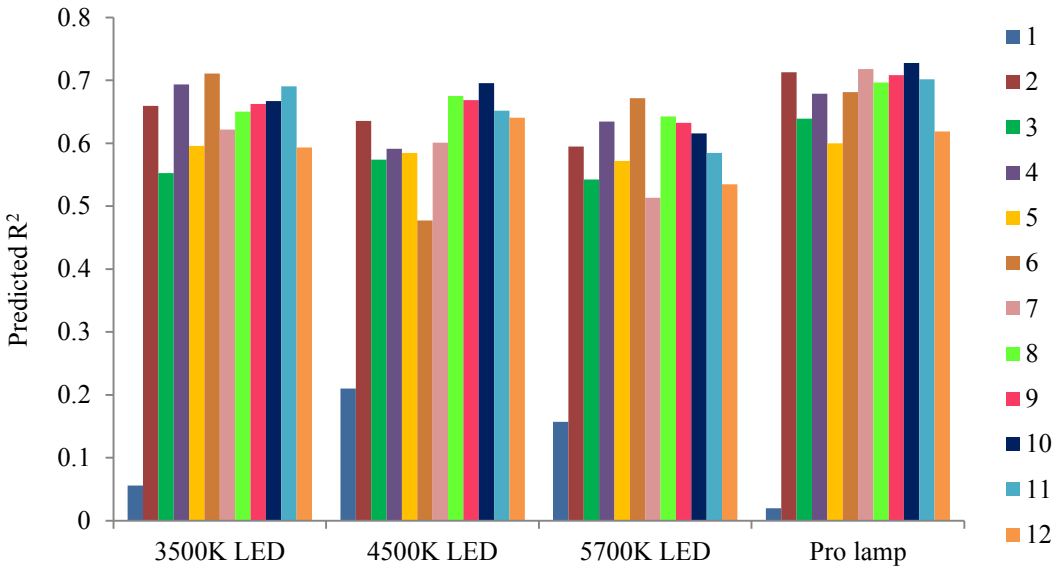

Figure 4.17 Overview graph of 12 model performances for SSC prediction of Sala Mango

Despite the results obtained are not satisfactory, the influence of lightings on spectroscopic measurement are now significant with wavelength selections for best predictive models of each of the lightings are different from one another unlike in pH case. Table 4.11 shows list of the best predictive models for SSC measurement of Sala Mango. Even wavelength selections for similar light source (LEDs with different CCTs) are different proving the hypothesis.

Therefore, it can be concluded that LED CCT indeed does affect spectroscopic measurement of Sala Mango and indirectly influence the calibration and prediction models' performance in correlating quality attributes of mango samples. The small difference in R^2 of best predictive models between halogen lamp and LEDs for pH shows potential of LED in replacing halogen lamp as lighting in spectroscopic measurement of Sala Mango.

Table 4.11 Summary of best predictive model for SSC prediction of Sala Mango

Light Source	Calibration Algorithm	Calibration		Prediction	
		R^2	RMSEC (^{o}Brix)	R^2	RMSEP (^{o}Brix)
D35	$SSC(^oBrix)=4.160 + 0.572R_{430} - 1.440R_{520} +0.846R_{540} - 1.786R_{690}+ 2.820R_{700}$	0.6361	1.2723	0.6903	1.1258
D45	$SSC(^oBrix)=7.500 + 0.700R_{470} - 0.770R_{520} +0.265R_{570} - 0.896R_{675}+1.431R_{700}$	0.5970	1.3390	0.6955	1.1210
D57	$SSC(^oBrix)=7.890 + 0.128R_{540} - 0.453R_{520} + 0.427R_{580} + 0.890R_{615} - 2.42R_{650}$	0.5860	1.3571	0.6424	1.2097
Halogen lamp	$SSC(^oBrix)=7.560 + 0.428R_{470} - 0.326R_{520} + 0.104R_{570} -0.087R_{675}+ 0.083R_{700}$	0.6059	1.3241	0.7276	1.0603

4.4 Direct Calibration Transfer of Sala Mango Visible Spectra between Different Light Sources

The section before discussed on the influence of LED CCT on visible spectroscopic measurement of SSC and pH of Sala Mango involving different lightings and the development of prediction models for respective quality attributes of mango using MLR method. Next, this section aims to access the potential of direct calibration transfer technique between calibration models generated from master lighting and after that predicted data from other light sources (slave lightings) are transferred directly into the models to get predicted R^2 and RMSEP. Difference in R^2 is calculated as a reference to stability of results obtained. Positive difference indicates increment in prediction accuracy while negative difference indicates reduction in prediction accuracy if compared to calibration R^2. The main purpose of this technique is to observe potential of interchanging light sources without recalibration process which is time-consuming, costly and energy-depleting. Only pH measurement is involved in this section as the results are highly stable and

strongly correlated to reflectance spectra as shown in the previous section. The results presented here along with the wavelength selection are chosen from combination of three regions wavelengths across visible range as they are found to give better results than one or two regions wavelengths algorithms.

4.4.1 D35 as Master lighting

For first calibration transfer set, D35 is treated as master lighting and thus, calibration algorithm produced by MLR method is transferred to other lightings to get prediction results as shown in Table 4.12. The best predictive model is shown in highlight. From Table 4.12, it is found that the percentage difference between calibrated R^2 and predicted R^2 are quite large after direct calibration transfer procedure. Out of the ten models, none of them can be fitted perfectly with high R^2 and low RMSEP for the other three slave lightings simultaneously. This shows that different predictive models have to be used when data is transferred between master and slave lightings. The best calibration model developed using master lighting for D45 as slave lighting is Model 9 as presented in Equation (4.9). The predicted R^2 has improved by 2.9% with value of 0.9289 and RMSEP of 0.2179 pH. The high R^2 (> 0.9) and low RMSEP has proven that this technique is workable in transferring spectra data from D45 lighting measurement into D35 calibration model.

$$pH = 2.332 + 0.370R_{470} - 0.405R_{520} + 0.133R_{570} - 0.438R_{675} + 0.769R_{700} \quad (4.9)$$

R^2_{cal} =0.9030; RMSEC =0.2654 pH

R^2_{pred} =0.9289; RMSEP =0.2179 pH

Table 4.12 Calibration and prediction results after Calibration Transfer using D35 as Master Lighting

Model	Wavelength(nm)	Light Source	Calibration R^2	Calibration RMSEC (pH)	Prediction R^2	Prediction RMSEP (pH)	*Diff. in R^2 (%)
1	400,430,480,520,620	Halogen lamp	0.7338	0.4396	0.4298	0.6171	-41.4
		D45			0.4165	0.6243	-43.2
		D57			0.0118	0.8124	-98.4
2	420,470,550,615,675	Halogen lamp	0.7887	0.3917	0.0076	0.8141	-99.0
		D45			0.6140	0.5078	-22.2
		D57			0.0096	0.8133	-98.8
3	455,480,585,625,700	Halogen lamp	0.8475	0.3327	0.8348	0.3322	-1.5
		D45			0.1710	0.7441	-79.8
		D57			0.1532	0.7521	-81.9
4	440,520,540,600,690	Halogen lamp	0.8559	0.3235	0.6884	0.4562	-19.6
		D45			0.8573	0.3087	+0.2
		D57			0.8586	0.3073	+0.3
5	435,470,510,620,670	Halogen lamp	0.8648	0.3133	0.0001	0.8172	-100.0
		D45			0.8021	0.3636	-7.3
		D57			0.5168	0.5681	-40.2
6	460,520,550,580,700	Halogen lamp	0.8839	0.2904	0.7469	0.4111	-15.5
		D45			0.9166	0.2360	+3.7
		D57			0.5917	0.5222	-33.1
7	450,520,580,615,650	Halogen lamp	0.8866	0.2869	0.0258	0.8066	-97.1
		D45			0.8705	0.2941	-1.8
		D57			0.4524	0.6048	-49.0
8	455,520,550,675,700	Halogen lamp	0.8971	0.2733	0.7962	0.3689	-11.2
		D45			0.9149	0.2384	+2.0
		D57			0.5745	0.5331	-36.0
9	470,520,570,675,700	Halogen lamp	0.9030	0.2654	0.7981	0.3672	-11.6
		D45			0.9289	0.2179	+2.9
		D57			0.3762	0.6455	-58.3
10	430,520,540,690,700	Halogen lamp	0.9117	0.2532	0.7407	0.4161	-18.8
		D45			0.9096	0.2458	-0.2
		D57			0.7759	0.3869	-14.9

For D57 as slave lighting, the best calibration algorithm developed using master lighting is Model 4 as shown in Equation (4.10). The R^2 of prediction has increased by 0.3% from 0.8559 to 0.8586, just a slight increment but at least stability of results is achieved.

$$pH = 1.808 + 0.089R_{440} - 1.010R_{520} + 0.704R_{540} - 0.008\,R_{600} + 0.058R_{690} \quad (4.10)$$

R^2_{cal} =0.8559; RMSEC =0.3235 pH

R^2_{pred} =0.8586; RMSEP =0.3073 pH

The third set is calibration transfer between D35 as master lighting and halogen lamp as slave lighting. Early prediction is that result for halogen lamp is worst as the difference in light source spectra should impact more than difference in correlated colour temperature of LED. The best calibration model generated using D35 is Model 3 as presented in Equation 4.11. R^2 prediction has a slight decrease of 1.5% after direct calibration transfer procedure.

$$pH = 1.546 + 0.870R_{455} - 2.510R_{480} + 0.208R_{585} - 0.255R_{625} + 0.860R_{700} \quad (4.11)$$

R^2_{cal} =0.8475; RMSEC =0.3327 pH

R^2_{pred} =0.8348; RMSEP =0.3322 pH

In summary, it is shown that direct calibration transfer technique is successfully applied from slave lightings into D35 calibration model with satisfactory results and acceptable R^2 difference (<5%) for each transfer. D45 possesses the best results after direct calibration transfer with prediction R^2 of 0.9289 and low RMSEP of 0.2179 pH. This might due to the smallest difference of its LED spectrum with D35's as shown in Figure 4.12. D57 has slightly better R^2 compared to halogen lamp but overall results are still stable with R^2 above 0.8.

4.4.2 D45 as Master lighting

For second set, D45 is considered as master lighting and the others (D35, D57 and halogen lamp) are treated as slave lightings. The spectra data from each slave lighting is transferred directly into calibration model generated by master lighting to get prediction results. The results are shown in Table 4.13 and the best predictive model is shown in highlight. From Table 4.13, similar to D35's results, it is found that different calibration models would actually affect the predictive results obtained. The range in difference of R^2 is wide therefore wavelength selection is

Table 4.13 Calibration and prediction results after Calibration Transfer using D45 as Master Lighting

Model	Wavelength(nm)	Light Source	Calibration		Prediction		*Diff. in R^2 (%)
			R^2	RMSEC (pH)	R^2	RMSEP (pH)	
1	400,430,480,520,620	Halogen lamp	0.7652	0.4128	0.1746	0.7425	-77.2
		D35			0.5880	0.5246	-23.2
		D57			0.0731	0.7868	-90.4
2	420,470,550,615,675	Halogen lamp	0.7795	0.4001	0.0341	0.8032	-95.6
		D35			0.6856	0.4583	-12.0
		D57			0.0647	0.7904	-91.7
3	455,480,585,625,700	Halogen lamp	0.8096	0.3717	0.6938	0.4523	-14.3
		D35			0.8475	0.3192	+4.7
		D57			0.7961	0.3691	-1.7
4	440,520,540,600,690	Halogen lamp	0.8382	0.3427	0.7693	0.3925	-8.2
		D35			0.8630	0.3024	+3.0
		D57			0.8223	0.3445	-1.9
5	435,470,510,620,670	Halogen lamp	0.8477	0.3325	0.0001	0.8172	-100.0
		D35			0.8713	0.2932	+2.8
		D57			0.3531	0.6573	-58.3
6	460,520,550,580,700	Halogen lamp	0.8760	0.3000	0.7417	0.4157	-15.3
		D35			0.8859	0.2760	+1.1
		D57			0.5590	0.5427	-36.2
7	450,520,580,615,650	Halogen lamp	0.8807	0.2943	0.0285	0.8055	-96.8
		D35			0.8979	0.2611	+2.0
		D57			0.5983	0.5180	-32.1
8	455,520,550,675,700	Halogen lamp	0.8942	0.2772	0.7862	0.3789	-12.1
		D35			0.9018	0.2568	+0.8
		D57			0.6010	0.5176	-32.8
9	430,520,540,690,700	Halogen lamp	0.8952	0.2758	0.7271	0.4270	-18.8
		D35			0.9107	0.2442	+1.7
		D57			0.8128	0.3536	-9.2
10	470,520,570,675,700	Halogen lamp	0.9121	0.2526	0.8009	0.3647	-12.2
		D35			0.9223	0.2278	+1.1
		D57			0.4498	0.6062	-50.7

important in finding the best calibration model developed from master lighting to predict acidity using spectra from slave lightings.The best calibration model found for calibration transfer between D35 (slave lighting) and D45 (master lighting) is Model 10 as shown in Equation (4.12). The high predicted R^2 (> 0.9) and increment

of 1.1% showing success of this technique in acidity measurement of Sala Mango even when spectra measured using different lighting is used.

$$pH=2.359 +0.265R_{470} -0.336R_{520} + 0.122R_{570} - 0.463R_{675} +0.749R_{700} \quad (4.12)$$

R^2_{cal} =0.9121; RMSEC =0.2526 pH

R^2_{pred} =0.9223; RMSEP =0.2278 pH

For D57 as slave lighting, the best calibration model is Model 4 as presented in Equation (4.13). R^2 obtained for D57 as slave lighting is lower compared to D35 showing

$$pH= 1.803 + 0.042R_{440} - 0.738R_{520} + 0.525R_{540} - 0.004R_{600} + 0.059R_{690} \quad (4.13)$$

R^2_{cal} =0.8382; RMSEC =0.3427 pH

R^2_{pred} =0.8223; RMSEP =0.3445 pH

Last but not least, calibration transfer between D45 as master lighting and halogen lamp as slave lighting is observed. Results from Table 4.13 shows this technique does not yield good results as the difference in R^2 for the ten calibration models are all decrement of more than 10%. The minimum decrement among the models is from Model 10 which also produces a decrement of 12.2% giving predicted R^2 of 0.8009 and RMSEP of 0.3647 pH.

Therefore, for direct calibration transfer of slave lightings into calibration models generated by D45 as master lighting, this technique is proved only successful for LEDs lightings and not halogen lamp. Difference in the original light source spectra is the key factor for this technique to be not applicable between these two lightings.

4.4.3 D57 as Master lighting

Table 4.14 shows the predictive models after direct calibration transfer procedure of spectra measured using slave lightings into calibration model generated from D57 as master lighting. The best predictive model is shown in highlight. From the table, once again, wide range in percentage difference of R^2 is observed for all the slave lightings as in D35 and D45 cases. Proper wavelength to generate calibration model is important to obtain predictive model with high R^2 and low RMSE and small difference in percentage difference of R^2.

Table 4.14 Calibration and prediction results after Calibration Transfer using D57 as Master Lighting

Model	Wavelength(nm)	Light Source	Calibration		Prediction		*Diff. in R^2 (%)
			R^2	RMSEC (pH)	R^2	RMSEP (pH)	
1	400,430,480,520,620	Halogen lamp	0.7423	0.4325	0.0475	0.7976	-93.6
		D35			0.4113	0.6271	-44.6
		D45			0.2157	0.7238	-70.9
2	420,470,550,615,675	Halogen lamp	0.7565	0.4204	0.4782	0.5903	-36.8
		D35			0.1936	0.7339	-74.4
		D45			0.0216	0.8084	-97.1
3	455,480,585,625,700	Halogen lamp	0.8443	0.3362	0.8342	0.3328	-1.2
		D35			0.3361	0.6659	-60.2
		D45			0.5711	0.5352	-32.4
4	440,520,540,600,690	Halogen lamp	0.8482	0.3320	0.8325	0.3344	-1.9
		D35			0.8880	0.2735	+4.7
		D45			0.8779	0.2856	+3.5
5	435,470,510,620,670	Halogen lamp	0.8539	0.3256	0.0030	0.8160	-99.6
		D35			0.8216	0.3452	-3.8
		D45			0.7716	0.3906	-9.6
6	430,520,540,690,700	Halogen lamp	0.8712	0.3058	0.7377	0.4185	-15.3
		D35			0.9059	0.2507	+4.0
		D45			0.9080	0.2479	+4.2
7	460,520,550,580,700	Halogen lamp	0.8734	0.3032	0.6965	0.4503	-20.3
		D35			0.8479	0.3187	-2.9
		D45			0.7586	0.4015	-13.1
8	450,520,580,615,650	Halogen lamp	0.8824	0.2922	0.0828	0.7827	-90.6
		D35			0.8401	0.3268	-4.8
		D45			0.9000	0.2584	+2.0
9	455,520,550,675,700	Halogen lamp	0.8938	0.2777	0.7699	0.3921	-13.9
		D35			0.8982	0.2608	+0.5
		D45			0.8392	0.3277	-6.1
10	470,520,570,675,700	Halogen lamp	0.8979	0.2722	0.7950	0.3701	-11.5
		D35			0.8075	0.3586	-10.1
		D45			0.6766	0.4648	-24.6

Besides, calibration algorithm which produces high calibration R^2 does not necessarily produce high prediction R^2 as shown by Model 10. The best calibration algorithm developed using master lighting and produces the best results for D35 as slave lighting is Model 6 as presented in Equation (4.14).

$$pH = 1.425 + 0.046R_{430} - 0.411R_{520} + 0.273R_{540} - 0.587R_{690} + 1.009R_{700} \quad (4.14)$$

R^2_{cal} =0.8712; RMSEC =0.3058 pH

R^2_{pred} =0.9059; RMSEP =0.2507 pH

Despite not having the highest RMSEC as compared to Model 7, 8, 9 and 10, this model produces the highest predicted R^2 and increment of 4.0% of R^2 showing applicability of this model.

Next, for calibration set between D57 as master lighting and D45 as slave lighting, the best calibration model is still Model 6 as presented in Equation (4.15). Similar to D35 case, predicted R^2 has increased by 4.2% to reach 0.9080 which is a satisfactory result.

$$pH = 1.425 + 0.046R_{430} - 0.411R_{520} + 0.273R_{540} - 0.587R_{690} + 1.009R_{700} \quad (4.15)$$

R^2_{cal} =0.8712; RMSEC =0.3058 pH

R^2_{pred} =0.9080; RMSEP =0.2479 pH

For halogen lamp as slave lighting, the best calibration can be obtained is Model 3 as presented in Equation (4.16). It is shown that results for halogen lamp is poorer compared to results for calibration transfer between LEDs. The R^2 obtained is only roughly 0.8 compared to white LEDs which can reach up to 0.9. The percentage difference in R^2 is insignificant with decrement of only 1.2%.

$$pH = 1.753 + 0.355R_{455} - 2.111R_{480} + 0.202R_{585} - 0.305R_{625} + 0.967R_{700} \quad (4.16)$$

R^2_{cal} =0.8443; RMSEC =0.3362 pH

R^2_{pred} =0.8342; RMSEP =0.3328 pH

Therefore, it can be deduced that direct calibration transfer technique using D57 as master lighting has successfully been applied to other slave lightings despite poorest result is obtained for halogen lamp with R^2 about 0.83 only. Most of the results show positive responses when direct calibration technique is applied between LEDs. In the next subsection, calibration transfer between halogen lamp as master lighting and LEDs is investigated instead.

4.4.4 Halogen lamp as Master lighting

Table 4.15 shows the calibration models generated using halogen lamp as master lighting and predictive results for white LEDs as slave lightings. From Table 4.15, it is shown that overall results for acidity prediction of Sala Mango after transferring of spectra from slave lightings into calibration model generated by master lighting has poorer results as compared to LEDs as master lighting. The highest calibration R^2 only reaches 0.8995 and difference in R^2 is also big (mostly greater than 10% of decrement). The best calibration model for D35 and D45 is Model 10 but their minimum percentages of decrement are big (7.3% for D35 and 10.7% for D45) hence, results are rejected for these two lightings. For D57 as slave lighting, the result is worst with best calibration model having even lower calibrated R^2 (0.8388) compared to another two LEDs (0.8995) and greater percentage of decrement up to 38.2% which is too big to be considered as true results. Thus, this technique is not successfully applied when halogen lamp is used as master lighting

as percentage of difference in R^2 between calibration and prediction values for the entire three slave lightings are great.

Table 4.15 Calibration and prediction results after Calibration Transfer using halogen lamp as Master Lighting

Model	Wavelength(nm)	Light Source	Calibration		Prediction		*Diff. in R^2 (%)
			R^2	RMSEC (pH)	R^2	RMSEP (pH)	
1	400,430,480,520,620	D35	0.6485	0.5051	0.1535	0.7519	-76.3
		D45			0.0532	0.7952	-91.8
		D57			0.0072	0.8143	-98.9
2	455,480,585,625,700	D35	0.8039	0.3773	0.0914	0.7790	-88.6
		D45			0.0069	0.8144	-99.1
		D57			0.0072	0.8143	-99.1
3	420,470,550,615,675	D35	0.8276	0.3538	0.7034	0.4451	-15.0
		D45			0.5885	0.5242	-28.9
		D57			0.0716	0.7875	-91.3
4	440,520,540,600,690	D35	0.8388	0.3421	0.5979	0.5182	-28.7
		D45			0.4463	0.6081	-46.8
		D57			0.5183	0.5672	-38.2
5	435,470,510,620,670	D35	0.8401	0.3407	0.2964	0.6855	-64.7
		D45			0.1064	0.7725	-87.3
		D57			0.0128	0.8120	-98.5
6	460,520,550,580,700	D35	0.8616	0.3170	0.7669	0.3945	-11.0
		D45			0.6441	0.4875	-25.2
		D57			0.4007	0.6327	-53.5
7	450,520,580,615,650	D35	0.8751	0.3012	0.4586	0.6014	-47.6
		D45			0.2520	0.7068	-71.2
		D57			0.4990	0.5784	-43.0
8	430,520,540,690,700	D35	0.8828	0.2917	0.0849	0.7818	-90.4
		D45			0.1671	0.7458	-81.1
		D57			0.1181	0.7675	-86.6
9	455,520,550,675,700	D35	0.8833	0.2911	0.7621	0.3986	-13.7
		D45			0.1902	0.7354	-78.5
		D57			0.2589	0.7035	-70.7
10	470,520,570,675,700	D35	0.8995	0.2702	0.8335	0.3335	-7.3
		D45			0.8032	0.3626	-10.7
		D57			0.2095	0.7266	-76.7

4.4.5 Summary

From this section, it is proven that direct calibration transfer technique involving different lightings in prediction of Sala Mango acidity has been successfully applied between LEDs with different CCT. This technique can be performed easily without any complex step yet at the same time can avoid the need of recalibration.

Figure 4.18 shows an overview graph of model performances for all light sources. From the graph, halogen lamp as master lighting shows the least performed results compared to other LEDs. D45 seems to have advantage as master lighting for D35 and vice versa while for D57, better results are obtained for both D35 and D45 as slave lightings.

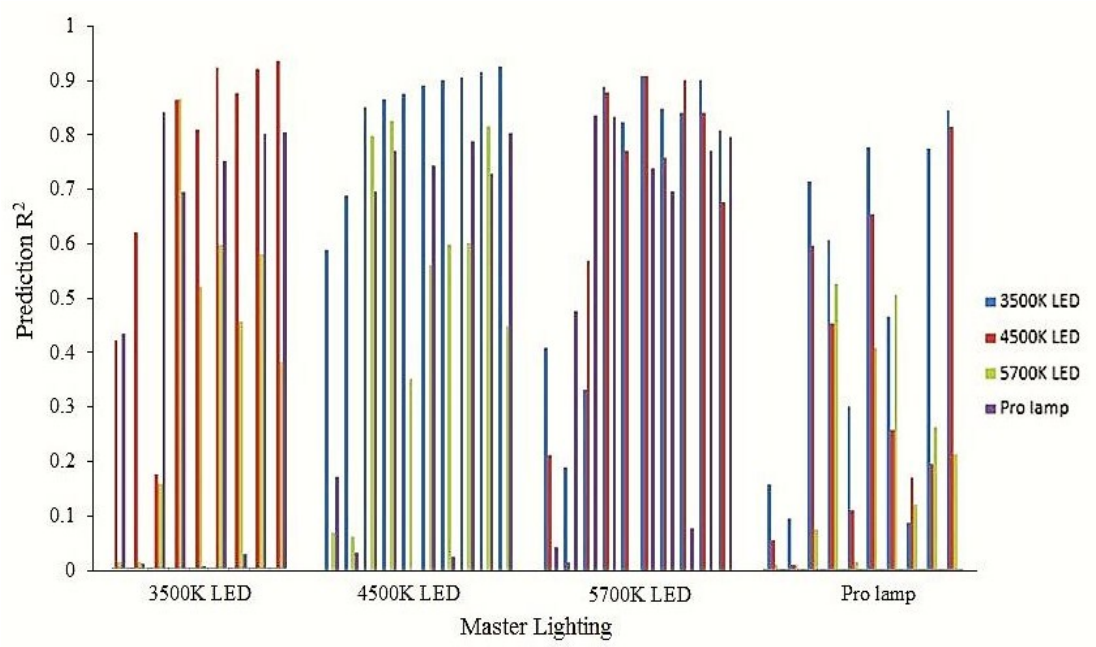

Figure 4.18 Overview of model performance of different light sources

The direct transfer procedure for D35 and D45 is workable for both ways which can be described as forward and backward directions as both of them produce good prediction of acidity as master lighting as illustrated in Figure 4.19.

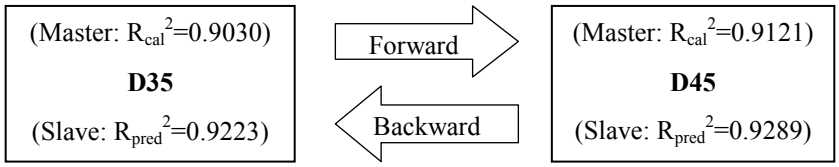

Figure 4.19 Illustration of forward and backward directions of direct calibration transfer

On the other hand, for D57, it produces good prediction results as master lighting for D35 and D45 as slave lightings but poor results are obtained when it acts as slave lighting (Not two ways). This observation can suggest limitation of this

procedure to be white LED of higher CCT should be master lighting rather than lower CCT LED else the accuracy of results might have to be compromised. Table 4.16 lists the overall results of the best predictive models after direct calibration transfer procedure between master and slave lightings. In summary, it can be deduced that this procedure is more applicable for calibration transfer between two similar light sources (LEDs with different CCTs) rather than two different spectra light sources (LED and halogen lamp).

Table 4.16 Summary of best predictive model results after direct calibration procedure between master and slave lightings

Master Lighting	Slave Lighting	Calibration Algorithm	Calibration		Prediction		Diff. in R^2 (%)
			R^2	RMSEC (pH)	R^2	RMSEP (pH)	
D35	D45	$pH=2.332+0.370R_{470} - 0.4052R_{520} +0.1327R_{570} -0.4382R_{675} + 0.769R_{700}$	0.9030	0.2654	0.9289	0.2179	+2.9
	D57	$pH=1.808+0.0891R_{440} - 1.010R_{520} +0.704R_{540} - 0.008R_{600} +0.058R_{690}$	0.8559	0.3235	0.8573	0.3087	+0.2
	Halogen lamp	$pH=1.546+0.870R_{455} - 2.510R_{480}+ 0.208R_{585} - 0.255R_{625} +0.860R_{700}$	0.8475	0.3327	0.8348	0.3322	-1.5
D45	D35	$pH=2.359+ 0.2650R_{470} -0.336R_{520}+0.122R_{570} - 0.463R_{675} +0.749R_{700}$	0.9121	0.2526	0.9223	0.2278	+1.1
	D57	$pH= 1.803 +0.042R_{440} - 0.738R_{520} +0.525R_{540} -0.004R_{600} + 0.059R_{690}$	0.8382	0.3427	0.8223	0.3445	-1.9
	Halogen lamp	-	0.8382	0.3427	0.7693	0.3925	-8.2
D57	D35	$pH = 1.425 +0.046R_{430} - 0.411R_{520}+ 0.273R_{540}- 0.587R_{690}+ 1.009R_{700}$	0.8712	0.3058	0.9059	0.2507	+4.0
	D45	$pH = 1.425 +0.046R_{430} - 0.411R_{520}+ 0.273R_{540} - 0.587R_{690}+ 1.009R_{700}$	0.8712	0.3058	0.9080	0.2479	+4.2
	Halogen lamp	$pH = 1.753 + 0.355R_{455} - 2.111R_{480}+ 0.202R_{585}- 0.305R_{625}+ 0.967R_{700}$	0.8443	0.3362	0.8342	0.3328	-1.2

CHAPTER 5

CONCLUSION AND FUTURE RECOMMENDATIONS

5.1 Conclusion

The present studies showed the investigation and application of the visible spectroscopy system in accessing acidity and soluble solids content of Sala Mango. This research can be summarized in such a way spectra of fruit samples are collected using reflectance mode of Jaz spectrometer under different lightings and then calibration algorithms are developed to correlate with the quality attributes. Prior to study of real sample, study on colour samples are first performed to check on the interaction of lighting with colour as measured by spectrometer.

The preliminary study is conducted to observe blue, red and green colour series illuminated by D35, D45, D57 and halogen lamp as measured using Jaz spectrometer. Results are given in peak wavelength and spectral gradient. Based on the results obtained, the peak wavelength for green and blue colour series has a slight difference but still consider near to halogen lamp's value. Red colour series is the only one which has significant difference. Spectral gradient which indicates the responsivity of colour measured by spectroscopy has more significant difference than peak wavelength. Blue and green colour series have better responsivity at higher CCT LED following the pattern of white diffuse reflectance spectra but in contrast for red colour series observation, responsivity is better for lower CCT LED. This has proven that composition of blue light and phosphor in white LED have influence on spectroscopic measurement of colour samples.

Second part of this study is to investigate the influence of LED CCT on visible spectroscopic measurement of intrinsic qualities of Sala Mango. From

preliminary study, lighting actually does change the colour measurement by spectrometer but further work is done to prove correlation to acidity and soluble solids content of mango samples. It was seen that LED spectra greatly altered the reflectance spectra of mango sample with the obvious blue radiation at 400-480 nm. Carotenoid pigments (~475-490 nm) are not observed from spectra due to the strong blue radiation from the LED itself but anthocyanins and chlorophyll-a are still observable which can be detected at roughly 550 nm and 675 nm. Despite the huge difference in reflectance spectra, it was found that algorithms developed using MLR are still able to produce good calibration and prediction performance for acidity and lower accuracy for SSC measurement. Nevertheless, LED CCT has shown direct influence on the model performance as represented in R^2 and RMSE. The highest prediction accuracy for acidity measurement produced using D35 is $R^2 = 0.9227$ and RMSEP = 0.2271 pH; for D45 is $R^2 = 0.9308$ and RMSEP = 0.2150 pH; D57 with $R^2 = 0.9145$ and RMSEP = 0.2390 pH and lastly halogen lamp with $R^{2=}$ 0.9114 and RMSEP = 0.2432 pH. For SSC measurement, the best prediction accuracy developed by best model for D35 is $R^2 = 0.6903$ and RMSEP = 1.1258 ^{o}Brix; for D45 is $R^2 =$ 0.6955 and RMSEP = 1.1210 ^{o}Brix; D57 with $R^2 = 0.6424$ and RMSEP = 1.2097 ^{o}Brix and halogen lamp with $R^2 = 0.7276$ and RMSEP = 1.0603 ^{o}Brix.

Last part of this study focuses on the exploration of possibility of direct calibration transfer procedure between similar type of light sources (LEDs with different CCT) and between different type of light sources (halogen lamp and LEDs). The calibration algorithm developed using master lighting is transferred to slave lightings for prediction of acidity measurement of Sala Mango. The best prediction accuracy obtained with D35 as master lighting and D45 as slave lighting is $R^2 = 0.9289$ and RMSEP = 0.2179 pH, $R^2 = 0.8586$ and RMSEP = 0.3073 pH for

D57 and lastly for halogen lamp as slave lighting, R^2 = 0.8348 and RMSEP = 0.3322 pH. For D45 as master lighting, the best prediction results are as follow. For D35 as slave lighting, R^2 = 0.9223 and RMSEP = 0.2278 pH are obtained, R^2 = 0.8223 and RMSEP = 0.3445 pH for D57 and lastly halogen lamp as slave lighting has a poor result with decrement of 12.2% from the calibration R^2 and hence, result is omitted. Next, for D57 acts as master lighting and D35, D45 and halogen lamp act as slave lightings. The results are as follow: R^2 = 0.9059 and RMSEP = 0.2507 pH for D35, R^2 = 0.9080 and RMSEP = 0.2479 pH for D45 and R^2 = 0.8342 and RMSEP = 0.3328 pH for halogen lamp. Based on the results obtained, LED CCT indeed does affect spectroscopic measurement of Sala Mango as poor results are obtained when direct calibration procedures are applied between lower CCT LEDs (D35 and D45) and high CCT LED (D57). D35 and D45 can be transferred perfectly in forward and backward directions with excellent performance in prediction R^2 while D57 only gives good results when it acts as master lighting. Hence, from this observation, it can be deduced that higher CCT can only be master lighting and its algorithm to be transferred to lower CCT LED as slave lightings and not vice versa. Lastly, when halogen lamp acts as master lighting, it was found that the results are not acceptable with error up high to 99%. The best result is only found for D35 as slave lighting but the percentage difference in R^2 is also more than 5% (decrement of 7.3%). Hence, it can be inferred that this procedure is not suitable for transfer between two different types of light sources. Nevertheless, this direct calibration transfer procedure is proven to be successfully utilized between LEDs with different CCT in prediction of acidity of Sala Mango without requiring complicated steps.

In summary, this research has explored the influence of LED CCT on colour measurement, confirmed the applicability of LED as lighting in spectroscopic

measurement of acidity and soluble solids content of Sala Mango and introduced the direct transfer calibration transfer method between similar types of light source (LEDs with different CCT).

5.2 Future Recommendations

This thesis has just presented the introduction of LED as lighting in spectroscopy instrumentation in measuring RGB colour samples and intrinsic properties of Sala Mango. However, further studies are still needed for future work to improve and maximise the utilization of this technology to be useful and beneficial in the future. Hence, several recommendations are suggested and enumerated as follows:

- The methodology used in this work has only been applied to mango samples. Therefore, it would be good to continue research line by testing on different fruit samples to further verify the applicability of LED as lighting in replacement of halogen lamp in spectroscopy instrumentation.
- Different measurements setup such as interactance, transmittance or fluorescence mode can be used to compare the results obtained in this thesis.
- Different chemometrics method such as PLS and PCA can be tested in dealing with spectral data. Area under curve analysis technique also can be applied on colour paper spectra to differentiate between glossy and non-glossy results.
- Optical filter such as long pass filter can be tried out to filter the blue light emitted from white LED and check on the differences in model performance
- Different type of white LED can be used in spectroscopic measurement to expand investigation and enhance practicability of LED for future prospect.

REFERENCES

Abbott, J. A. (1999). Quality measurement of fruits and vegetables. *Postharvest biology and technology, 15*(3), 207-225.

Abdi, H. (2003). Multivariate analysis *Encyclopedia for research methods for the social sciences* (pp. 699-702).

Barbut, S. (2001). Effect of illumination source on the appearance of fresh meat cuts. *Meat science, 59*(2), 187-191.

Behar-Cohen, F., Martinsons, C., Viénot, F., Zissis, G., Barlier-Salsi, A., Cesarini, J., Enouf, O., Garcia, M., Picaud, S., & Attia, D. (2011). Light-emitting diodes (LED) for domestic lighting: Any risks for the eye? *Progress in retinal and eye research, 30*(4), 239-257.

Birth, G. (1976). *How light interacts with foods. In "Quality Detection in Foods" Ed. Gaffney, JJ*: American Society of Agricultural Engineers, St. Joseph, MI.

Blanco, M., & Villarroya, I. (2002). NIR spectroscopy: a rapid-response analytical tool. *TrAC Trends in Analytical Chemistry, 21*(4), 240-250.

Bobelyn, E., Serban, A.-S., Nicu, M., Lammertyn, J., Nicolai, B. M., & Saeys, W. (2010). Postharvest quality of apple predicted by NIR-spectroscopy: study of the effect of biological variability on spectra and model performance. *Postharvest biology and technology, 55*(3), 133-143.

Brownleader, M., Jackson, P., Mobasheri, A., Pantelides, A., Sumar, S., Trevan, M., & Dey, P. (1999). Molecular aspects of cell wall modifications during fruit ripening. *Critical Reviews in Food Science and Nutrition, 39*(2), 149-164.

Camps, C., & Christen, D. (2009). Non-destructive assessment of apricot fruit quality by portable visible-near infrared spectroscopy. *LWT-Food Science and Technology, 42*(6), 1125-1131.

Cen, H., Bao, Y., He, Y., & Sun, D.-W. (2007). Visible and near infrared spectroscopy for rapid detection of citric and tartaric acids in orange juice. *Journal of Food Engineering, 82*(2), 253-260.

Chen, J. Y., Zhang, H., & Matsunaga, R. (2006). Rapid determination of the main organic acid composition of raw Japanese apricot fruit juices using near-infrared spectroscopy. *Journal of agricultural and food chemistry, 54*(26), 9652-9657.

Chen, P. (1978). Use of optical properties of food materials in quality evaluation and materials sorting. *Journal of Food Process Engineering, 2*(4), 307-322.

Cho, S., Han, A., Taylor, M. H., Huck, A. C., Mishler, A. M., Mattal, K. L., Barker, C. A., & Seo, H.-S. (2015). Blue lighting decreases the amount of food consumed in men, but not in women. *Appetite, 85*, 111-117.

Cortés, V., Ortiz, C., Aleixos, N., Blasco, J., Cubero, S., & Talens, P. (2016). A new internal quality index for mango and its prediction by external visible and near-infrared reflection spectroscopy. *Postharvest biology and technology, 118*, 148-158.

Davey, M. W., Saeys, W., Hof, E., Ramon, H., Swennen, R. L., & Keulemans, J. (2009). Application of visible and near-infrared reflectance spectroscopy (Vis/NIRS) to determine carotenoid contents in banana (Musa spp.) fruit pulp. *Journal of agricultural and food chemistry, 57*(5), 1742-1751.

De Almeida, A., Santos, B., Paolo, B., & Quicheron, M. (2014). Solid state lighting review–Potential and challenges in Europe. *Renewable and Sustainable Energy Reviews, 34*, 30-48.

Delwiche, S. R., Mekwatanakarn, W., & Wang, C. Y. (2008). Soluble solids and simple sugars measurement in intact mango using near infrared spectroscopy. *HortTechnology, 18*(3), 410-416.

Department of Energy, U. S. (2014). True Colors (E. E. a. R. Energy, Trans.) (pp. 8).

El-Ramady, H. R., Domokos-Szabolcsy, É., Abdalla, N. A., Taha, H. S., & Fári, M. (2015). Postharvest Management of Fruits and Vegetables Storage *Sustainable Agriculture Reviews* (pp. 65-152): Springer.

ElMasry, G., Wang, N., ElSayed, A., & Ngadi, M. (2007). Hyperspectral imaging for nondestructive determination of some quality attributes for strawberry. *Journal of Food Engineering, 81*(1), 98-107.

Esbensen, K. H., Guyot, D., Westad, F., & Houmoller, L. P. (2002). *Multivariate Data Analysis: In Practice : an Introduction to Multivariate Data Analysis and Experimental Design*: CAMO.

Etienne, A., Génard, M., Lobit, P., Mbeguié-A-Mbéguié, D., & Bugaud, C. (2013). What controls fleshy fruit acidity? A review of malate and citrate accumulation in fruit cells. *Journal of experimental botany, 64*(6), 1451-1469.

Fonollosa, J., Fernández, L., Gutiérrez-Gálvez, A., Huerta, R., & Marco, S. (2016). Calibration transfer and drift counteraction in chemical sensor arrays using Direct Standardization. *Sensors and Actuators B: Chemical*.

Francis, F. (1995). Quality as influenced by color. *Food quality and preference, 6*(3), 149-155.

Fu, X.-p., Li, J.-p., Zhou, Y., Ying, Y.-b., Xie, L.-j., Niu, X.-y., Yan, Z.-k., & Yu, H.-y. (2009). Determination of soluble solid content and acidity of loquats based on FT-NIR spectroscopy. *Journal of Zhejiang University Science B, 10*(2), 120-125.

Gómez, A. H., He, Y., & Pereira, A. G. (2006). Non-destructive measurement of acidity, soluble solids and firmness of Satsuma mandarin using Vis/NIR-spectroscopy techniques. *Journal of Food Engineering, 77*(2), 313-319.

Guidetti, R., Beghi, R., & Giovenzana, V. (2012). *Chemometrics in food technology*: INTECH Open Access Publisher.

Guo, Z., Huang, W., Chen, L., Wang, X., & Peng, Y. (2013). *Nondestructive evaluation of soluble solid content in strawberry by near infrared spectroscopy.* Paper presented at the Third International Conference on Photonics and Image in Agriculture Engineering (PIAGENG 2013).

Held, G. (2016). *Introduction to light emitting diode technology and applications*: CRC Press.

Hemming, D. (2013). *Plant Sciences Reviews 2012*: CABI.

Hu, R., & Xia, J. (2011). *Calibration transfer of near infrared spectroscopy based on DS algorithm.* Paper presented at the Electric Information and Control Engineering (ICEICE), 2011 International Conference on.

Hunter, R. S. (1987). *The measurement of appearance*: John Wiley & Sons.

Ignat, T. (2012). *Non-destructive methods for determination of quality attributes of bell peppers.* PhD Thesis, Corvinus University of Budapest.

Jamshidi, B., Minaei, S., Mohajerani, E., & Ghassemian, H. (2012). Reflectance Vis/NIR spectroscopy for nondestructive taste characterization of Valencia oranges. *Computers and electronics in agriculture, 85*, 64-69.

Jha, S., Chopra, S., & Kingsly, A. (2005). Determination of sweetness of intact mango using visual spectral analysis. *Biosystems engineering, 91*(2), 157-161.

Jha, S., Jaiswal, P., Narsaiah, K., Gupta, M., Bhardwaj, R., & Singh, A. K. (2012). Non-destructive prediction of sweetness of intact mango using near infrared spectroscopy. *Scientia Horticulturae, 138*, 171-175.

Jha, S., Kingsly, A., & Chopra, S. (2006). Non-destructive determination of firmness and yellowness of mango during growth and storage using visual spectroscopy. *Biosystems engineering, 94*(3), 397-402.

Jha, S., Narsaiah, K., Sharma, A., Singh, M., Bansal, S., & Kumar, R. (2010). Quality parameters of mango and potential of non-destructive techniques for their measurement—a review. *Journal of food science and technology, 47*(1), 1-14.

Jha, S. N. (2010). Near infrared spectroscopy *Nondestructive Evaluation of Food Quality* (pp. 141-212): Springer.

Jost-Boissard, S., Fontoynont, M., & Blanc-Gonnet, J. (2009). Perceived lighting quality of LED sources for the presentation of fruit and vegetables. *Journal of Modern Optics, 56*(13), 1420-1432.

Kenkel, J. (2010). *Analytical Chemistry for Technicians, Third Edition*: CRC Press.

Knee, M. (2002). *Fruit Quality and Its Biological Basis*: Sheffield Academic Press.

Lawless, H. T., & Heymann, H. (2010). Color and appearance *Sensory Evaluation of Food* (pp. 283-301): Springer.

Leader Tech, I. (2016). The Basics of the Electromagnetic Spectrum Retrieved August 22, 2016, from https://leadertechinc.com/blog/basics-electromagnetic-spectrum/

Li, J., Huang, W., Zhao, C., & Zhang, B. (2013). A comparative study for the quantitative determination of soluble solids content, pH and firmness of pears by Vis/NIR spectroscopy. *Journal of Food Engineering, 116*(2), 324-332.

Liew, C., & Lau, C. (2012). Determination of quality parameters in Cavendish banana during ripening by NIR spectroscopy. *Int Food Res J, 19*(2), 751-758.

Lin, H., & Ying, Y. (2009). Theory and application of near infrared spectroscopy in assessment of fruit quality: a review. *Sensing and instrumentation for food quality and safety, 3*(2), 130-141.

Litz, R. E. (2009). *The mango: botany, production and uses*: CABI.

Liu, R. H. (2003). Health benefits of fruit and vegetables are from additive and synergistic combinations of phytochemicals. *The American journal of clinical nutrition, 78*(3), 517S-520S.

Luo, W., Huan, S., Fu, H., Wen, G., Cheng, H., Zhou, J., Wu, H., Shen, G., & Yu, R. (2011). Preliminary study on the application of near infrared spectroscopy and pattern recognition methods to classify different types of apple samples. *Food chemistry, 128*(2), 555-561.

McMurry, V. (2006). *Mastering Color*: North Light Books.

Ministry of Agriculture and Agro-Based Industry, M. (2015). Agrofood Statistics 2014 (pp. 22).

Ministry of Agriculture and Agro-Based Industry, M. (2016). Mango Retrieved January 4, 2016, from http://www.moa.gov.my/buah-buahan

Munawar, A. A., von Hörsten, D., Mörlein, D., Pawelzik, E., & Wegener, J. K. (2013). *Rapid and non-destructive prediction of mango sweetness and acidity using near infrared spectroscopy.* Paper presented at the GIL Jahrestagung.

Nicolai, B. M., Beullens, K., Bobelyn, E., Peirs, A., Saeys, W., Theron, K. I., & Lammertyn, J. (2007). Nondestructive measurement of fruit and vegetable quality by means of NIR spectroscopy: A review. *Postharvest biology and technology, 46*(2), 99-118.

Nicolaï, B. M., Defraeye, T., De Ketelaere, B., Herremans, E., Hertog, M. L., Saeys, W., Torricelli, A., Vandendriessche, T., & Verboven, P. (2014). Nondestructive measurement of fruit and vegetable quality. *Annual review of food science and technology, 5*, 285-312.

Nip, W.-K. (1993). *Determining Internal Quality of Mango Fruit.* Paper presented at the Conference on Mango in Hawaii, Honolulu, Hawaii.

Noh, S.-H., & Choi, K.-H. (2006). *Nondestructive quality evaluation technology for fruits and vegetables.* Paper presented at the International Seminar on Enhancing Export Competitiveness of Asian Fruits, Bangkok, Thailand.

Ocean Optics, I. (2010). Jaz Installation and Operation Manual. Retrieved from http://oceanoptics.com///wp-content/uploads/Jazinstallationandoperation.pdf

Omar, A., & MatJafri, M. (2013). Principles, methodologies and technologies of fresh fruit quality assurance. *Quality Assurance and Safety of Crops & Foods, 5*(3), 257-271.

Omar, A. F. (2013). Spectroscopic profiling of soluble solids content and acidity of intact grape, lime, and star fruit. *Sensor Review, 33*(3), 238-245.

Osram Opto, S. (2011). LCW W5AM.PC - Golden Dragon Plus White (English/Deutsch) (Datasheet). Retrieved 8 May 2017 http://uk.rs-online.com/webdocs/102d/0900766b8102d17a.pdf

Osram Opto, S. (2015a). LCW W5AM - Golden Dragon Plus White (English/Deutsch) (Datasheet). Retrieved 8 May 2017 http://www.osram-os.com/Graphics/XPic6/00199188_0.pdf/LCW%20W5AM%20-%20GD%20PLUS%20WHITE%20(EnglishDeutsch).pdf

Osram Opto, S. (2015b). LUW W5AM - Golden Dragon Plus White (English/Deutsch) (Datasheet). Retrieved 8 May 2017 http://www.osram-os.com/Graphics/XPic9/00197237_0.pdf/LUW%20W5AM%20-%20GD%20PLUS%20WHITE%20(EnglishDeutsch).pdf

Paz, P., Sánchez, M.-T., Pérez-Marín, D., Guerrero, J. E., & Garrido-Varo, A. (2009). Instantaneous quantitative and qualitative assessment of pear quality using near infrared spectroscopy. *Computers and electronics in agriculture, 69*(1), 24-32.

Peng, J., Peng, S., Jiang, A., & Tan, J. (2011). Near-infrared calibration transfer based on spectral regression. *Spectrochimica Acta Part A: Molecular and Biomolecular Spectroscopy, 78*(4), 1315-1320.

Pholpho, T., Pathaveerat, S., & Sirisomboon, P. (2011). Classification of longan fruit bruising using visible spectroscopy. *Journal of Food Engineering, 104*(1), 169-172.

Pode, R., & Diouf, B. (2011). *Solar Lighting*: Springer London.

Prelovsek, M., & Bizjak, G. (2006). Variations of color correlated temperature of white led light. *INFORMACIJE MIDEM-JOURNAL OF MICROELECTRONICS ELECTRONIC COMPONENTS AND MATERIALS, 36*(3), 134-139.

Rajkumar, P., Wang, N., EImasry, G., Raghavan, G., & Gariepy, Y. (2012). Studies on banana fruit quality and maturity stages using hyperspectral imaging. *Journal of Food Engineering, 108*(1), 194-200.

Rencher, A. C. (2003). *Methods of multivariate analysis* (Vol. 492): John Wiley & Sons.

Richarme, M. (2002). Eleven Multivariate Analysis Techniques: Key Tools In Your Marketing Research Survival Kit.

Romano, G. S., Cittadini, E. D., Pugh, B., & Schouten, R. (2006). Sweet cherry quality in the horticultural production chain. *Stewart Postharvest Review, 2*(6), 1-9.

Ruiz-Altisent, M., Ruiz-Garcia, L., Moreda, G., Lu, R., Hernandez-Sanchez, N., Correa, E., Diezma, B., Nicolaï, B., & García-Ramos, J. (2010). Sensors for product characterization and quality of specialty crops—A review. *Computers and Electronics in Agriculture, 74*(2), 176-194.

Salguero-Chaparro, L., Palagos, B., Peña-Rodríguez, F., & Roger, J. (2013). Calibration transfer of intact olive NIR spectra between a pre-dispersive instrument and a portable spectrometer. *Computers and Electronics in Agriculture, 96*, 202-208.

Seymour, G., Tucker, G. A., Poole, M., & Giovannoni, J. (2013). *The Molecular Biology and Biochemistry of Fruit Ripening*: Wiley.

Seymour, G. B., Taylor, J. E., & Tucker, G. A. (2012). *Biochemistry of Fruit Ripening*: Springer Netherlands.

Shao, Y., & He, Y. (2008). Nondestructive measurement of acidity of strawberry using Vis/NIR spectroscopy. *International Journal of Food Properties, 11*(1), 102-111.

Siddiqui, M. W. (2015). *Postharvest Biology and Technology of Horticultural Crops*.

Sinelli, N., Spinardi, A., Di Egidio, V., Mignani, I., & Casiraghi, E. (2008). Evaluation of quality and nutraceutical content of blueberries (Vaccinium corymbosum L.) by near and mid-infrared spectroscopy. *Postharvest biology and technology, 50*(1), 31-36.

Singh, Z., Singh, R. K., Sane, V. A., & Nath, P. (2013). Mango-postharvest biology and biotechnology. *Critical Reviews in Plant Sciences, 32*(4), 217-236.

Spinelli, L., Rizzolo, A., Vanoli, M., Grassi, M., Zerbini, P. E., de Azevedo Pementel, A. M., & Torricelli, A. (2013). *Nondestructive assessment of fruit biological age in Brazilian mangoes by time-resolved reflectance spectroscopy in the 540-900 nm spectral range.* Paper presented at the InsideFood Symposium, 9-12 April 2013, Leuven, Belgium.

Subedi, P., & Walsh, K. B. (2011). Assessment of sugar and starch in intact banana and mango fruit by SWNIR spectroscopy. *Postharvest biology and technology, 62*(3), 238-245.

Taguchi, T. (2008). Present status of energy saving technologies and future prospect in white LED lighting. *IEEJ Transactions on Electrical and Electronic Engineering, 3*(1), 21-26.

Tharanathan, R., Yashoda, H., & Prabha, T. (2006). Mango (Mangifera indica L.),"The king of fruits"—An overview. *Food Reviews International, 22*(2), 95-123.

Thomas, N. C. (1991). The early history of spectroscopy. *Journal of chemical education, 68*(8), 631.

Timkhum, P., & Terdwongworakul, A. (2012). Non-destructive classification of durian maturity of 'Monthong'cultivar by means of visible spectroscopy of the spine. *Journal of Food Engineering, 112*(4), 263-267.

Titova, T. P., Nachev, V. G., & Damyanov, C. I. (2015). Food quality evaluation according to their color characteristics. *Facta Universitatis, Series: Automatic Control and Robotics, 14*(1), 1-10.

Tominaga, S., & Wandell, B. A. (1989). Standard surface-reflectance model and illuminant estimation. *JOSA A, 6*(4), 576-584.

Utzinger, U., & Richards-Kortum, R. R. (2003). Fiber optic probes for biomedical optical spectroscopy. *Journal of Biomedical Optics, 8*(1), 121-147.

Van Duyn, M. A. S., & Pivonka, E. (2000). Overview of the health benefits of fruit and vegetable consumption for the dietetics professional: selected literature. *Journal of the American Dietetic Association, 100*(12), 1511-1521.

Wang, S.-s., Sun, H.-n., Chen, J., & Sun, A.-d. (2012). Determination of soluble solids content of blueberries with near infrared spectroscopy [J]. *Science and Technology of Food Industry, 1*, 093.

Wanitchang, P., Terdwongworakul, A., Wanitchang, J., & Nakawajana, N. (2011). Non-destructive maturity classification of mango based on physical, mechanical and optical properties. *Journal of Food Engineering, 105*(3), 477-484.

Wonderful Technology, C. L. (2016). LED Color Temperature Correlation Example Retrieved October 7, 2016, from http://www.wonderfulled.com/led-color-temperature-correlation-example/

Yahaya, O., MatJafri, M., Aziz, A., & Omar, A. (2015). Visible spectroscopy calibration transfer model in determining pH of Sala mangoes. *Journal of Instrumentation, 10*(05), T05002.

Yang, F. L., Cho, S., & Seo, H. S. (2015). Effects of Light Color on Consumers' Acceptability and Willingness to Eat Apples and Bell Peppers. *Journal of Sensory Studies*.

Yuan, L. m., Sun, L., Cai, J. r., & Lin, H. (2015). A Preliminary Study on Whether the Soluble Solid Content and Acidity of Oranges Predicted by Near Infrared Spectroscopy Meet the Sensory Degustation. *Journal of Food Process Engineering, 38*(4), 309-319.

Zerbini, P. E. (2006). Emerging technologies for non-destructive quality evaluation of fruit. *Journal of fruit and ornamental plant research, 14*, 13.

Zerbini, P. E., Vanoli, M., Rizzolo, A., Grassi, M., de Azevedo Pimentel, R. M., Spinelli, L., & Torricelli, A. (2015). Optical properties, ethylene production and softening in mango fruit. *Postharvest biology and technology, 101*, 58-65.

Zhang, H., Huang, J., Li, T., Wu, X., Svanberg, S., & Svanberg, K. (2014). Studies of tropical fruit ripening using three different spectroscopic techniques. *Journal of Biomedical Optics, 19*(6), 067001-067001.

Zhang, H., Wang, J., & Ye, S. (2008). Predictions of acidity, soluble solids and firmness of pear using electronic nose technique. *Journal of Food Engineering, 86*(3), 370-378.

Ziosi, V., Noferini, M., Fiori, G., Tadiello, A., Trainotti, L., Casadoro, G., & Costa, G. (2008). A new index based on vis spectroscopy to characterize the progression of ripening in peach fruit. *Postharvest biology and technology, 49*(3), 319-329.